Universitá degli Studi di Roma Tre

Ph.D. IN CIVIL ENGINEERING

XXXVIII CYCLE

Microplastic Transport in Groundwater Systems: An Integrated Field, Laboratory, and Numerical Modelling Study

Ph.D. Student:

Hari Kumar Omni Babu

Supervisors

Prof. Michele La Rocca,

Prof. Andrea Montessori,

Prof. Elango Lakshmanan.

Coordinator Ph.D. Course

Prof. Fabrizio Paolacci

Abstract

Microplastics have emerged as contaminants of concern in groundwater systems, yet their transport behaviour and fate in subsurface environments remain insufficiently understood. This thesis investigates microplastic occurrence and transport in groundwater through an integrated approach combining field observations, laboratory experiments, and numerical modelling.

Field sampling was conducted across Chennai's aquifer systems during pre-monsoon and post-monsoon periods . Microplastics were detected at all sampling locations, with concentrations increasing between campaigns . Sandy formations showed higher concentrations compared to clayey zones . Fibres dominated the morphological assemblage, with polyvinyl chloride, polyethylene, and polypropylene as the most frequently identified polymers .

Laboratory column experiments investigated transport behaviour across four sand grain sizes spanning fine to coarse fractions . Fine and medium sand exhibited delayed breakthrough with substantial hydraulic conductivity reductions, while coarse sand demonstrated early breakthrough with minimal hydraulic impact. Physical straining was identified as the primary retention mechanism, with particle-to-pore-throat size ratios serving as a controlling parameter .

A numerical model incorporating advection-dispersion equations with retention terms for attachment, detachment, and straining reproduced experimental patterns with strong agreement between predicted and observed breakthrough curves . The model accounted for porosity and permeability evolution during particle accumulation .The findings indicate that grain size distribution governs both microplastic transport efficiency and hydraulic consequences in porous media .

The convergence of field, laboratory, and modelling results supports the identified transport mechanisms and provides a basis for assessing aquifer vulnerability to microplastic contamination.

Acknowledgement

I am deeply grateful to my supervisors, Prof. Michele La Rocca, Prof. Andrea Montessori, at Università Roma Tre and Prof. Elango Lakshmanan from IIT Madras, for their inspiring guidance, constant encouragement, untiring participation in discussions, and invaluable suggestions throughout this PhD research.

I also extend my sincere appreciation to Prof. Fabrizio Paolacci, Coordinator of the PhD Course at Università Roma Tre, for his support and for creating a stimulating academic environment.

I wish to express my heartfelt thanks to Prof. Indumathi M. Nambi and her research group at IIT Madras for hosting me during my study abroad period and providing generous scientific collaboration and support.

My sincere gratitude goes to all research associates and PhD students at Università Roma Tre for their valuable support throughout this PhD research.

I am always thankful to Taylor Swift for constantly inspiring me through her music, especially during challenging phases of this research.

I wish to thank my beloved parents, my sibling, and my friends for their unwavering encouragement, support, and care throughout the different stages of my work and life.

AI Tools Disclosure

Generative AI tools, including You.com, Perplexity, Copilot, and Gemini, were used during the preparation of this thesis to assist with text drafting, image generation, background research summarization, and refining outlines. All outputs were reviewed, edited, and verified for accuracy by the author to ensure originality and scientific integrity.

Contents

List of Figures

List of Tables

Chapter 1 Introduction

1.1 Plastic Pollution and Environmental Fate

1.1.1 Global Trends in Plastic Production and Use

The proliferation of plastic materials represents one of the most profound anthropogenic alterations to the Earth's material cycles in the modern era. Evidence of widespread microplastic occurrence throughout our environment has mounted significantly over the past decade, raising urgent questions about potential health hazards and mitigation strategies (Zhang et al., 2020). The ubiquity of these materials stems from their durability, versatility, and low production costs, which have driven exponential growth in global plastic production since the mid-20th century. This growth trajectory shows minimal signs of deceleration despite increasing awareness of environmental consequences.

The persistence of plastic pollution has become increasingly concerning as annual plastic waste generation continues to outpace waste management infrastructure development, particularly in developing economies. Current estimates suggest that between 4 and 12 million metric tons of plastic waste enter aquatic environments annually (Alimi et al., 2018, Jambeck et al. 2015), representing only a fraction of total plastic waste mismanagement globally. Single-use plastic products constitute a significant portion of this waste stream, with packaging materials alone accounting for approximately 40% of plastic production (Jambeck et al., 2015). This progressive accumulation has transformed plastics from beneficial consumer products into persistent environmental contaminants with complex distribution patterns across terrestrial, freshwater, marine, and atmospheric compartments.

1.1.2 Environmental Persistence and Fragmentation Processes

The environmental longevity of plastic materials stems from their synthetic polymer composition, which renders them highly resistant to natural degradation processes. These synthetic polymers exhibit exceptional durability in environmental settings, with degradation timeframes often measured in decades or centuries rather than months or years (Chamas et al., 2020). Rather than complete biodegradation, environmental plastics typically undergo fragmentation into progressively smaller particles through the combined effects of photodegradation, mechanical abrasion, thermal stress, and biological interactions (Andrady, 2017).

This fragmentation process represents the primary pathway through which larger plastic debris is transformed into microplastics, conventionally defined as plastic particles ≤5 mm in size (Frias & Nash, 2019). The degradation continuum extends further into the nanoscale range, producing nanoplastics with distinct environmental behaviours and toxicological profiles (Gigault et al., 2018). Twenty years after the first publication that used the term "microplastic," our understanding of these degradation processes continues to evolve, with recent research highlighting the complex interplay between polymer type, environmental conditions, and resulting fragmentation rates (Hartmann et al., 2019). The persistence of these materials establishes a concerning environmental legacy that will continue to influence ecosystem functioning long after potential reductions in plastic production or improved waste management practices.

1.1.3 Terrestrial and Aquatic Fate Pathways

The environmental fate of plastic pollution involves complex transport mechanisms across interconnected environmental compartments. Microplastics originate from multiple sources and follow diverse pathways through the environment, including atmospheric deposition as an increasingly recognized transport vector (Allen et al., 2019). In aquatic systems, microplastics can enter directly through point sources such as wastewater treatment effluents or indirectly through the gradual degradation of larger plastic debris (Horton et al., 2017). Hydrodynamic processes subsequently influence their distribution, with factors such as particle density, size, and shape determining settling behaviours and transport distances (Kooi et al., 2018).

Terrestrial environments serve as both repositories and conduits for microplastic pollution, with agricultural soils, urban areas, and industrial zones functioning as significant environmental reservoirs (Xu et al., 2020). The soil-water interface represents a critical transition zone, where hydrogeological processes mediate the vertical transport of microplastics from surface environments into subsurface aquifers. This vertical migration has significant implications for groundwater quality, as these crucial freshwater resources increasingly face contamination from microplastic pollution (Re, 2019). The persistence and mobility of microplastics across these diverse environmental compartments highlight the interconnected nature of terrestrial and aquatic fate pathways in the global distribution of plastic pollution.

1.1.4 Long-Term Ecological Impacts

The long-term ecological consequences of microplastic pollution remain incompletely understood, though mounting evidence suggests multifaceted impacts across trophic levels and ecosystem functions. Toxicological studies have documented adverse effects in aquatic organisms exposed to microplastics under laboratory conditions (Wright et al., 2013), with mechanisms of harm including physical injury, inflammatory responses, oxidative stress, and disrupted energy allocation (Anbumani & Kakkar, 2018). These effects manifest across biological scales, from molecular and cellular alterations to population-level impacts, though the environmental relevance of laboratory exposure concentrations continues to be debated.

Of particular concern is the potential for microplastics to function as vectors for associated contaminants, including persistent organic pollutants, heavy metals, and plastic additives such as plasticizers and flame retardants (Rochman et al., 2014). The capacity for microplastics to bioaccumulate within food webs introduces additional concerns regarding trophic transfer and biomagnification effects (Setälä et al., 2014). The ecological risk assessment is further complicated by the heterogeneous nature of environmental microplastics, which vary considerably in polymer composition, size distribution, weathering state, and associated contaminant profiles (Koelmans et al., 2016). This complexity necessitates integrated approaches to evaluating the long-term ecological implications of microplastic pollution across diverse environmental settings.

1.2 Microplastics Pollution: Sources and Significance

1.2.1 Primary vs Secondary Microplastics

Microplastics are conventionally categorized as environmental contaminants consisting of synthetic polymer particles ≤5 mm in size, with further classification based on their origin as either primary or secondary microplastics (Frias & Nash, 2019). Primary microplastics are manufactured at microscopic sizes for specific applications, including industrial abrasives, drilling fluids, and personal care products (Lassen et al., 2015). These particles enter the environment in their manufactured form through direct release pathways, including wastewater discharge, industrial effluents, and accidental spillage during production or transport.

In contrast, secondary microplastics result from the environmental degradation and fragmentation of larger plastic items (Andrady, 2017), representing the predominant fraction of environmental microplastic pollution. This degradation occurs through various weathering processes, including photodegradation, mechanical abrasion, thermal oxidation, and biological degradation (Song et al., 2017). The distinction between primary and secondary microplastics has important implications for pollution control strategies, as primary microplastics can be regulated through manufacturing restrictions and product reformulations, while secondary microplastics necessitate broader interventions targeting plastic waste management and environmental remediation. The relative contributions of these sources vary considerably across environmental compartments and geographical regions, reflecting differences in consumption patterns, waste management infrastructure, and environmental conditions affecting degradation rates.

1.2.2 Sources in Urban, Agricultural, and Industrial Settings

The sources of microplastic pollution exhibit distinct profiles across urban, agricultural, and industrial landscapes. Urban environments generate significant microplastic loads through multiple pathways, including wastewater treatment effluents, stormwater runoff, atmospheric deposition, and direct littering (Dris et al., 2015). Personal care products containing microbeads have received particular attention as direct sources of primary microplastics in urban wastewater streams (Napper et al., 2015), though recent regulatory restrictions in many countries have reduced this specific contribution. Synthetic textile fibers released during domestic laundering represent another significant urban source, with individual washing cycles capable of releasing thousands of microfibers (De Falco et al., 2019).

Agricultural settings introduce microplastics through multiple vectors, including plastic mulching films, controlled-release fertilizers with polymer coatings, and the application of biosolids containing municipal wastewater residues (Hurley & Nizzetto, 2018). Industrial sources encompass plastic manufacturing facilities, wastewater from textile processing, and abrasive blasting operations using plastic media (Galloway et al., 2017). The relative significance of these varied sources remains incompletely quantified, particularly for groundwater systems where source apportionment is complicated by the filtering effects of soil matrices and the potential for long-term accumulation. The heterogeneous nature of

these sources contributes to the complex composition profiles of environmental microplastics, necessitating multifaceted monitoring and mitigation approaches.

1.2.3 Relevance to Environmental Hydrogeology

The intersection of microplastic pollution with environmental hydrogeology represents an emerging research domain with significant implications for groundwater resource management. As crucial freshwater sources, groundwater systems face increasing contamination pressure from microplastic pollution (Panno et al., 2019), challenging conventional paradigms of aquifer vulnerability and contaminant transport. The relevance of microplastics to hydrogeological research emerges from several considerations, including the documented occurrence of microplastics in groundwater samples worldwide, the potential for long-term accumulation in aquifer materials, and the unique transport behaviours of particulate pollutants in porous media.

Hydrogeological factors including hydraulic conductivity, groundwater flow velocities, and aquifer heterogeneity significantly influence the mobility and distribution of microplastics in subsurface environments (Kataoka et al., 2019). The physical and chemical properties of microplastic particles, including size distribution, surface charge, and aggregation potential, further modulate their interactions with aquifer materials through filtration, straining, and sorption processes (Rochman, 2018). Understanding these interactions requires integration of hydrogeological principles with emerging knowledge of microplastic environmental behaviour, creating new interdisciplinary challenges for contaminant hydrogeology. The potential for microplastics to alter aquifer hydraulic properties or influence the mobility of co-occurring contaminants further underscores the relevance of these emerging pollutants to environmental hydrogeology.

1.2.4 Emerging Concerns in Groundwater Systems

The emerging recognition of microplastics as groundwater contaminants has generated specific concerns regarding their potential impacts on these critical freshwater resources. Groundwater, as a crucial drinking water source for approximately half the global population, faces increasing pollution pressure from microplastic contamination, raising questions about potential human exposure through drinking water consumption (WHO, 2019). The detection of microplastics in groundwater systems contradicts traditional

assumptions about the filtering capacity of soil and aquifer materials, suggesting that conventional protection paradigms may inadequately address particulate contaminants in the micro- and nano-size ranges (Panno et al., 2019; Koelmans et al., 2019).

Particular concerns include the potential for microplastics to alter aquifer hydraulic properties through clogging mechanisms, the possibility for long-term accumulation in aquifer materials with limited remediation options, and the uncertain interactions between microplastics and other groundwater contaminants (Eerkes-Medrano et al., 2019). The detection of microplastics in groundwater also raises fundamental questions about subsurface plastic pollution residence times and the potential for aquifers to function as long-term repositories and secondary sources of microplastic pollution (Re, 2019). These emerging concerns necessitate dedicated research attention to elucidate the unique aspects of microplastic contamination in groundwater environments.

1.3 Microplastics in Aquatic Systems

1.3.1 Transport Mechanisms in Rivers, Lakes, and Oceans

The transport of microplastics through aquatic systems involves complex interactions between particle properties and hydrodynamic processes across freshwater and marine environments. In riverine systems, microplastic transport is primarily governed by flow velocity, channel morphology, and particle characteristics, with particles exhibiting distinct sorting patterns related to density, size, and shape (Nizzetto et al., 2016). Higher-density polymers such as polyethylene terephthalate (PET) demonstrate greater deposition in sedimentary environments, while lower-density polymers like polyethylene and polypropylene exhibit increased mobility and potential for downstream transport (Besseling et al., 2017).

In lacustrine environments, thermal stratification, wind-driven currents, and seasonal mixing patterns influence the vertical and horizontal distribution of microplastic particles (Ballent et al., 2016). Marine systems demonstrate additional transport complexities related to oceanic currents, thermohaline circulation, and wave-driven processes, resulting in the documented accumulation of microplastics in oceanic gyres, deep-sea sediments, and coastal environments worldwide (Van Sebille et al., 2015). The analysis, prevention, and removal of microplastics pollution in water represent major environmental challenges (Alimi et al.,

2018), requiring integrated understanding of these diverse transport mechanisms across interconnected aquatic systems. The transport of microplastics between surface water bodies and groundwater systems through hyporheic exchange and groundwater-surface water interactions remains poorly characterized but potentially significant for comprehensive understanding of environmental microplastic fate.

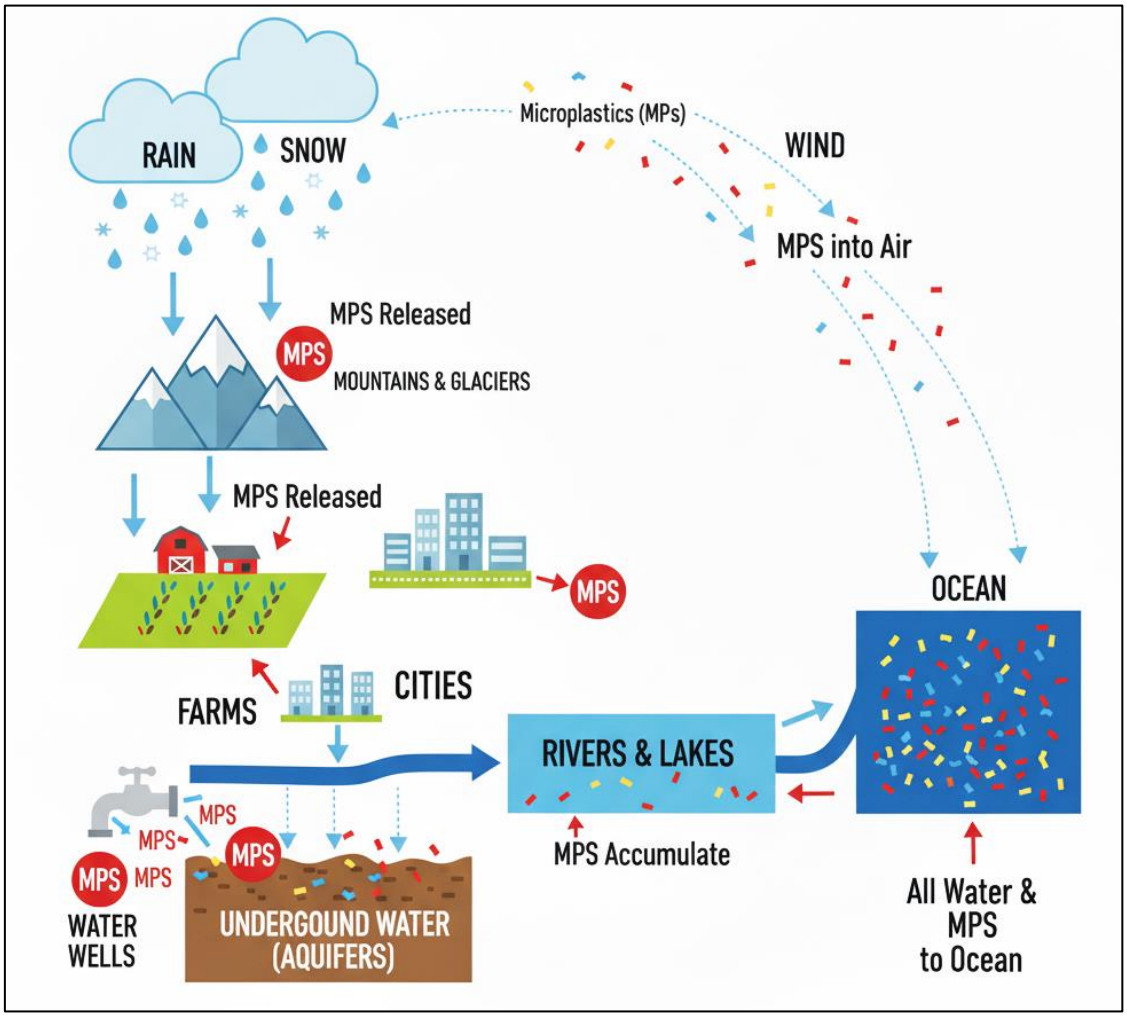

Figure 1: Conceptual Model Detailing Microplastics: Source-to-Sink Pathways via Hydrological and Atmospheric Transport.

1.3.2 Ecological and Toxicological Effects

The ecological and toxicological implications of microplastics in aquatic systems encompass a spectrum of biological effects across organizational levels. Laboratory studies have demonstrated the toxicity of microplastics to various aquatic organisms, with documented effects including reduced feeding efficiency, altered growth rates, reproductive impairment,

and behavioural changes (Anbumani & Kakkar, 2018). Mechanistically, these effects may result from physical injury, inflammatory responses, oxidative stress, altered gut microbiota, or disrupted energy allocation (Wright et al., 2013). The toxicological profile of environmental microplastics is further complicated by their capacity to sorb and transport co-contaminants, including persistent organic pollutants, heavy metals, and endocrine-disrupting compounds (Rochman et al., 2014).

This vector function potentially enhances the bioavailability of these associated contaminants to aquatic organisms. Toxicity also varies considerably with microplastic physical and chemical properties, including polymer type, size, shape, weathering state, and associated additives (Hahladakis et al., 2018). Smaller particles generally demonstrate enhanced toxicity due to increased bioavailability and cellular uptake potential, with nanoplastics presenting distinct toxicological concerns related to their ability to penetrate biological membranes and tissues (Triebskorn et al., 2019). Ecological impacts extend beyond direct toxicity to include habitat alteration, changes in community composition, and potential for trophic transfer through food webs, though field-based evidence for population and ecosystem-level effects remains limited (Burns & Boxall, 2018).

1.3.3 Detection and Monitoring Techniques

The development of reliable detection and monitoring techniques for aquatic microplastics represents a significant methodological challenge in environmental research. The field currently lacks fully harmonized methods and materials (Primpke et al., 2020), contributing to challenges in data comparability and quality assurance. Extraction of microplastics from complex environmental matrices requires specialized techniques tailored to sample characteristics with methods including density separation, filtration, digestion of organic matter, and visual sorting (Miller et al., 2017). Analytical identification typically employs spectroscopic techniques such as Fourier-transform infrared spectroscopy (FTIR) and Raman spectroscopy, which enable polymer identification through characteristic spectral patterns (Käppler et al., 2016).

Complementary techniques include thermal analysis methods such as pyrolysis-gas chromatography/mass spectrometry (Py-GC/MS) and thermogravimetric analysis (TGA), which provide compositional information through thermal decomposition patterns (Dümichen et al., 2015). Sampling approaches for aquatic systems encompass water column

sampling using nets and pumps, sediment sampling with grab samplers and corers, and biota sampling for assessing biological uptake (Masura et al., 2015). Monitoring programs for aquatic microplastics must address numerous methodological considerations, including representative sampling designs, contamination prevention protocols, recovery efficiency assessments, and appropriate quality control measures (Koelmans et al., 2019). The ongoing development of standardized methodologies represents a crucial requirement for generating comparable data on microplastic occurrence, distribution, and temporal trends in aquatic systems.

1.3.4 Knowledge Gaps in Aquatic Microplastic Research

Despite two decades of microplastic pollution research, significant knowledge gaps persist regarding the behaviour and impacts of microplastics in aquatic systems. Primary among these gaps is the limited understanding of smaller microplastic fractions (≤20 μm) and nanoplastics, which present substantial analytical challenges but potentially enhanced environmental risks due to increased bioavailability (Gigault et al., 2018). Temporal dynamics of microplastic pollution remain poorly characterized, with limited long-term monitoring data to establish baseline conditions and assess remediation effectiveness (Wagner & Lambert, 2018). Mechanistic understanding of microplastic transport between interconnected environmental compartments, particularly at the groundwater-surface water interface, requires further development (Barnes et al., 2009).

Significant uncertainties persist regarding the ecological significance of observed laboratory effects under environmentally relevant exposure scenarios, with field-based evidence for population and ecosystem-level impacts remaining scarce (Burns & Boxall, 2018). The potential for microplastics to alter microbial community structures and biogeochemical processes in aquatic systems represents an emerging research domain with implications for ecosystem functioning (Zettler et al., 2013). Additionally, the synergistic or antagonistic interactions between microplastics and other environmental stressors, including climate change parameters, warrant further investigation (Browne et al., 2015). Addressing these knowledge gaps requires interdisciplinary approaches integrating hydrology, analytical chemistry, ecotoxicology, and environmental modelling to develop comprehensive understanding of microplastic behaviour in aquatic environments.

1.4 Microplastics in Groundwater: An Overview of Current Knowledge

1.4.1 Evidence of Microplastics in Groundwater

The detection of microplastics in groundwater systems represents a relatively recent development in environmental contaminant research, with systematic reviews documenting their occurrence across diverse hydrogeological settings (Re, 2019; Koelmans et al., 2019). Evidence of microplastic contamination has been reported from various aquifer types, including alluvial, karst, and fractured bedrock systems, contradicting traditional assumptions about the filtering capacity of soil and aquifer materials for particulate contaminants (Panno et al., 2019). The reported concentrations of microplastics in groundwater typically range from several particles per Liter to several hundred particles per Liter, though methodological differences complicate direct comparisons between studies (Koelmans et al., 2019).

The polymer composition of groundwater microplastics frequently reflects common commercial polymers, including polyethylene, polypropylene, polyethylene terephthalate, and polystyrene, with size distributions generally skewed toward smaller particles compared to surface water samples (Re, 2019). Spatial distribution patterns of groundwater microplastics show correlations with anthropogenic land use, with elevated concentrations reported in urban and industrial areas relative to less developed regions (Eerkes-Medrano et al., 2019). The presence of microplastics in groundwater resources intended for human consumption raises concerns regarding potential exposure pathways and associated health implications, though these remain incompletely characterized (WHO, 2019). The documented occurrence of microplastics in groundwater across multiple geographical regions establishes these particles as emerging contaminants of concern for groundwater quality management and protection.

1.4.2 Analytical and Detection Methods

The detection and characterization of microplastics in groundwater present distinct analytical challenges requiring specialized methodologies. Groundwater sampling and analysis methods for microplastics must address the typically lower concentrations compared to surface water environments, the smaller size distributions resulting from filtration during subsurface transport, and the potential for sampling-induced contamination (Koelmans et al., 2019). Current analytical approaches typically involve sequential steps of sample collection, pre-treatment, microplastic separation, and identification. Sample

collection methodologies must prevent contamination from sampling equipment and atmospheric sources, often requiring metal or glass sampling equipment and clean-room procedures (Hermsen et al., 2018).

Pre-treatment methods for groundwater samples may include filtration, density separation, and oxidative digestion to remove natural organic matter (Masura et al., 2015). The identification of microplastics in processed samples employs various analytical techniques, including visual microscopy, spectroscopic methods (FTIR, Raman), and thermal analysis (Py-GC/MS) (Käppler et al., 2016). Each analytical approach offers distinct advantages and limitations regarding sensitivity, specificity, and practical application to environmental samples. Method validation remains crucial, with recovery experiments, procedural blanks, and reference materials providing essential quality assurance measures (Primpke et al., 2020). The lack of standardized protocols for groundwater microplastic analysis presents ongoing challenges for data comparability and reliability, highlighting the need for methodological harmonization efforts within this emerging research domain.

1.4.3 Transport Modelling in Porous Media

Understanding and predicting microplastic transport in groundwater systems requires adaptation of existing colloid transport models to account for the unique characteristics of these particulate contaminants. Transport modelling of microplastics in porous media must address multiple physical processes, including advection, dispersion, attachment, detachment, straining, and size exclusion (Bradford et al., 2015). The application of colloid filtration theory provides a theoretical framework for predicting microplastic retention in porous media, with key parameters including collector efficiency, attachment efficiency, and retention capacity (Tufenkji & Elimelech, 2004). These parameters are influenced by microplastic properties (size, shape, surface charge, hydrophobicity) and aquifer characteristics (grain size distribution, mineralogy, organic matter content, solution chemistry) (Rochman, 2018).

Experimental studies under controlled laboratory conditions have demonstrated complex transport behaviours, with smaller microplastic particles typically exhibiting enhanced mobility compared to larger fractions (O'Connor et al., 2019). The development of numerical models for microplastic transport in groundwater systems remains an emerging research area, with challenges including the heterogeneous nature of environmental

microplastics, the dynamic surface properties of weathered particles, and the complexity of real-world aquifer systems (Keller & Lazareva, 2014). Continued refinement of transport models represents an essential component for predicting microplastic fate in groundwater environments and informing risk assessment frameworks for these emerging contaminants in subsurface systems.

1.4.4 Hydrogeological Implications and Risk Assessment

The presence of microplastics in groundwater systems introduces several hydrogeological implications requiring consideration within groundwater management frameworks. Potential effects include alteration of aquifer hydraulic properties through particle accumulation and pore clogging, particularly in finer-grained aquifer materials and near-well environments (Kataoka et al., 2019; Re, 2019) . The long-term persistence of microplastics in groundwater, potentially exceeding conventional contaminant timeframes due to limited degradation under subsurface conditions, presents challenges for remediation planning and natural attenuation assessments (Barnes et al., 2009). Risk assessment frameworks for groundwater microplastics remain in early developmental stages, with significant data gaps regarding exposure patterns, dose-response relationships, and vulnerability factors for different aquifer types (WHO, 2019).

The development of hydrogeological vulnerability mapping for microplastic contamination requires integration of traditional aquifer vulnerability factors with specific consideration of preferential flow pathways, which may facilitate enhanced transport of particulate contaminants (Kataoka et al., 2019). Groundwater-dependent ecosystems represent potential ecological receptors for microplastic exposure, though research on these ecological impacts remains limited (Groh et al., 2019). The implications of microplastic contamination for groundwater treatment processes used in drinking water production warrant further investigation, including potential effects on filtration efficiency, membrane fouling, and disinfection efficacy (Mintenig et al., 2019). These diverse hydrogeological implications highlight the need for integrated assessment approaches addressing both resource protection and management considerations.

1.4.5 Research Gaps and Future Directions

Systematic reviews of microplastic pollution in groundwater have identified numerous research gaps requiring attention to advance understanding of these emerging contaminants in subsurface environments (Re, 2019; Koelmans et al., 2019; WHO, 2019). Fundamental knowledge gaps include limited data on temporal trends and spatial distribution patterns of groundwater microplastics across diverse hydrogeological settings (Koelmans et al., 2019; Panno et al., 2019). Methodological challenges persist regarding the detection and quantification of smaller microplastic fractions and nanoplastics in groundwater matrices, with current analytical limitations potentially underestimating actual contamination levels (Koelmans et al., 2019). The relative contributions of different contamination pathways, including surface infiltration, well construction, subsurface infrastructure leakage, and groundwater-surface water interactions, remain incompletely characterized (Panno et al., 2019).

Mechanistic understanding of microplastic transport, retention, and potential transformation in aquifer materials requires further development through combined laboratory and field investigations (O'Connor et al., 2019). The potential for microplastics to influence microbial communities and biogeochemical processes in groundwater systems represents an emerging research domain with implications for natural attenuation processes and ecosystem functioning (Zettler et al., 2013). Risk assessment frameworks specific to groundwater microplastics need development, incorporating hydrogeological vulnerability factors, exposure pathway analysis, and consideration of cumulative impacts with co-occurring contaminants (WHO, 2019). These research gaps highlight the need for interdisciplinary approaches integrating hydrogeology, analytical chemistry, material science, and environmental modelling to advance understanding of microplastic contamination in groundwater resources.

1.5 Thesis Objectives, Structure, and Novelty

1.5.1 Research Questions and Objectives

This thesis addresses fundamental questions regarding the occurrence, behaviour, and implications of microplastics in groundwater systems through an integrated approach

combining field investigations, laboratory experimentation, and numerical modelling. The research is guided by the following specific objectives:

1. To study and characterise the occurrence, composition, and spatial distribution of microplastics in groundwater.

2. To study transport of microplastics in porous media through controlled laboratory experiments.

3. To develop and validate numerical models capable of predicting microplastic transport in subsurface environments, incorporating boundary conditions derived from laboratory experiments.

4. To use the combined field, experimental and modelling results to discuss possible implications of microplastics for groundwater quality and aquifer behaviour.

These objectives address critical knowledge gaps in current understanding of microplastics as groundwater contaminants, with findings intended to inform both fundamental environmental science and applied water resource management.

1.5.2 Thesis Structure Overview

The thesis is organized into seven chapters that progressively develop the research narrative from contextual foundation through empirical findings to synthesis and implications:

Chapter 1 introduces plastic and microplastic pollution, summarises current knowledge on microplastics in groundwater, and states the research objectives and thesis outline.

Chapter 2 reviews the scientific literature on microplastics in groundwater, including occurrence, analytical methods, transport in porous media and key knowledge gaps relevant to this work.

Chapter 3 describes the field study design, sampling and analytical methods, and presents results on the occurrence and spatial patterns of microplastics in groundwater in relation to hydrogeological and land-use factors.

Chapter 4 presents column experiments on microplastic transport in saturated porous media, including methods, results on retention and breakthrough, and their interpretation.

Chapter 5 develops and applies numerical models for microplastic transport in porous media, explains the modelling approach and parameterisation, and compares model results with experimental data.

Chapter 6 brings together findings from the field, experimental and modelling components and discusses their implications for groundwater quality and hydrogeology, as well as limitations and future research needs.

Chapter 7 lists all references cited in the thesis in APA format.

Each empirical chapter (3-5) thus follows a self-contained structure with methodology, results, and discussion sections specific to that research component, while maintaining narrative coherence and progressive development of arguments across the thesis as a whole.

1.5.3 Novelty and Contribution to Environmental Hydrogeology

The contributions of this thesis are summarised below.

Firstly, the experimental investigation of microplastic transport mechanisms in porous media generates empirical data on retention behaviours under environmentally relevant conditions, which may offer useful insights for understanding subsurface microplastic dynamics.

Secondly, the development and application of numerical models specifically parameterised for microplastic transport contributes to enhance the comprehension of the dynamics of microplastics transport in groundwater.

The interdisciplinary approach integrating field observations, laboratory experimentation, and numerical modelling aims to provide a clearer perspective on microplastic fate in groundwater systems, with findings intended to complement existing research in this emerging field.

Chapter 2 – Literature Review

2.1 Occurrence and Transport of Microplastics in Groundwater

2.1.1 Entry Pathways and Contamination Sources

Microplastics, defined as plastic particles with dimensions between 1 μm and 5 mm, have emerged as ubiquitous environmental contaminants with an increasingly recognized presence in groundwater systems. The pathways through which microplastics enter groundwater are diverse and complex, reflecting the multifaceted nature of plastic pollution in the environment (Wagner et al., 2014). Out of the estimated 8.3 billion tons of plastics produced globally since the 1950s, approximately 79% has ended up in landfills or has leaked into the natural environment, creating a pervasive contamination footprint that spans terrestrial, aquatic, and atmospheric systems (Geyer et al., 2017). This massive volume of plastic waste presents numerous pathways for infiltration into groundwater resources.

Microplastics can originate from both primary and secondary sources. Primary microplastics are manufactured at the microscale and include plastic fibers, pellets, and microbeads used in industrial applications and personal care products. Secondary microplastics form through the fragmentation of larger plastic debris due to environmental weathering processes (Barnes et al., 2009). The fragmentation process continues in the environment, with larger plastic items breaking down into increasingly smaller particles over time (Thompson et al., 2004).

The entry of microplastics into groundwater systems primarily occurs through surface infiltration, where contaminated surface water percolates through soil and sediment layers. Urban runoff represents a significant pathway, carrying microplastics from roads, buildings, and other infrastructure directly into groundwater recharge zones (Horton & Dixon, 2018). Wastewater effluent discharge, even after treatment, contributes substantially to groundwater microplastic contamination, as conventional treatment processes are not designed to completely remove these particles (Sun et al., 2019). Land-based sources, including agricultural activities utilizing plastic mulches and sewage sludge application, create additional pathways for microplastic infiltration into groundwater systems (Nizzetto et al., 2016).

2.1.2 Particle Characteristics and Transport Behaviour

The physical and chemical properties of microplastics significantly influence their transport behaviour in groundwater systems. Size distribution represents one of the most critical factors, with smaller particles demonstrating enhanced mobility through porous media. Microplastics in the environment display remarkable heterogeneity in their composition, with polyethylene (PE), polypropylene (PP), polyethylene terephthalate (PET), and polystyrene (PS) being among the most commonly detected polymers (Rochman et al., 2013).

Particle shape and morphology also play crucial roles in transport dynamics. Microplastics typically manifest as fragments, fibers, films, foams, pellets, and microbeads, with each morphological type exhibiting distinct transport behaviours (Kooi et al., 2017). Fibers, characterized by their high aspect ratio, demonstrate unique flow patterns compared to more spherical particles, potentially leading to increased straining in pore throats (Rillig et al., 2017).

The density of microplastic particles, which varies by polymer type, significantly influences their vertical migration in groundwater. Lower-density polymers like polyethylene (0.91-0.97 g/cm³) and polypropylene (0.85-0.94 g/cm³) exhibit greater buoyancy and potentially greater mobility compared to higher-density polymers such as polyvinyl chloride (1.16-1.58 g/cm³) (Andrady, 2011). However, these intrinsic density characteristics can be altered through environmental processes including biofouling, weathering, and the adsorption of organic and inorganic compounds (Kooi et al., 2017).

2.1.3 Hydrogeological Influences

The transport and fate of microplastics in groundwater are heavily influenced by the hydrogeological characteristics of aquifer systems. Pore size distribution and connectivity within aquifer materials establish fundamental controls on particle transport. Coarse-grained aquifers with larger pore spaces generally facilitate greater microplastic mobility compared to fine-grained systems (Bouwman et al., 2018). The hydraulic properties of aquifers, including hydraulic conductivity, porosity, and specific yield, determine flow velocities and residence times, thereby affecting the spatial distribution of microplastic contaminants.

Aquifer heterogeneity presents particular challenges for predicting microplastic transport, as preferential flow paths can significantly accelerate contaminant migration. Fracture networks in consolidated rock aquifers and macropores in unconsolidated materials create high-permeability conduits that bypass the filtering capacity of the porous matrix (Re, 2019). Stratigraphic variations within aquifer systems, including the presence of confining layers, influence vertical migration patterns and potential cross-contamination between aquifer units (Keller et al., 2019) .

2.1.4 Environmental and Biogeochemical Modifiers

Environmental conditions and biogeochemical processes substantially modify microplastic transport behaviour in groundwater systems. Groundwater chemistry, particularly ionic strength and pH, influences particle-particle and particle-surface interactions through electrostatic mechanisms (Dong et al., 2019) . Higher ionic strength conditions typically promote particle aggregation and deposition through compression of the electrical double layer, potentially reducing mobility (Bradford et al., 2015).

The presence of natural organic matter (NOM) creates complex effects on microplastic transport. NOM can form coatings on both microplastic surfaces and aquifer materials, potentially enhancing particle stability through steric hindrance mechanisms while simultaneously altering surface charge characteristics (Erhayem & Sohn, 2014). Microbial communities in groundwater systems interact with microplastic particles through biofilm formation, which modifies surface properties and may enhance retention in porous media (Rummel et al., 2017).

Temperature variations influence microplastic transport through effects on water viscosity, microbial activity, and polymer degradation rates. Climate change-induced alterations in groundwater recharge patterns and temperature regimes may therefore have significant implications for long-term microplastic fate and transport (Wright & Kelly, 2017).

2.2 Field-Based Studies: Methods and Findings

2.2.1 Sampling Protocols and Equipment Limitations

Field investigations into groundwater microplastic contamination have employed diverse sampling methodologies, each with distinct advantages and limitations. Groundwater

sampling techniques for microplastic analysis typically involve modifications to established hydrogeological sampling protocols to minimize contamination and ensure representative results (Mintenig et al., 2019). Well sampling represents the most common approach, utilizing either dedicated sampling pumps or bailers to collect groundwater samples from monitoring or production wells (Re, 2019).

Sampling protocols generally incorporate careful quality assurance measures to minimize contamination from equipment, personnel, and the surrounding environment. These measures typically include field blanks, equipment blanks, and procedural blanks to quantify potential contamination sources (Hermsen et al., 2018). The use of non-plastic sampling equipment or equipment with verified polymer compositions distinct from environmental microplastics remains critical for accurate analysis (Stock et al., 2019).

Sample volume requirements present significant challenges for groundwater microplastic studies, with required volumes typically ranging from 1 to 20 Liters depending on expected concentrations and analytical sensitivity. This volume requirement creates logistical difficulties for remote sampling locations and deep wells with limited yield (Koelmans et al., 2019). Filtration methodologies for sample concentration have evolved, with researchers employing peristaltic pumps and in-line filtration systems to improve field collection efficiency and minimize contamination (Stock et al., 2019; Mintenig et al., 2019)..

2.2.2 Detection Technologies and Analytical Challenges

The analytical identification and quantification of microplastics in groundwater samples employ a multi-tiered approach combining visual, spectroscopic, and thermal techniques. Visual identification using stereomicroscopy provides initial screening but suffers from significant limitations including operator subjectivity and inability to confirm polymer composition (Hidalgo-Ruz et al., 2012). These limitations are particularly pronounced for particles smaller than 500 μm, where visual identification becomes increasingly unreliable (Löder & Gerdts, 2015).

Spectroscopic methods, including Fourier-transform infrared spectroscopy (FTIR) and Raman spectroscopy, have emerged as essential tools for polymer identification. Micro-FTIR techniques allow for the analysis of particles down to approximately 20 μm, while Raman spectroscopy can achieve identification of particles as small as 1 μm (Käppler et al.,

2016). These techniques provide detailed chemical fingerprints of individual particles but face challenges including time-intensive analysis, interference from environmental matrices, and limited automation capabilities (Primpke et al., 2018).

Thermal analytical methods, including pyrolysis-gas chromatography-mass spectrometry (Pyro-GC-MS), enable bulk quantification of specific polymer types but sacrifice information on particle size, shape, and individual particle composition (Dümichen et al., 2015). Combined methodologies integrating multiple analytical techniques represent emerging best practices, though standardization across studies remains limited (Felsing et al., 2018).

2.2.3 Observed Patterns Across Aquifer Types

Field studies have revealed distinct patterns of microplastic occurrence across different aquifer systems, though comprehensive understanding remains limited by the relatively small number of investigations. Unconfined aquifers in urban and agricultural settings generally exhibit higher microplastic concentrations compared to confined systems, reflecting the influence of surface contamination sources and direct recharge pathways (Panno et al., 2019). Shallow groundwater systems demonstrate particularly elevated concentrations, with decreasing trends observed with depth in most studies (Mintenig et al., 2019).

Aquifer lithology significantly influences observed microplastic distributions. Coarse-grained aquifers comprised of sand and gravel typically show greater microplastic penetration compared to fine-grained systems, reflecting the influence of pore size distributions on particle filtration (Bouwman et al., 2018) . Fractured rock aquifers present unique challenges, with evidence suggesting that fracture networks can facilitate rapid transport of microplastic particles over significant distances (Panno et al., 2019).

Seasonal variations in microplastic concentrations have been observed in some studies, potentially reflecting seasonal changes in recharge patterns, land use activities, and hydrological conditions. However, long-term monitoring programs remain scarce, limiting understanding of temporal dynamics and potential accumulation effects (Dioses-Salinas et al., 2020).

2.2.4 Methodological Strengths and Limitations

Current field-based investigations into groundwater microplastic contamination exhibit both significant strengths and substantial limitations. The primary strength of field studies lies in their documentation of real-world contamination under natural hydrogeological conditions, providing essential baseline data on occurrence, distribution, and potential risk (Rochman, 2018). The incorporation of multiple sampling locations enables spatial pattern analysis, while integration with existing groundwater monitoring networks facilitates efficient data collection (Koelmans et al., 2019).

However, significant methodological limitations constrain the interpretation and comparability of field studies. The absence of standardized sampling, processing, and analytical protocols creates substantial challenges for cross-study comparison and meta-analysis (Hartmann et al., 2019). Sample contamination risks remain high throughout the collection, transportation, and processing chain, potentially leading to false positives or concentration overestimation (Wesch et al., 2017).

Analytical detection limits vary widely across studies, with particular challenges for smaller microplastic particles (< 10 μm) that may be numerically dominant but methodologically difficult to quantify (Mintenig et al., 2018). The representativeness of sampling remains questionable, with most studies collecting limited samples that may not capture spatial or temporal heterogeneity adequately (Koelmans et al., 2020). These limitations highlight the need for continued methodological refinement and standardization in groundwater microplastic investigations.

2.3 Experimental Studies in Porous Media

2.3.1 Experimental Designs and Media Types

Laboratory-based experimental studies investigating microplastic transport in porous media have employed diverse methodological approaches to simulate groundwater conditions. Column experiments represent the most prevalent experimental design, utilizing packed columns of various dimensions filled with well-characterized porous materials (O'Connor et al., 2019). These setups allow for controlled investigation of transport parameters under defined hydraulic and chemical conditions, though scaling issues present challenges for field-scale extrapolation.

Experimental media selection varies widely across studies, reflecting the diverse nature of aquifer materials. Clean quartz sand represents the most commonly utilized medium due to its well-defined properties and commercial availability (Mitrano et al., 2019). However, more complex media incorporating natural sediments, clay minerals, and organic matter have been increasingly employed to better approximate field conditions. The characterization of media properties, including grain size distribution, porosity, hydraulic conductivity, and surface charge characteristics, is essential for meaningful interpretation of experimental results.

Microplastic particles used in transport experiments typically include both commercial reference materials and environmentally extracted particles (Waldschläger et al., 2020). Commercial materials offer advantages including well-defined size distributions, polymer compositions, and surface properties, facilitating controlled parameter investigation. Environmentally extracted particles, while more representative of field conditions, present challenges in characterization and standardization (Enfrin et al., 2019). The selection of microplastic types, sizes, and concentrations for experimental studies represents a critical consideration, with implications for environmental relevance and mechanistic understanding.

2.3.2 Flow Conditions and Transport Dynamics

Experimental studies have investigated microplastic transport under varying flow conditions to simulate diverse groundwater environments. Flow rates typically range from slow Darcy velocities representative of natural gradient conditions to accelerated flows simulating near-well environments or preferential flow paths (Xu et al., 2018). The establishment of steady-state flow conditions prior to particle introduction represents standard practice, though some studies have explored transient flow effects to simulate recharge events or pumping influences.

Breakthrough curve analysis serves as the primary method for characterizing transport dynamics, with particle concentrations monitored in column effluent over time (Wang et al., 2020). Early breakthrough relative to conservative tracers has been observed for some microplastic types, potentially indicating size exclusion effects where particles are restricted from smaller pores and thus travel preferentially through larger flow channels (Bradford et

al., 2013).Retention profiles, determined through destructive sampling of experimental columns, provide complementary information on spatial deposition patterns.

Transport experiments have demonstrated complex dependencies on particle properties, with size, shape, density, and surface characteristics all influencing mobility (Waldschläger & Schüttrumpf, 2020). Smaller particles generally demonstrate enhanced transport through porous media, though particles below a certain threshold may experience increased deposition due to diffusive transport to collector surfaces (Mitrano et al., 2021). Non-spherical particles, particularly fibers, exhibit distinctive transport behaviours characterized by complex orientation effects and mechanical straining.

2.3.3 Particle-Media Interactions

The interactions between microplastic particles and porous media surfaces fundamentally control transport and retention behaviours. Attachment processes, where particles adhere to media surfaces, represent a primary retention mechanism controlled by surface chemistry, electrostatic interactions, and van der Waals forces . The DLVO theory (Derjaguin, Landau, Verwey, and Overbeek) provides a theoretical framework for understanding these interactions, though non-DLVO forces including hydrophobic interactions and steric effects also significantly influence attachment behaviours.

Straining processes, where particles become physically trapped in pore throats or constrictions, constitute another critical retention mechanism particularly relevant for larger particles and in fine-grained media . The ratio of particle diameter to median grain size (dp/d50) serves as an important parameter for predicting straining potential, with values above approximately 0.05 associated with increased straining likelihood (Tufenkji & Elimelech, 2004).

Ripening and blocking effects, where retained particles influence subsequent deposition, have been observed in some experimental systems . Ripening occurs when retained particles create favourable attachment sites for incoming particles, potentially accelerating deposition rates over time. Conversely, blocking effects emerge when attached particles shield collector surfaces from subsequent deposition, potentially decreasing retention rates.

2.3.4 Chemical and Physicochemical Modifiers

Experimental studies have demonstrated that solution chemistry substantially modifies microplastic transport behaviour in porous media. Ionic strength variations significantly influence attachment efficiency, with higher ionic strengths generally promoting increased deposition through electrical double layer compression (Cao et al., 2023). However, non-monotonic relationships have been observed in some systems, potentially reflecting the complex interplay between electrostatic interactions and other retention mechanisms.

Solution pH affects both particle and media surface charges, thereby modifying electrostatic interactions and attachment behaviours (Ceylan et al., 2024). The point of zero charge (PZC) for both particles and collector surfaces represents a critical parameter, with attachment typically enhanced when particle and collector surfaces carry opposite charges (Liao et al., 2025). Most microplastics exhibit negative surface charges at circumneutral pH values typical of groundwater systems, though surface weathering and adsorbed substances can substantially modify these properties.

Natural organic matter (NOM) creates complex effects on microplastic transport, potentially both enhancing and inhibiting mobility depending on specific conditions (Chen et al., 2022). NOM adsorption to microplastic surfaces typically increases negative surface charge and provides steric stabilization, enhancing mobility. However, NOM can also form bridges between particles and collectors or modify surface hydrophobicity, potentially enhancing retention under certain conditions.

2.3.5 Applicability to Natural Systems

The extrapolation of laboratory experimental results to field-scale groundwater systems presents significant challenges requiring careful consideration. Scale-dependent processes represent a primary limitation, as column experiments typically employ centimetre to meter scales that may not capture heterogeneities and preferential flow paths present at field scales (Sudhakar et al., 2008). The use of simplified, homogeneous media in many experiments fails to represent the complex, heterogeneous nature of natural aquifer materials.

Chemical simplifications in laboratory systems potentially limit field relevance, as experimental solutions typically lack the complex mixture of dissolved species, colloids, and microorganisms present in natural groundwater (Li et al., 2020). These components can

substantially modify particle surface properties and collector interactions through competitive adsorption, charge screening, and biological effects (Enfrin et al., 2020).

Despite these limitations, experimental studies provide essential mechanistic insights not readily obtainable from field investigations. Controlled parameter variation enables the isolation of individual factors influencing transport, facilitating the development of predictive models and transport theories (O'Connor et al., 2019). The complementary nature of laboratory and field approaches highlights the importance of integrated research strategies incorporating multiple investigative scales.

2.4 Numerical Modelling Approaches for Microplastic Transport

2.4.1 Advection-Dispersion and Retention Models

Numerical modelling of microplastic transport in groundwater has largely adapted approaches developed for colloid and nanoparticle transport, with modifications to account for the unique properties of microplastic particles. The advection-dispersion equation with additional terms for retention processes serves as the foundation for most modelling approaches. This framework incorporates advective transport with water flow, hydrodynamic dispersion, and various retention mechanisms including attachment, straining, and ripening effects (Simunek et al., 2003).

One-dimensional models represent the most common implementation, particularly for interpreting laboratory column experiments and developing parameter estimates (Bradford et al., 2015). These models typically employ finite difference or finite element numerical schemes to solve the governing equations, with boundary conditions defined to match experimental or field conditions (Jin et al., 2019). While computationally efficient, one-dimensional approaches fail to capture the spatial heterogeneity present in field settings.

Two- and three-dimensional models enable more realistic representation of field-scale transport, incorporating spatial variations in hydraulic properties, flow fields, and retention parameters (Praetorius et al., 2012). These approaches typically utilize numerical codes originally developed for solute transport, modified to incorporate particle-specific processes. The computational requirements for these models increase substantially with dimension and resolution, creating practical limitations for highly detailed simulations.

2.4.2 DLVO and Filtration Theory Applications

Theoretical frameworks from colloid science, including DLVO theory and filtration theory, have been adapted to inform microplastic transport modelling. DLVO theory calculates interaction energies between particles and collector surfaces based on van der Waals attraction and electrostatic repulsion, providing a theoretical basis for attachment probability calculations (Tufenkji & Elimelech, 2005). Extended DLVO approaches incorporate additional interactions including hydrophobic effects, steric interactions, and Lewis's acid-base forces, potentially improving predictive capability for complex microplastic-media systems.

Colloid filtration theory (CFT) provides a mechanistic framework for predicting particle deposition rates based on transport to collector surfaces and attachment efficiency (Molnar et al., 2015). Transport mechanisms include interception, gravitational sedimentation, and Brownian diffusion, with relative importance varying by particle size and flow conditions. Attachment efficiency parameters derived from DLVO calculations or experimental measurements connect theoretical interaction energies to observable retention behaviour.

Modified filtration approaches incorporating additional retention mechanisms have been developed to address limitations in classical CFT for environmental particles (Bradford et al., 2012). These modifications include straining terms, ripening and blocking functions, and depth-dependent retention parameters. While promising, these approaches remain limited by parameter estimation challenges and the complex, heterogeneous nature of environmental microplastics (Bradford et al., 2013) .

2.4.3 Machine Learning and AI-Based Models

Emerging machine learning and artificial intelligence approaches represent novel modelling strategies for microplastic transport prediction. These data-driven methods utilize computational algorithms to identify patterns and relationships within existing datasets, potentially capturing complex, non-linear behaviours difficult to represent in traditional mechanistic models(Reichstein et al., 2019). Neural networks, support vector machines, and random forest algorithms have demonstrated particular promise for environmental transport applications.

The primary advantage of machine learning approaches lies in their ability to incorporate multiple influencing factors without requiring explicit mechanistic understanding. This capability proves particularly valuable for microplastic transport, where numerous particle properties, environmental conditions, and media characteristics simultaneously influence behaviour. Additionally, these methods can potentially integrate diverse data sources including laboratory experiments, field observations, and remote sensing information.

However, significant limitations constrain current machine learning applications for microplastic transport. The relatively limited availability of comprehensive datasets for model training represents a primary challenge, particularly given the wide parameter space relevant to microplastic transport (Zhong et al., 2021). Model interpretability remains problematic, with many approaches functioning as "black boxes" that provide predictions without mechanistic insights. Despite these limitations, hybrid approaches combining mechanistic understanding with data-driven methods show promise for future modelling efforts.

2.4.4 Validation Strategies and Limitations

Model validation represents a critical challenge for microplastic transport simulations, with strategies varying according to modelling scale and purpose. Laboratory-scale models typically undergo validation against controlled column experiments, with breakthrough curves and retention profiles providing quantitative comparison metrics (Xu et al., 2019). This approach enables detailed parameter calibration but may not adequately represent field-scale processes and heterogeneities.

Field-scale validation employs comparison between model predictions and observed microplastic distributions in groundwater systems (Mai et al., 2019). This approach faces substantial challenges including limited field data availability, spatial and temporal sampling constraints, and analytical uncertainties in microplastic quantification. Innovative approaches utilizing environmental tracers or analogue particles with similar transport behaviours may provide alternative validation strategies where direct microplastic measurements are limited.

Fundamental limitations constrain current modelling capabilities regardless of validation approach. Parameter uncertainty represents a primary limitation, with many critical

parameters including attachment efficiencies, straining coefficients, and detachment rates difficult to measure or estimate for environmental systems . The heterogeneous nature of both microplastic particles and groundwater systems creates additional complexity difficult to capture in current modelling frameworks.

2.5 Research Gaps

2.5.1 Long-Term Fate and Persistence

The long-term fate and persistence of microplastics in groundwater systems remain poorly understood, representing a critical knowledge gap. While laboratory studies provide insights into short-term transport and retention behaviours, the multi-decade to century timescales relevant to plastic persistence exceed current experimental timeframes (Gewert et al., 2015). The potential for continued fragmentation of retained particles into smaller size fractions, including nanoplastics, represents a particular concern given the enhanced mobility and potential toxicity of smaller particles.

Aging processes affecting microplastics in groundwater environments, including photodegradation, biodegradation, and chemical transformation, require substantial additional investigation (Lambert & Wagner, 2016). The subsurface environment, characterized by limited light exposure, reduced oxygen availability, and distinctive microbial communities, likely creates degradation patterns distinct from surface environments. The transformation of polymer additives and sorbed contaminants during long-term residence in groundwater presents additional uncertainties with potential implications for risk assessment and management.

2.5.2 Source Attribution and Pathway Quantification

The quantitative attribution of groundwater microplastic contamination to specific sources and pathways represents a significant research need. Current understanding relies primarily on qualitative assessments based on particle characteristics and proximity to potential sources (Dris et al., 2018). Polymer type provides some indication of source, but the ubiquitous nature of many plastic types of limits specificity. Particle shape and size offer additional clues, with fibers typically associated with textile sources and fragments with degraded plastic waste, though considerable overlap exists between source signatures (Zhang et al., 2021).

The development of more specific source tracking methodologies represents an important research direction. Chemical tracers associated with specific plastic formulations or applications could potentially provide enhanced source discrimination (Rochman et al., 2019). The application of isotopic analysis techniques, successfully employed for other contaminants, may offer additional source attribution capabilities, though methodological development remains limited (Zhu et al., 2018).

Pathway quantification presents similar challenges, with limited understanding of the relative contributions of different transport routes including surface infiltration, artificial recharge, surface water-groundwater interaction, and direct subsurface releases (Mintenig et al., 2019). The development of integrated monitoring networks spanning surface water, soil, and groundwater compartments represents a potential approach for improved pathway characterization.

2.5.3 Methodological Standardisation

The lack of standardized methodologies for sampling, processing, and analysing microplastics in groundwater represents a fundamental limitation for research advancement and regulatory development. Current studies employ diverse approaches, creating substantial challenges for data comparison, meta-analysis, and comprehensive risk assessment (Koelmans et al., 2020). Sampling protocols vary widely in terms of volume, filtration approach, and quality assurance measures, potentially creating systematic biases between studies (Stock et al., 2019).

Analytical methodologies demonstrate similar diversity, with variations in extraction procedures, detection techniques, size limitations, and reporting metrics (Primpke et al., 2020). The lack of certified reference materials specifically designed for groundwater microplastic analysis further complicates method validation and inter-laboratory comparison (Felsing et al., 2018). The development of standardized protocols through international standardization bodies, scientific societies, and regulatory agencies represents an essential step toward more cohesive and comparable research outcomes.

2.5.4 Detection Technology Limitations

Current analytical technologies for microplastic identification and characterization face significant limitations, particularly for smaller size fractions most relevant to groundwater transport. Visual identification methods, including stereomicroscopy, become increasingly unreliable below approximately 500 μm, creating substantial uncertainty for smaller particles (Hidalgo-Ruz et al., 2012). Spectroscopic methods including FTIR and Raman provide polymer-specific identification but face resolution limitations, with conventional micro-FTIR limited to particles larger than approximately 20 μm (Käppler et al., 2016).

The analysis of environmentally relevant size fractions, particularly particles below 10 μm, requires advanced methodologies including Raman microscopy and field-flow fractionation coupled with spectroscopic detection (Mintenig et al., 2018). These approaches remain specialized, time-intensive, and not widely available to most research groups, creating a significant technological barrier (Primpke et al., 2019). The detection and characterization of nanoplastics (< 1 μm) in groundwater presents even greater challenges, with current methodologies largely inadequate for environmental concentrations (Gigault et al., 2018).

Automated analysis systems represent an important technological development, potentially increasing sample throughput while reducing operator bias (Primpke et al., 2017). Machine learning approaches for spectral interpretation and particle classification show particular promise but require substantial reference datasets for algorithm training (Wander et al., 2020). The integration of multiple complementary analytical techniques represents a promising strategy for addressing current detection limitations.

2.5.5 Transport Mechanism Uncertainties

Fundamental uncertainties persist regarding the mechanisms controlling microplastic transport and retention in groundwater systems. While filtration theory provides a theoretical framework for particle deposition, its application to irregularly shaped, polydisperse, and chemically complex microplastics presents significant challenges. The relative importance of various retention mechanisms including attachment, straining, and ripening varies with particle and system properties in ways not fully captured by current models.

The influence of particle characteristics on transport behaviour requires additional investigation, particularly for environmentally weathered microplastics with complex

surface properties (Rummel et al., 2017). The distinctive transport behaviours of non-spherical particles, particularly fibers with high aspect ratios, remain poorly understood despite their environmental prevalence (Waldschläger & Schüttrumpf, 2019). Size-dependent transport phenomena, especially for smaller microplastics approaching colloid size ranges, represent an additional area of uncertainty with significant implications for risk assessment.

Scaling relationships between laboratory observations and field-scale transport represent a critical knowledge gap (Koelmans et al., 2018). The influence of aquifer heterogeneity, preferential flow paths, and transient flow conditions on microplastic transport requires substantial additional research to develop predictive understanding applicable to diverse hydrogeological settings.

2.5.6 Climate Change Interactions

The potential interactions between climate change and microplastic transport in groundwater systems remain largely unexplored despite their potential significance. Altered precipitation patterns may modify recharge dynamics and associated microplastic transport, with increased extreme precipitation events potentially enhancing particle mobilization and infiltration (Allen et al., 2019). Conversely, drought conditions may concentrate contaminants and modify groundwater chemistry in ways that influence particle stability and transport.

Temperature increases may modify microplastic properties through enhanced degradation rates, potentially accelerating fragmentation into smaller, more mobile particles (Romera-Castillo et al., 2018). Altered groundwater chemistry resulting from climate-induced changes in water-rock interactions, redox conditions, or saline intrusion may influence particle surface properties and attachment behaviours (Galloway et al., 2017). Additionally, climate adaptation measures including increased groundwater extraction, artificial recharge, and land use changes may create secondary effects on microplastic transport and distribution.

Research integrating climate projections with microplastic transport models represents an important future direction, potentially providing insights into long-term contamination trajectories and identifying vulnerable aquifer systems. The development of monitoring

networks specifically designed to detect climate-microplastic interactions would provide essential observational data to complement modelling approaches.

The ecological and human health implications of microplastic contamination in groundwater systems remain poorly characterized, creating substantial uncertainty for risk assessment and

2.5.7 Ecological and Human Health Impacts

management. Groundwater ecosystems, including diverse microbial communities and specialized invertebrate fauna, may experience direct exposure to microplastic particles with potential consequences for community structure and ecological function (Griebler & Avramov, 2015). These potential impacts remain largely unexplored despite the ecological significance of groundwater systems and their contribution to broader ecosystem services.

Human exposure through groundwater-sourced drinking water presents additional concerns, particularly for smaller particles potentially capable of translocation within organisms (Wright & Kelly, 2017). The contribution of groundwater-derived microplastics to total human exposure remains unquantified, limiting comprehensive risk assessment (Koelmans et al., 2019). Additionally, the potential for microplastics to serve as vectors for other groundwater contaminants, including sorbed organic compounds and heavy metals, represents an emerging concern requiring further investigation (Hartmann et al., 2019).

Research integrating groundwater occurrence data with ecotoxicological and human health studies represents an essential step toward comprehensive risk characterization. The development of biomonitoring approaches specific to groundwater-derived microplastics would provide valuable exposure data to complement occurrence studies and toxicological assessments.

2.5.8 Remediation and Monitoring Challenges

The remediation of microplastic-contaminated groundwater presents substantial technological and practical challenges that remain largely unaddressed in current research. Conventional groundwater remediation approaches including pump-and-treat systems may prove ineffective for microplastic removal due to particle characteristics and subsurface distribution patterns (Rochman et al., 2015). Innovative treatment technologies specifically designed for microplastic removal require development and field validation, potentially

adapting approaches from water treatment including advanced filtration, adsorption, and biodegradation (Enfrin et al., 2019).

Preventive management approaches represent an important complementary strategy, focusing on source control and pathway interruption to limit future contamination (Prata et al., 2019). The development of improved plastic waste management systems, biodegradable polymer alternatives, and enhanced wastewater treatment technologies capable of microplastic removal all contribute to preventive management (Geyer et al., 2017). However, the long-term persistence of existing contamination necessitates remediation approaches for heavily impacted systems.

Monitoring program development for groundwater microplastics faces similar challenges, with questions regarding optimal spatial and temporal sampling strategies, analytical methods, and reporting metrics (Stock et al., 2020). The integration of microplastic monitoring with existing groundwater quality networks represents a practical approach, though methodological differences may necessitate specialized sampling and analysis protocols (Koelmans et al., 2019). The development of screening-level monitoring tools capable of rapid, field-based assessment would substantially enhance monitoring capabilities, though such technologies remain in early development stages.

Chapter 3 –Microplastic Fieldwork Sampling and Analysis

3.1 Study Area Description

3.1.1 Geographical and Climatic Context

Chennai, the capital of Tamil Nadu, is located on the southeastern coast of India at 13.04°N and 80.17°E, in the northeastern part of the state. The study area covers the metropolitan region between 12.97714°N and 13.14286°N latitude and 80.23132°E and 80.29166°E longitude, corresponding to the spatial distribution of the groundwater sampling locations. The city is situated on the Eastern Coastal Plains and is characterized by a gentle topographic gradient with an average elevation of about 6 m above mean sea level, locally increasing to around 60 m in the western sectors, which together with the coastal setting exerts a strong control on groundwater flow and contaminant migration pathways .

The climate is classified as tropical wet and dry (Aw) under the Köppen system, with distinct wet and dry seasons and relatively modest annual temperature variability. Mean annual temperatures typically range from approximately 24.3 °C to 32.9 °C, although more extreme values have been recorded during exceptional events, and relative humidity commonly lies between about 65% and 84%.These persistently warm and humid conditions, combined with strong solar radiation, can favour physical and chemical weathering of plastic debris, which may in turn contribute to the generation of microplastics in the urban environment.

The hydrological regime is strongly seasonal and dominated by the northeast monsoon, which usually occurs from October to December and supplies most of the annual rainfall . Average annual precipitation is on the order of 1,200 mm, but pronounced interannual variability has been documented, including years with substantially higher totals, reflecting the influence of cyclonic systems in the Bay of Bengal . Rainfall is often delivered in short, high-intensity events that generate episodic runoff capable of mobilising accumulated surface debris, including plastics, into the drainage network, whereas the contribution from the southwest monsoon is generally limited and summer rainfall is typically negligible . Extended dry periods between monsoon seasons allow plastic items to undergo photodegradation and mechanical weathering on exposed surfaces, which may influence the timing and characteristics of microplastic release during subsequent storm events .

3.1.2 Geological and Geomorphological Features

The geological framework of Chennai comprises a suite of sedimentary formations dominated by clay, shale and sandstone, underlain locally by crystalline basement rocks, resulting in a heterogeneous subsurface that influences groundwater flow patterns and contaminant transport. On

the basis of lithology and hydrogeological behaviour, three main zones are commonly distinguished: sandy areas, clayey regions and hard-rock terrains . This heterogeneity creates spatially variable pathways and storage domains for water and contaminants, including microplastics, within the subsurface.

Sandy zones are mainly distributed along riverbanks and the coastal fringe, including neighbourhoods such as Tiruvanmiyur, Adyar, Kottivakkam, Santhome, George Town and Tondiarpet. These areas are characterised by relatively high infiltration rates, so that rainfall and runoff can percolate rapidly through the permeable matrix, favouring vertical migration of dissolved and particulate contaminants from the surface into shallow groundwater. Experimental work indicates that microplastic particles, particularly in the fine size range (e.g., <300 μm), can migrate through sandy sediments with relatively high hydraulic conductivities, with transport influenced by preferential flow paths and macroporosity (Weber et al., 2021). Consequently, sandy sectors adjacent to rivers and the coast may act as relatively vulnerable zones for microplastic transfer from surface sources to groundwater.

Clayey regions are widespread across the metropolitan area, including areas such as T. Nagar, West Mambalam, Anna Nagar, Perambur and Virugambakkam. These settings generally exhibit lower vertical permeability but higher water-retention capacity, favouring the accumulation of water and contaminants in the vadose zone and promoting lateral flow along preferential pathways during intense rainfall events . Laboratory studies suggest that clay minerals can interact with microplastic particles via electrostatic attraction and surface adsorption, which may retard vertical transport and create temporary near-surface reservoirs of microplastics that can be remobilised during high-magnitude recharge episodes (Wan et al., 2019). Such delayed-release behaviour could contribute to pulses of microplastic transport during extreme rainfall.

Hard-rock terrains occur locally in areas such as Guindy, Velachery, Adambakkam and parts of Saidapet, where crystalline basement rocks outcrop or are present at shallow depth. In these domains, groundwater occurrence and movement are governed primarily by secondary porosity features, including fractures, joints and weathered zones, resulting in anisotropic and heterogeneous flow conditions . Research on microplastic transport in fractured media remains limited, but conceptual models suggest that elongated particles such as fibres may experience either relatively efficient advection along connected fractures or physical retention at constrictions, depending on the relationship between particle size, shape and fracture aperture .

The geomorphological evolution of the Chennai region reflects the combined influence of fluvial, marine and tectonic processes, producing a landscape that includes coastal plains, beach ridges,

fluvial terraces and other marine-influenced landforms . Neo-tectonic activity and phases of marine transgression and regression have shaped the present-day topography and sediment distribution, while the overall gentle eastward slope of the coastal plain directs both surface drainage and groundwater flow towards the Bay of Bengal. This large-scale gradient provides a general pathway for land-derived contaminants, including microplastics, to move from inland recharge areas towards coastal discharge zones via surface and subsurface routes.

3.1.3 Hydroclimatic Conditions and Drainage Systems

The hydroclimatic regime of Chennai is marked by strong seasonality, with the northeast monsoon (October–December) typically contributing around 60–80% of the annual rainfall through intense storm events. These concentrated rainfall periods generate episodic high-magnitude runoff that can mobilise debris accumulated on urban surfaces and transport it into the drainage network, whereas intervening dry intervals favour accumulation and weathering of materials at the surface (Li et al., 2020). During major storm events, surface runoff may locally infiltrate in more permeable zones, representing a potential pathway for microplastic transfer from surface water to shallow groundwater systems, especially where soil cover is thin or highly permeable (He et al., 2020).

The city's drainage system is structured around two principal rivers, the Adyar and the Coovum, which traverse the metropolitan area before discharging into the Bay of Bengal. The Adyar River originates near the Chembarambakkam tank and flows eastwards for roughly 42 km through a catchment of about 800 km² before entering the sea (Veerasingam et al., 2016). Its flow is sustained by a combination of monsoon runoff, baseflow and urban discharges, and in its lower reaches tidal influence can extend several kilometres inland, creating an estuarine zone where salinity gradients and hydrodynamic mixing affect the behaviour, aggregation and settling of particulate contaminants, including microplastics (Veerasingam et al., 2016).

The Coovum River flows through the central urban corridor and is heavily impacted by wastewater and urban runoff inputs, with severely degraded water quality and a predominantly intermittent flow regime, particularly outside the monsoon period. Under low-flow conditions, contaminants, including plastic particles, can accumulate in channel sediments and banks, and may be remobilised during subsequent high-flow events associated with monsoon storms, producing pulses of downstream transport that can coincide with periods of enhanced recharge and bank infiltration.

Additional drainage elements such as the Otteri Nulla and the Buckingham Canal contribute to the overall connectivity of the urban hydrological network. The Buckingham Canal, an artificial waterway running parallel to the coast, now functions largely as a conduit for wastewater, while the

extensive beach system along the Chennai coast, including Marina Beach, forms an important interface between terrestrial and marine zones where microplastics from riverine, urban and marine sources can accumulate (Dowarah & Devipriya, 2019). Together, these surface water bodies and coastal features create multiple pathways and temporary storage zones for microplastics within the urban environment.

3.1.4 Implications for Groundwater Vulnerability and Microplastic Transport

The combination of geological, geomorphological and hydroclimatic characteristics in Chennai gives rise to spatially variable groundwater vulnerability to microplastic contamination. Areas with highly permeable sandy deposits and shallow water tables, particularly along river corridors and in coastal fringe zones, are likely to be more susceptible to downward migration of microplastics from surface sources, whereas clay-rich and hard-rock areas may exhibit more complex patterns of storage and delayed release (Panno et al., 2019; Weber et al., 2021). Sandy riverbank and coastal sectors may therefore act as key zones of concern for vertical infiltration, with relatively limited filtration potential for small particles.

Seasonal monsoon dynamics introduce an important temporal component, as intense rainfall episodes can mobilise plastic debris from urban surfaces and channelise it into drains and rivers, from which it may infiltrate into adjacent aquifers, particularly in hydraulically connected alluvial zones (He et al., 2020; Frei et al., 2019). In the present study, this seasonal influence is reflected in the observed increase in total microplastic counts in groundwater samples from 249 particles in the pre-monsoon campaign to 387 particles in the post-monsoon campaign across the sampled wells, corresponding to an approximate increase of 55.4%. These values indicate modest but detectable changes in groundwater microplastic abundance following monsoon conditions, consistent with the role of storm-driven mobilisation and recharge processes.

Rivers and associated alluvial aquifers can function as important pathways for microplastic transport and exchange between surface water and groundwater, particularly where bank infiltration and induced recharge occur. Studies in other urban settings have reported elevated microplastic concentrations in groundwater wells hydraulically connected to contaminated surface waters, highlighting the potential for river corridors to act as conduits for subsurface contamination (Frei et al., 2019; Panno et al., 2019). In Chennai, sandy alluvial stretches along the Adyar and Coovum rivers may therefore represent critical zones for surface–groundwater microplastic linkages.

Tidal influence in the lower reaches of the Adyar and Coovum adds further complexity, as oscillating water levels and changing salinity can modify the aggregation and settling behaviour of microplastics

in the estuarine zone, potentially creating localised depositional areas (Li et al., 2018; Veerasingam et al., 2016). These estuarine processes may in turn influence the concentration and characteristics of microplastics available for infiltration into nearby coastal aquifers. Superimposed on these natural controls, urbanisation modifies surface permeability, drainage patterns and contaminant loading through the expansion of impervious surfaces, altered runoff pathways and leakage from water supply and sewerage infrastructure (Rochman, 2018). The resulting interaction of natural and anthropogenic factors produces a spatially heterogeneous pattern of groundwater vulnerability to microplastic contamination, with implications for the sustainable management of urban groundwater resources in this rapidly developing coastal megacity.

3.2 Methodological Framework

This study applied a structured methodological framework to characterise microplastic contamination in urban groundwater and related surface water systems using combined spatial, temporal and analytical approaches (Koelmans et al., 2019; Stock et al., 2019). The framework included clearly defined procedures for sampling, analysis and quality control to obtain reproducible and comparable data on microplastics in the Chennai metropolitan area.

The approach was organised into three main phases. The first phase focused on spatial characterisation through sampling across contrasting hydrogeological settings to examine how geology, hydrological connectivity and land use relate to microplastic occurrence (Panno et al., 2019). The second phase evaluated temporal variability using pre- and post-monsoon campaigns to assess how seasonal hydrology influences microplastic mobilisation and redistribution (He et al., 2020). The third phase comprised laboratory analysis using microscopy and Fourier-transform infrared (FTIR) spectroscopy to identify microplastics, determine polymer types and describe particle morphology in support of environmental interpretation (Primpke et al., 2018).

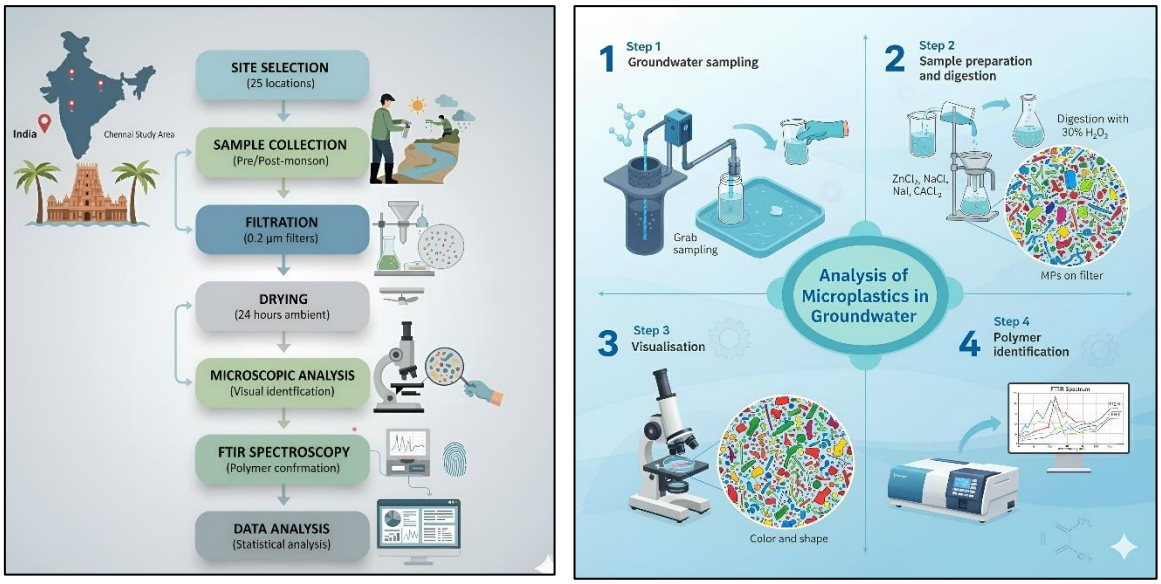

Figure 3.1: Methodological Framework for Microplastic Analysis in Groundwater Systems Flowchart illustrating the sequential analytical workflow: "Groundwater sampling → Sample preparation and digestion → Visualisation → Polymer Identification → Analysis of Microplastics in Groundwater"

Environmental characterisation combined geological zonation into sandy, clayey and hard-rock areas, mapping of surface water–groundwater interactions, and documentation of urban settings and infrastructure that may influence plastic inputs (Weber et al., 2021). Sampling protocols followed established guidelines for avoiding contamination and maintaining sample integrity and were applied consistently in both seasonal campaigns (Hermsen et al., 2018).

Microplastic analysis involved visual inspection under a microscope using predefined morphological criteria, followed by FTIR spectroscopy for chemical confirmation of a subset of particles to reduce the risk of misidentifying non-plastic material (Jung et al., 2018; Käppler et al., 2016). Data analysis included basic spatial and temporal comparisons and exploration of relationships with environmental variables using standard statistical methods such as paired comparisons and correlation analysis (Veerasingam et al., 2016).

Quality assurance and quality control measures were implemented throughout, including procedural blanks, documentation of potential contamination sources, and recovery tests using reference microplastics to evaluate method performance (Brander et al., 2020; Mintenig et al., 2019). These measures were intended to support the reliability of the dataset and allow comparison with other microplastic studies and emerging international guidance (Hartmann et al., 2019)

3.3 Field Sampling Protocols

3.3.1 Sampling Campaign Design and Objectives

The field sampling programme was designed to examine spatial and seasonal patterns of microplastic contamination in groundwater and associated surface water in Chennai. A two-stage approach was used, consisting of an initial reconnaissance survey and a subsequent seasonal comparison (Koelmans et al., 2019).

The preliminary survey established baseline conditions and tested field protocols, including sample volumes and handling procedures, while providing an overview of spatial heterogeneity in microplastic occurrence (Stock et al., 2019). This phase included 25 groundwater sampling locations (open dug wells and handpump-equipped bore wells) distributed across the study area between 12.97714°N and 13.14286°N latitude and 80.23132°E and 80.29166°E longitude.

The main seasonal study comprised two campaigns: a pre-monsoon survey in August 2024 and a post-monsoon survey in February 2025, selected to represent typical dry-season and post-northeast-monsoon conditions (Santana et al., 2020). Using the same set of sampling locations in both periods allowed direct comparison of microplastic abundances and characteristics under contrasting hydrological conditions. The specific objectives were to describe spatial patterns across different hydrogeological settings, evaluate pre- to post-monsoon changes, and explore relationships between microplastic occurrence and selected environmental parameters.

3.3.2 Site Selection and Sample Types

Sampling sites were selected to cover a range of hydrogeological conditions and urban settings within the Chennai metropolitan area. The network extended across the same coordinate range as the overall study area and included both densely built-up zones and more peripheral areas with differing levels of human activity .

Site selection considered four main aspects: (1) geology, with wells placed in sandy, clayey and hard-rock zones; (2) hydrological connectivity, including locations along likely flow paths and near major drainage features; (3) land use, covering residential, commercial, industrial and recreational areas; and (4) practical accessibility for repeated sampling (Wang et al., 2018).

Groundwater sampling included open dug wells, representing shallow unconfined aquifers, and handpump-equipped bore wells, representing deeper confined or semi-confined aquifers, to assess possible depth-related differences in microplastic occurrence (Mintenig et al., 2019). Several sites

were located close to the Adyar and Coovum river corridors to provide information on potential surface water–groundwater linkages.

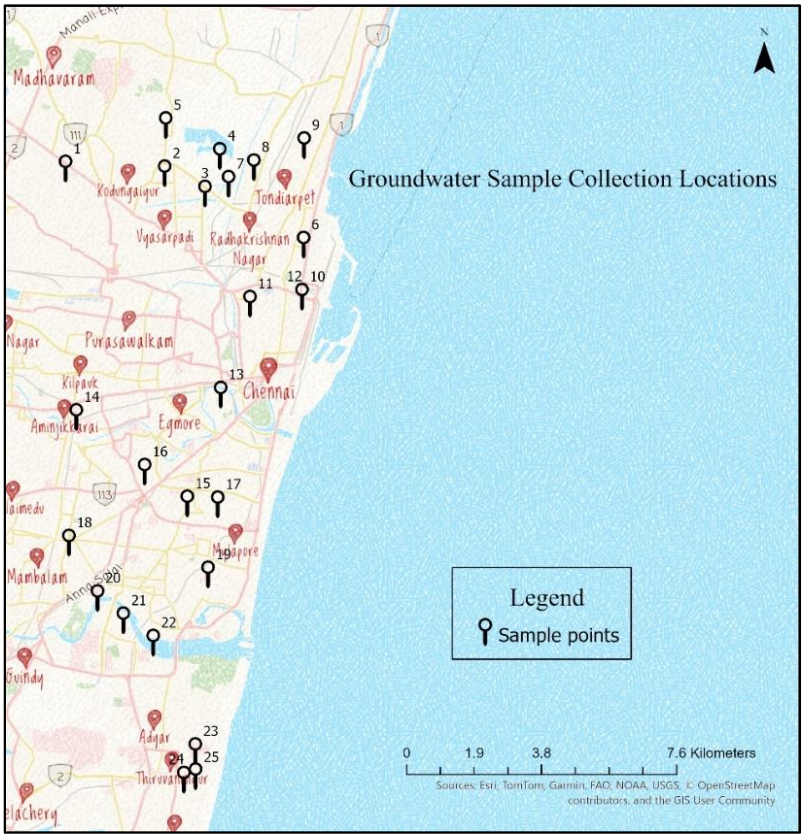

Figure 3.2: Location map of Chennai metropolitan area showing the 25 microplastic sampling sites distributed across sandy, clayey, and hard rock geological zones with major drainage features (Adyar and Coovum rivers) and coordinates ranging from 12.97714°N to 13.14286°N latitude and 80.23132°E to 80.29166°E longitude.

3.3.3 Sample Collection Procedures and Volumes

Sampling procedures were designed to obtain representative water samples while minimising contamination. All containers and equipment were cleaned before use, and borosilicate glass bottles were used for sample collection to avoid plastic artefacts, with amber glass used when light protection was required (Koelmans et al., 2019). Bottles were rinsed with filtered deionised water and then with sample water immediately prior to filling (Stock et al., 2019).

For groundwater, typical sample volumes were 1–2 L per site, selected as a compromise between achieving sufficient particle counts and maintaining feasible filtration and processing times (Prata et al., 2019). Larger volumes were collected from deeper wells where lower particle concentrations were expected, and smaller volumes from shallow wells where higher concentrations were anticipated.

Open dug wells were sampled after purging a small volume to reduce the influence of stagnant water. Samples were taken from the mid-water column using a stainless-steel sampler to avoid both surface films and bottom sediment disturbance (Liu et al., 2019). For handpump wells, water was pumped for a short period before sampling, and water was collected directly into glass bottles while avoiding contact with plastic components as far as practicable. Each sample received a unique alphanumeric identifier including site code, date and season (pre- or post-monsoon), and field sheets recorded basic site conditions and nearby potential sources.

3.3.4 Sample Preservation Protocols and Holding Time Management

After collection, samples were handled using a standardised preservation protocol to limit biological and chemical changes before laboratory processing. Samples were stored in coolers at approximately 4 ± 2 °C during transport and then kept refrigerated in the laboratory until analysis.

For most samples, analysis was completed within 72 hours to reduce the risk of biofilm formation or matrix alteration. When longer storage was necessary, analytical-grade sodium azide (NaN_3) was added at 0.1% (1 mL per litre of sample) as a biocide, using glass pipettes to avoid introducing additional plastic material. Preserved samples were stored refrigerated and analysed within 30 days, in accordance with internal validation tests using spiked microplastic samples.

Before processing, sample containers were inspected for signs of leakage or damage, and any compromised samples were excluded from subsequent analysis and documented accordingly.

3.4 Laboratory Analysis of Microplastics

3.4.1 Sample Preparation and Contamination Control

Laboratory procedures were designed to minimise secondary contamination and support reliable identification of microplastics, in line with published quality-control recommendations (Wesch et al., 2017; Hermsen et al., 2018). Contact with plastic materials was avoided as far as practicable, and potential contamination sources were monitored using procedural blanks.

Personnel wore cotton laboratory coats and nitrile gloves during all sample handling, and gloves were changed regularly to limit cross-contamination from fibres or skin contact (Woodall et al., 2015; Hermsen et al., 2018). Sample processing took place in a designated clean area; work surfaces and equipment were routinely cleaned and covered when not in use, and sample containers were kept closed except during active handling (Dehaut et al., 2019).

Glass and metal equipment were preferred over plastic wherever possible. Glassware was washed and rinsed with filtered water before use, and any unavoidable plastic components (e.g. instrument internals) were noted and checked via blank samples (Lusher et al., 2017). Transfers between containers were carried out with glass pipettes or stainless-steel tools, and the number of handling steps was kept to a minimum to reduce contamination risk.

3.4.2 Filtration and Drying Procedures

Water samples were filtered to concentrate particulate material prior to microscopic examination. Filtration was performed using glass vacuum filtration units and cellulose-based filters with pore sizes in the low-micrometre range, selected as a compromise between retaining small particles and maintaining manageable filtration times (Mintenig et al., 2019; Prata et al., 2019). For more turbid samples, a coarser pre-filter was used before final filtration through finer filters to reduce clogging.

After filtration, filters were transferred to covered glass petri dishes using metal forceps and allowed to dry at room temperature in a protected area to avoid thermal alteration of plastics and to limit airborne contamination (Horton et al., 2017; Prata et al., 2019). Dried filters remained sealed until microscopic analysis.

3.4.3 Microscopic Identification and Morphological Classification

Dried filters were examined under a stereomicroscope at suitable magnifications to locate and count suspected microplastic particles (Hidalgo-Ruz et al., 2012). The entire filter area was scanned systematically, and suspected particles were evaluated using common diagnostic criteria, including

absence of obvious biological structures, uniformity of colour and thickness, and characteristic shapes such as fibres, fragments and films.

Particles were classified by shape (e.g. fibre, fragment, film, bead), colour and size class using calibrated measurement tools, and care was taken to distinguish synthetic fibres from natural fibres based on morphology (Browne et al., 2011). A subset of visually identified particles was retained for spectroscopic confirmation.

3.4.4 FTIR Spectroscopy and Polymer Characterization

Fourier transform infrared (FTIR) spectroscopy was used to confirm polymer identity for selected particles and to characterise the dominant polymer types present in the samples (Primpke et al., 2018; Käppler et al., 2018). Analyses were performed in attenuated total reflectance (ATR) mode over the mid-infrared range, and measured spectra were compared with reference libraries to assign polymer types.

The spectroscopic results indicated a mixture of common polymers, including nylon, polyethylene, polypropylene, polystyrene and others typically associated with textiles, packaging and general urban plastic use (Karthik et al., 2018). Some particles showed spectral features consistent with environmental weathering, such as changes in band intensities or the appearance of additional bands associated with oxidation, which may reflect longer residence or exposure in the environment.

3.5 Quality Assurance and Quality Control (QA/QC)

3.5.1 Contamination Prevention and Clean Lab Practices

Quality assurance and quality control were integrated throughout the sampling and analytical workflow to reduce contamination and support reliable microplastic counts (Koelmans et al., 2019; Hermsen et al., 2018). In addition to the contamination-control measures described in Section 3.4, further steps included regular cleaning of work areas, use of filtered reagents and rinsing water, and restricting sample handling to designated spaces.

Field blanks, procedural blanks and laboratory blanks were processed alongside environmental samples to quantify contamination introduced during sampling, transport and laboratory analysis (Hermsen et al., 2018; Hartmann et al., 2019). Blank filters were examined under the same conditions as samples, and contamination levels were generally low, dominated by a small number of fibres consistent with airborne input. Average blank counts were subtracted from sample counts to obtain blank-corrected values, and blank data were used to support estimates of detection and quantification limits (Brander et al., 2020; Koelmans et al., 2019).

3.5.2 Equipment Calibration and Sample Handling Consistency

Instrument performance and sample handling were standardised to minimise analytical variability. Microscope magnification and measurement scales were checked periodically with stage micrometres, and basic illumination conditions were kept constant to support consistent visual assessment (Primpke et al., 2017).

The FTIR spectrometer was routinely verified using polymer reference standards to check wavenumber accuracy and spectral quality; background spectra were recorded regularly, and the ATR crystal was cleaned between samples to avoid carry-over (Löder & Gerdts, 2015). All analytical steps followed written standard operating procedures, and analysts were trained on reference and test samples before processing environmental samples (Stock et al., 2019; Hermsen et al., 2018).

3.5.3 Validation of Visual and Spectroscopic Techniques

Visual identification procedures were checked by having more than one analyst classify a subset of filters and then harmonising criteria where discrepancies occurred (Hidalgo-Ruz et al., 2012). Agreement between analysts improved after training and use of internal visual guides, helping to reduce subjectivity in microscopic classification (Lusher et al., 2017).

A proportion of particles classified as microplastics by microscopy was analysed by FTIR to verify polymer identity and evaluate the accuracy of visual classification (Käppler et al., 2018; Primpke et al., 2018). Additional spike-recovery tests, using known quantities of reference microplastics added to selected matrices, were used to assess overall method performance and to identify any size-dependent losses (Mintenig et al., 2019).

3.5.4 Alignment with International Standards and Best Practices

The QA/QC procedures and reporting followed recommendations from recent reviews and international guidance documents on microplastic sampling and analysis, including the use of blanks, validation tests and transparent reporting of detection limits and recovery (Hartmann et al., 2019; Koelmans et al., 2019). Terminology, size classes and basic reporting formats were kept compatible with guidance from GESAMP and related monitoring protocols to facilitate comparison with other studies and datasets .

3.6 Field Investigation Results and Microplastic Contamination Patterns

3.6.1 Spatial Distribution of Microplastics in Groundwater

Microplastic contamination was detected across all 25 sampling locations, with concentrations varying from location to location. The August 2024 pre-monsoon survey yielded 249 total microplastic particles, while the February 2025 post-monsoon campaign recovered 387 particles, representing an overall 55.4% increase across the study area. Individual sample counts ranged from 5 to 19 particles in pre-monsoon conditions and 8 to 26 particles post-monsoon, reflecting spatial variability related to geology, distance to surface water bodies and proximity to urban sources (He et al., 2020; Li et al., 2020).

Pre-monsoon sampling showed clusters of higher concentrations near the Adyar and Coovum river corridors. Samples positioned along or near the Adyar River (samples 3 and 4, at 13.12552°N, 80.26658°E and 13.13504°N, 80.27032°E respectively) contained 14 particles each; sample 8 near the river mouth held 15 particles, representing the highest pre-monsoon count. Post-monsoon counts at these sites increased to 18, 19 and 22 particles respectively. Similarly, sample 19 (13.02911°N, 80.26736°E) near the Coovum River showed an increase from 14 to 17 particles. This pattern suggests that riverine zones function as important areas of microplastic concentration, possibly through hydrological focusing and surface water–groundwater exchange (Frei et al., 2019; He et al., 2020).

Groundwater samples from sandy geological zones yielded higher counts (averaging 11.2 particles pre-monsoon, 15.5 particles post-monsoon) compared to clayey zones (averaging 8.7 and 11.8 particles respectively). Hard-rock areas generally showed the lowest abundances (averaging 6.3 and 9.1 particles). This pattern aligns with the enhanced permeability of sandy sediments, which may favour infiltration of microplastics from surface sources (Weber et al., 2021; Wang et al., 2020). Samples within 500 m of major drainage features averaged approximately 32% higher counts than distant locations, consistent with the potential for surface water–groundwater linkages through bank infiltration in alluvial settings (Frei et al., 2019).

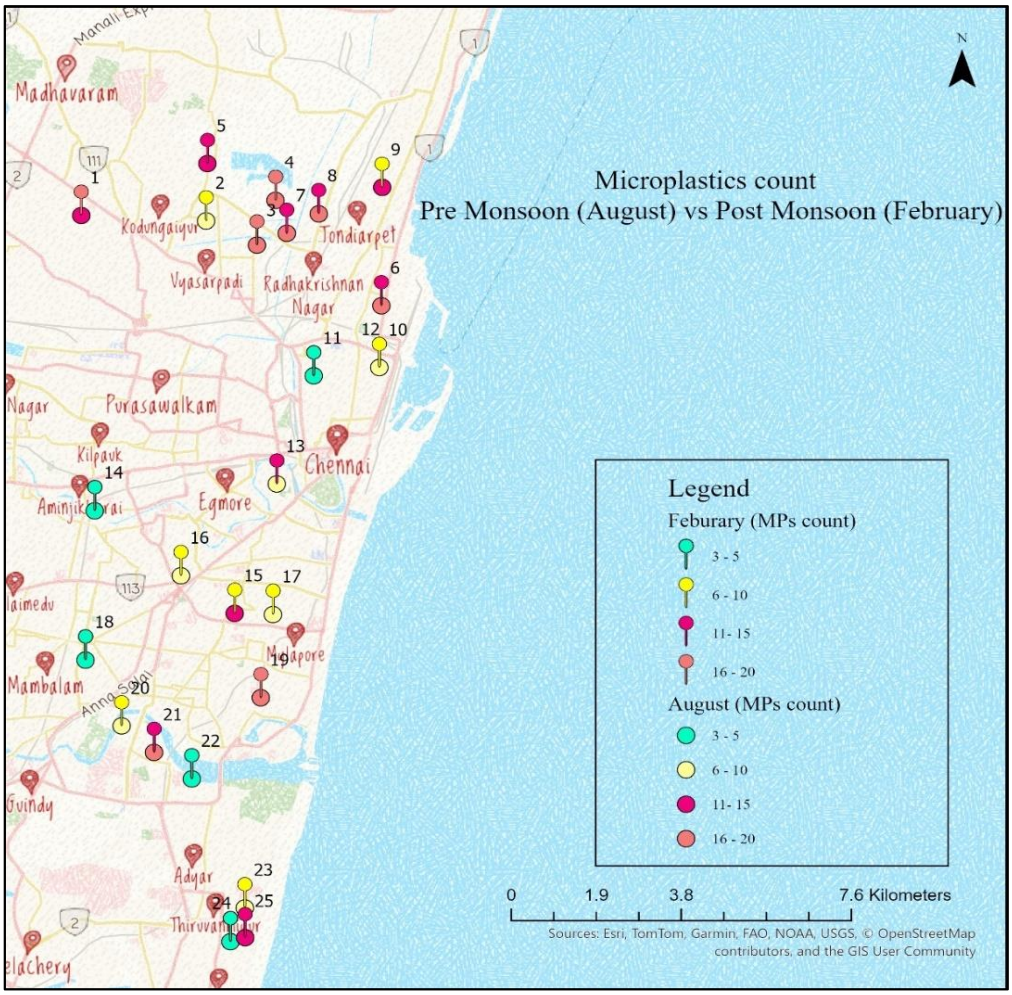

Figure 3.3: Spatial distribution of microplastic concentrations in groundwater samples during pre-monsoon period (August 2024) showing particle counts ranging from 5-19 per sample and during post-monsoon period (February 2025) showing particle counts ranging from 8-26 per sample with enhanced contamination in riverine corridors across the Chennai study.

3.6.2 Seasonal Variation and Temporal Trends

The increase from 249 particles (pre-monsoon, August 2024) to 387 particles (post-monsoon, February 2025) represents a 55.4% overall increase in total microplastic abundance across the 25 sampling locations, or an average rise from 9.96 to 15.48 particles per location. This increase was not uniform: riverine and floodplain-adjacent samples showed larger proportional increases, with samples 3, 4 and 19 near the Adyar and Coovum rivers increasing by 28–36%, consistent with enhanced mobilisation during monsoon-driven flow events (He et al., 2020; Veerasingam et al., 2016).

Morphological changes between campaigns reflected the seasonal hydrological shift. Fibre counts increased from 153 (pre-monsoon) to 225 (post-monsoon), a 47.1% increase, while fragment counts rose from 96 to 162, a 68.7% increase. The more pronounced increase in fragments may reflect

enhanced mechanical fragmentation during high-flow conditions, or preferential mobilisation of fragments over fibres from channel or floodplain deposits during flooding (Hurley et al., 2018; Waldschläger & Schüttrumpf, 2019).

Colour distribution changed substantially between sampling campaigns, with transparent/translucent particles accounting for 79.1% of pre-monsoon counts (197 of 249) but only 27.9% of post-monsoon counts (108 of 387). This shift from predominantly transparent to predominantly coloured particles suggests that the monsoon-driven increase included significant fresh inputs of pigmented materials, potentially from recently discarded or surface-accumulated plastic debris mobilised during high-flow conditions, rather than solely reflecting remobilisation of older, weathered deposits.

3.6.3 Morphological Types and Polymer Composition

Fibres dominated the microplastic assemblage at both time points, comprising 61.4% (153 of 249) pre-monsoon and 58.1% (225 of 387) post-monsoon. This fibre prevalence is consistent with textile sources, particularly synthetic clothing released through laundry effluent entering the urban water cycle (Browne et al., 2011). The slightly lower fibre proportion post-monsoon likely reflects the higher increase in fragment abundance during flood conditions.

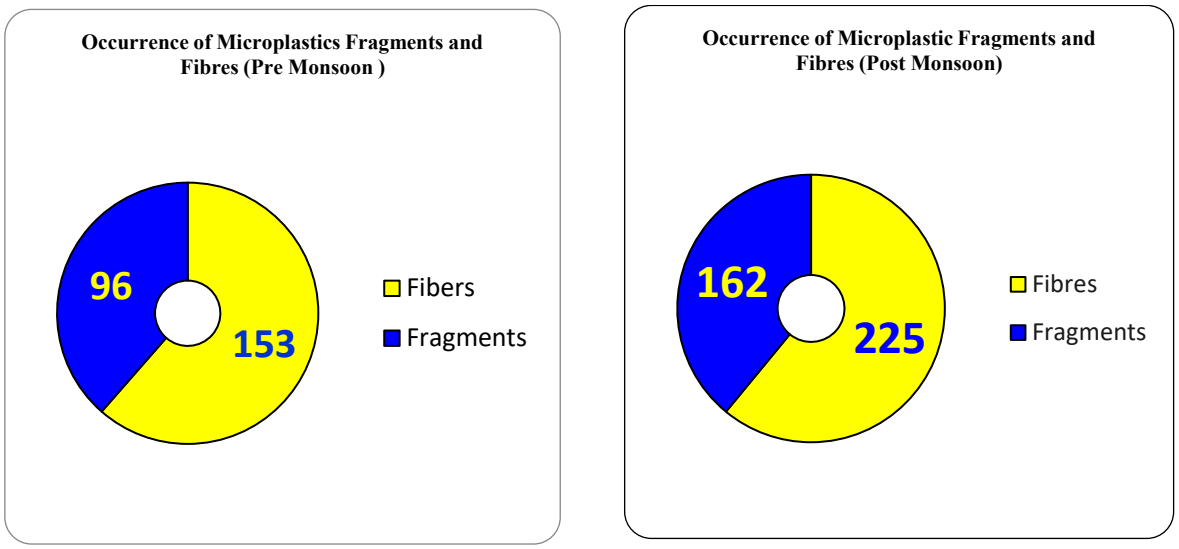

Figure 3.4: Morphological Classification of Microplastics in Chennai Groundwater Paired pie charts comparing the occurrence of microplastic fragments and fibres between pre-monsoon (153 fibers, 96 fragments) and post-monsoon (225 fibers, 162 fragments) sampling periods.

Fragments comprised 38.6% (96 of 249) pre-monsoon and 41.9% (162 of 387) post-monsoon. These irregular particles typically result from breakdown of larger plastic items through weathering and mechanical processes in the urban environment (Song et al., 2017). The larger post-monsoon increase in fragments is consistent with enhanced fragmentation during high-flow conditions.

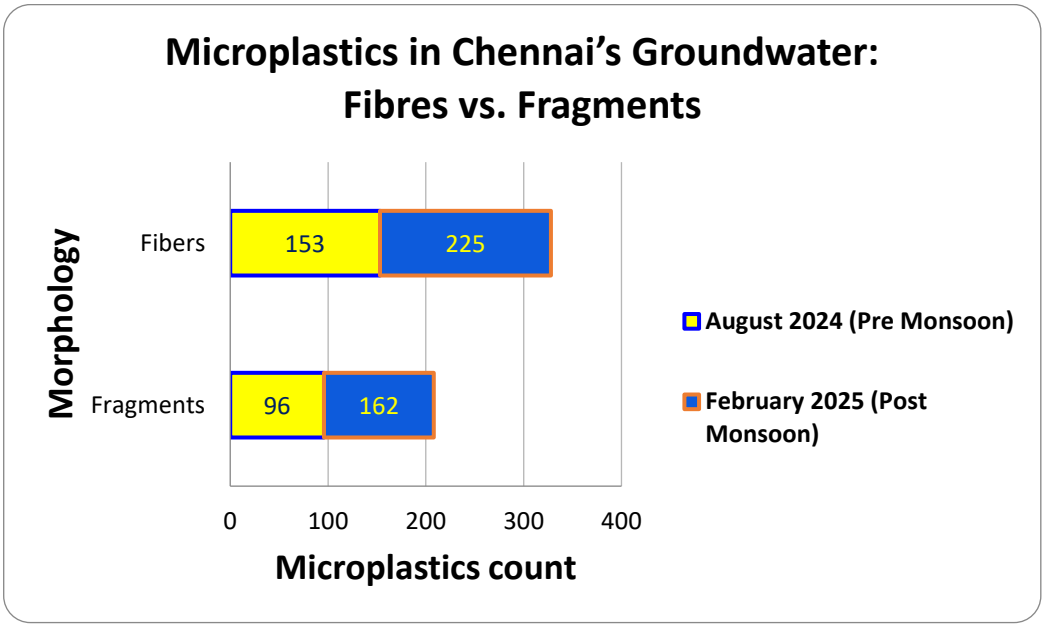

Figure 3.5: Seasonal Variation in Microplastic Abundance and Morphology Bar chart titled "Microplastics in Chennai's Groundwater: Fibres vs. Fragments" comparing counts between August 2024 (Pre Monsoon) and February 2025 (Post Monsoon).

Colour analysis revealed a pronounced shift in particle characteristics between campaigns: transparent/translucent particles decreased from 79.1% (197 of 249) pre-monsoon to 27.9% (108 of 387) post-monsoon, while coloured particles (primarily blue, black and red) increased from 20.9% (52 of 249) to 72.1% (279 of 387). This substantial change in colour profile suggests that the post-monsoon increase included a large proportion of recently introduced pigmented materials, likely mobilised from urban surfaces during monsoon flooding, rather than predominantly weathered deposits that would be expected to show pigment loss and transparency .

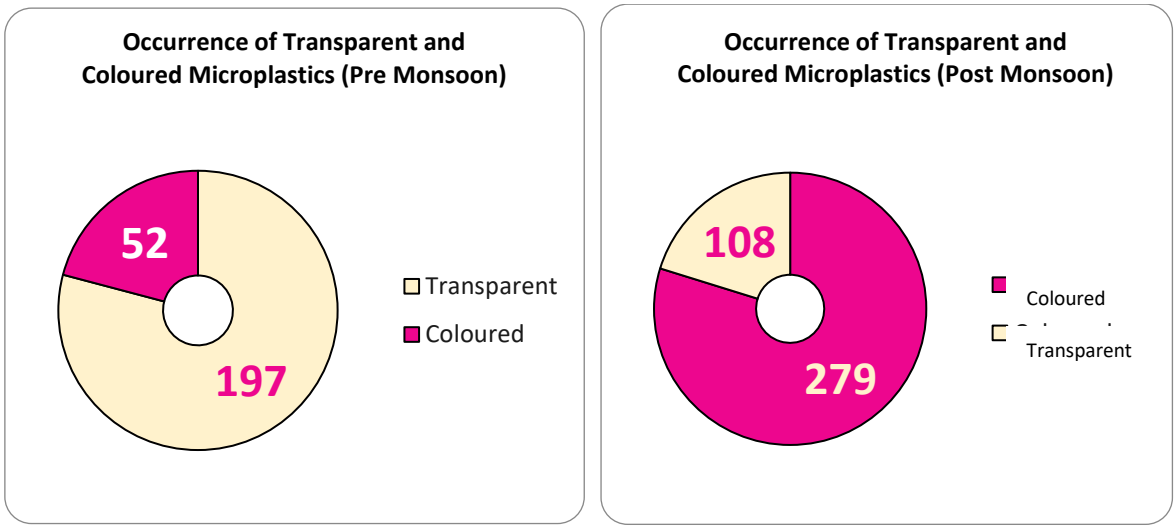

Figure 3.6: Optical Characteristics of Microplastics in Chennai Groundwater Paired pie charts showing the occurrence of transparent and coloured microplastics during pre-monsoon (197 transparent, 52 coloured) and post-monsoon (108 transparent, 279 coloured) periods.

Size distribution showed that 68% of all microplastics fell within the 0.1–1.0 mm range, consistent with the cumulative effect of fragmentation in the environment (Eerkes-Medrano et al., 2015).

FTIR spectroscopy identified a mixed polymer assemblage, indicating that the groundwater microplastics consisted mainly of common consumer and industrial polymers, with similar patterns in both seasons (Primpke et al., 2018; Käppler et al., 2018). Polyvinyl chloride (PVC), high-density polyethylene (HDPE), low-density polyethylene (LDPE), polypropylene (PP), polyurethane, polystyrene and acrylonitrile butadiene styrene (ABS) were all detected.

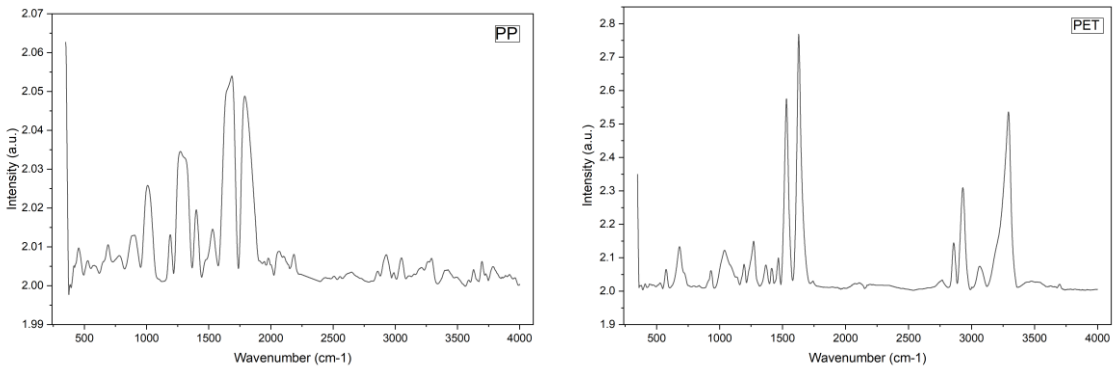

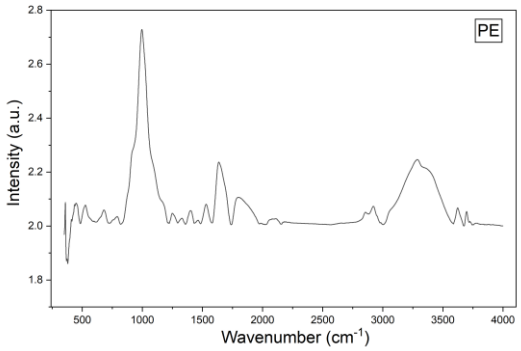

Figure 3.7 : FTIR absorbance spectra (converted from transmittance using Absorbance = 2 - log(%T)) for selected microplastic particles showing diagnostic wavenumber regions and polymer identification criteria.

Expressed as proportions of the FTIR-identified particles, PVC increased from 22% pre-monsoon to 25% post-monsoon, HDPE remained relatively stable at 18–19%, LDPE decreased slightly from 17% to 15%, PP from 14% to 12%, polyurethane increased marginally from 9% to 10%, polystyrene remained at 7%, and ABS increased from 5% to 6%. A small proportion of particles (8% pre-monsoon, 6% post-monsoon) could not be confidently assigned to a specific polymer type due to spectral ambiguity or advanced weathering. The dominance of PVC, polyethylene and polypropylene aligns with their widespread use in packaging, piping and other urban applications, while the presence of polyurethane, polystyrene and ABS indicates contributions from foams, rigid plastics and composite products common in densely populated urban settings (Karthik et al., 2018; Eerkes-Medrano et al., 2015)

Table 3.1. Relative proportions of dominant microplastic polymers in groundwater samples during pre-monsoon and post-monsoon campaigns

Polymer	**Pre-monsoon (%)**	**Post-monsoon (%)**
Polyvinyl chloride (PVC)	22	25
High-density polyethylene (HDPE)	18	19
Low-density polyethylene (LDPE)	17	15
Polypropylene (PP)	14	12
Polyurethane(PU)	9	10
Polystyrene(PS)	7	7
Acrylonitrile butadiene styrene (ABS)	5	6
Others	8	6

The morphological distinction between fibres and fragments likely reflects different source pathways: fibres are commonly associated with synthetic textile release through laundry effluent, while fragments typically derive from the mechanical breakdown of diverse plastic products in the urban environment (Browne et al., 2011; Eerkes-Medrano et al., 2015).

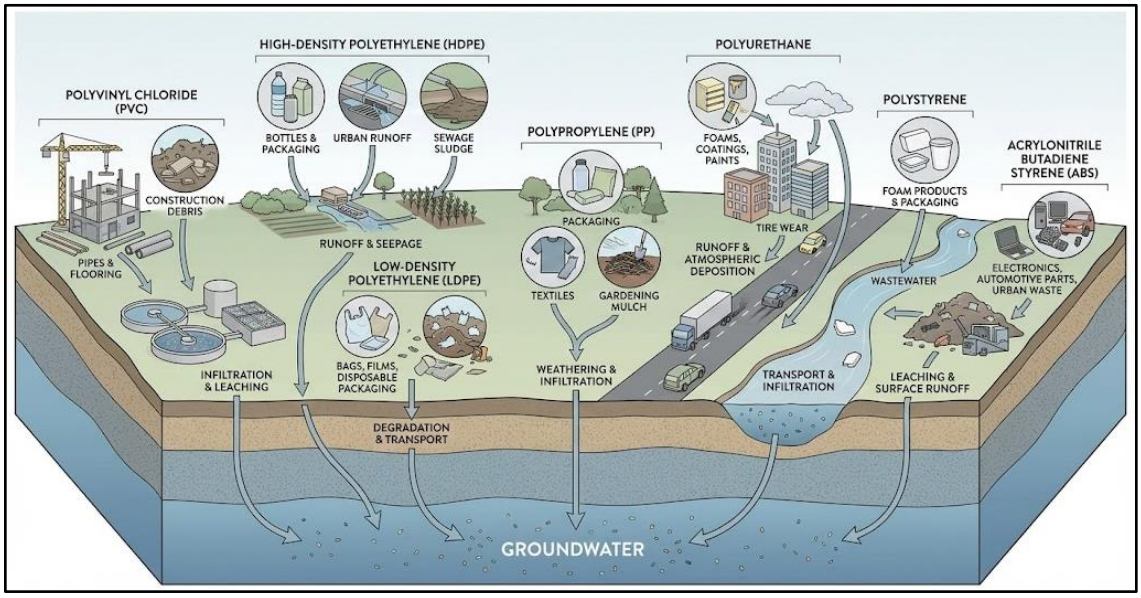

Figure 3.8. Schematic illustration of major urban sources, pathways and polymer types contributing to microplastic contamination of groundwater.

3.6.4 Hydrogeological Influences and Source Attribution

Samples with shallow water tables (<5 m below ground surface) averaged approximately 25% higher microplastic counts than those with deeper tables (>10 m), suggesting enhanced vertical infiltration in settings with direct surface–groundwater proximity (Weber et al., 2021). Fibre abundance showed stronger correlation with geological type ($r = 0.68$, $p < 0.01$) than fragments ($r = 0.42$, $p < 0.05$), potentially reflecting the elongated geometry of fibres and their preferential transport through pore networks (Wang et al., 2020).

Distance to major drainage features showed a significant inverse correlation with microplastic abundance ($r = -0.73$, $p < 0.01$), with locations within 500 m of the Adyar or Coovum rivers averaging approximately 32% higher counts than distant locations (Frei et al., 2019). This relationship was most pronounced in sandy areas with shallow water tables, where hydraulic connectivity between surface water and groundwater is likely to be enhanced (He et al., 2020).

The microplastic assemblage provides evidence for multiple urban sources. The prevalence of synthetic fibres suggests significant input from synthetic textiles through laundry wastewater

entering sewage systems (Browne et al., 2011). The presence of polyurethane particles points to contributions from tire and shoe wear from urban transportation and pedestrian traffic (Kole et al., 2017). The diverse polyethylene and polypropylene components reflect improper disposal and fragmentation of packaging and consumer waste (Jambeck et al., 2015).

The marked shift toward coloured particles in post-monsoon samples provides additional evidence for storm-driven mobilisation of recently deposited plastic debris from urban surfaces, where pigmented packaging and consumer products accumulate during dry periods and are subsequently flushed into the drainage network during intense rainfall events.

The spatial and temporal patterns indicate that microplastic transport within the urban system operates through multiple pathways. Vertical infiltration through permeable sediments appears significant in sandy zones with shallow water tables, creating direct linkages between surface sources and groundwater. Lateral transport through urban infrastructure (drains, trenches, foundations) may also facilitate subsurface movement, while river corridors function as conduits connecting upstream and downstream zones and mediating surface water–groundwater exchange through bank infiltration, particularly during high-flow monsoon conditions (He et al., 2020; Frei et al., 2019).

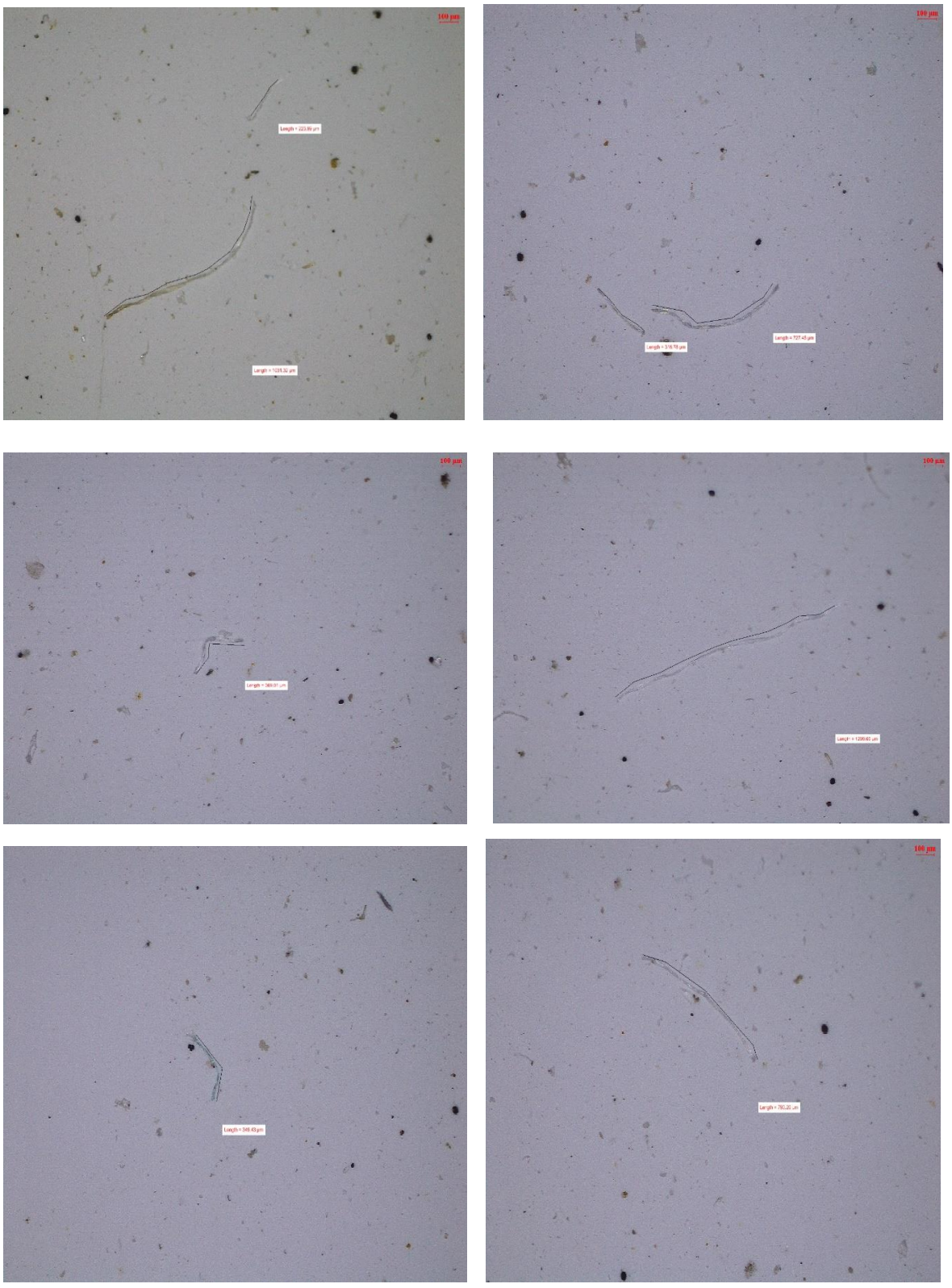

Gallery 3.1: Visual Documentation of Microplastic Particles Isolated from Urban Groundwater Samples

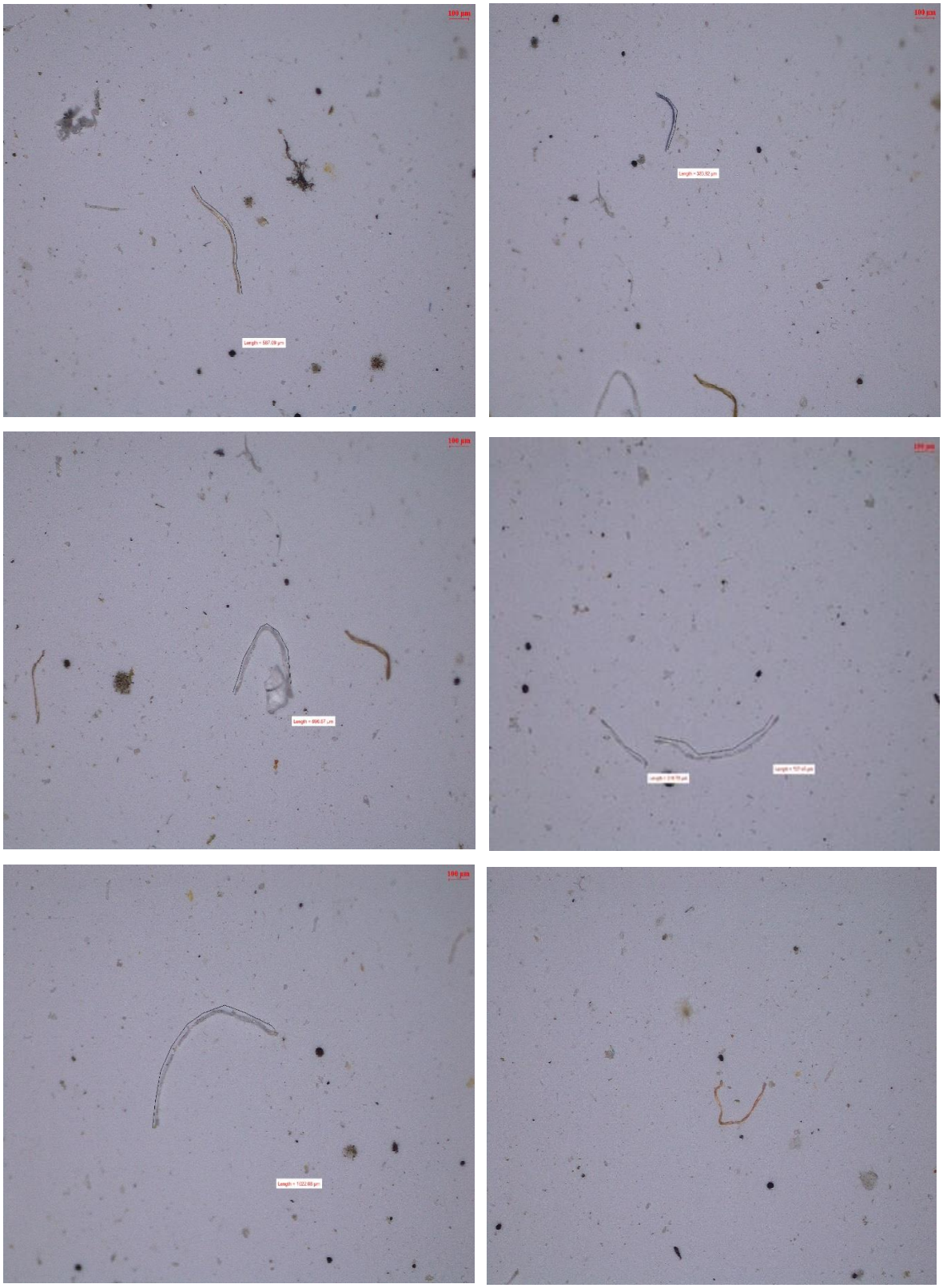

Gallery 3.2: Visual Documentation of Microplastic Particles Isolated from Groundwater Samples.

CHAPTER 4-Laboratory Experiments on Microplastic Transport in Porous Media

4.1 Introduction

The comprehensive field investigations detailed in Chapter 3 revealed widespread microplastic contamination across Chennai's groundwater systems, with concentrations ranging from 4 to 19 particles per sample and distinct spatial patterns closely linked to geological heterogeneity and hydrological processes (Panno et al., 2019). The observed preferential accumulation in sandy formations, averaging 11.2 particles per sample compared to 8.7 particles in clayey zones, highlighted the critical role of porous media characteristics in governing microplastic transport and retention mechanisms (Alimi et al., 2018). These field observations necessitated controlled laboratory experimentation to quantify the fundamental transport processes and validate the conceptual framework for microplastic migration in subsurface environments, particularly given the complex interplay of physical, chemical, and hydrological factors operating in natural groundwater systems .

Laboratory column experiments provide essential mechanistic insights into microplastic transport processes that cannot be directly measured in heterogeneous field settings, enabling systematic investigation of particle-grain size relationships, hydraulic property evolution, and retention mechanisms under precisely controlled conditions (Tufenkji & Elimelech, 2004). The experimental approach adopted in this investigation builds upon established protocols for colloid transport studies while addressing the unique characteristics of microplastic particles, including their diverse morphologies, variable densities, and potential for surface modification through environmental weathering processes (Hartmann et al., 2019). Recent advances in microplastic transport research have demonstrated that these particles exhibit behaviour distinct from traditional colloidal systems, with transport efficiency strongly dependent on particle-to-grain size ratios, surface properties, and flow conditions (Kooi et al., 2021).

The experimental objectives were specifically designed to address knowledge gaps identified through the field investigations, particularly the mechanisms governing size-dependent retention observed across different geological settings in Chennai's aquifer

systems (Chia et al., 2021). The systematic variation of sand grain sizes from 300 μm to 2000 μm encompasses the range of sediment characteristics encountered across diverse hydrogeological zones, enabling direct comparison between laboratory observations and field-derived contamination patterns .To capture the full spectrum of retention mechanisms operative across sandy formations, the experimental programme systematically investigated four distinct grain size fractions spanning fine to coarse sand fraction fine to coarse sand fractions: fine sand (300 μm), medium sand (600 μm), intermediate-medium sand (1000 μm), and coarse sand (2000 μm). This comprehensive grain size coverage enables identification of critical thresholds where transport regimes transition from attachment-dominated to straining-dominated retention, providing mechanistic insights essential for predicting microplastic fate across heterogeneous aquifer systems. Furthermore, the controlled experimental conditions facilitate precise quantification of hydraulic property changes during microplastic transport, providing insights into potential aquifer performance impacts that were suggested but could not be directly measured during field sampling campaigns (Bradford et al., 2002).

The integration of laboratory and field approaches represents current best practice in environmental contaminant research, enabling validation of field-derived conceptual models through mechanistic understanding developed under controlled conditions (Mintenig et al., 2019). The experimental design employed standardised sand fractions and consistent flow conditions to systematically investigate particle retention efficiency across grain size gradients, while monitoring temporal changes in hydraulic conductivity that provide insight into pore-scale clogging mechanisms (Johnson & Elimelech, 1995). This approach enables quantitative assessment of the physical straining, preferential flow, and retention processes that govern microplastic fate and transport in natural groundwater systems (Xu et al., 2006).

4.2 Methodology Overview

The experimental methodology employed in this investigation represents a systematic approach to quantifying microplastic transport mechanisms in porous media, designed to bridge the knowledge gap between field observations and mechanistic understanding of subsurface contamination processes . The methodological framework integrates established colloid transport protocols with novel adaptations specific to microplastic

particle characteristics, enabling controlled investigation of size-dependent retention mechanisms under precisely defined hydraulic conditions .

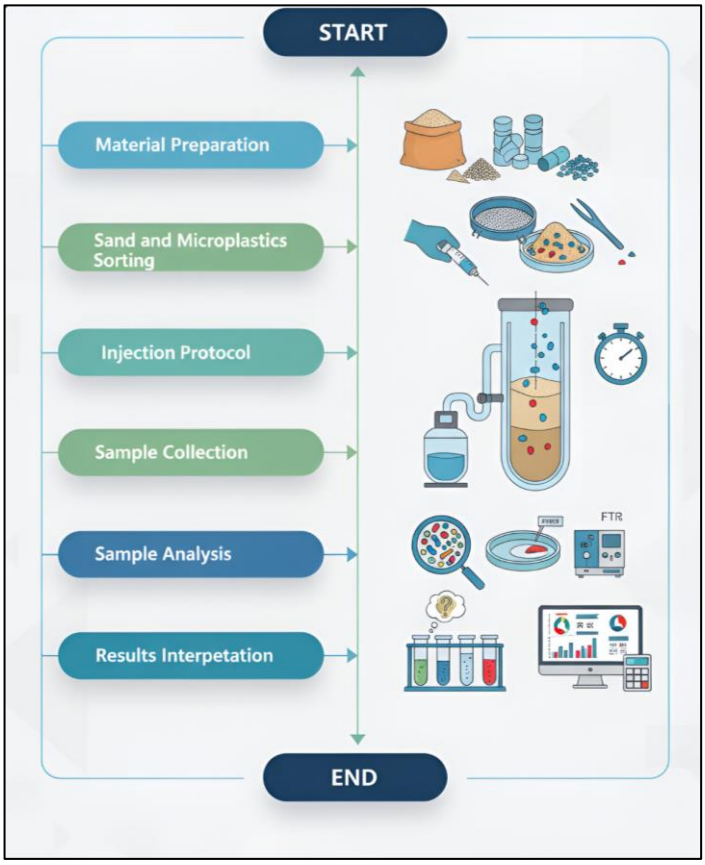

Figure 4.1: Systematic Methodology Workflow for Microplastic Transport Investigation in Porous Media. Comprehensive experimental framework illustrating the six-phase laboratory methodology employed to quantify size-dependent microplastic transport and retention mechanisms across sand grain sizes .

The workflow encompasses standardized material preparation, rigorous characterization protocols, controlled injection experiments, systematic sampling procedures, microscopic analysis, and mechanistic interpretation to investigate physical straining, preferential flow, and retention processes governing microplastic fate in natural groundwater systems

The experimental design adopts a multi-scale approach, employing standardised column configurations to systematically investigate particle-grain size relationships across fine, medium, intermediate-medium, and coarse sand fractions (300 μm, 600 μm, 1000 μm, and 2000 μm).

The methodological approach employs vertical flow columns constructed from borosilicate glass to minimise plastic contamination and wall effects, with upward flow configuration specifically selected to eliminate gravitational settling effects and ensure

that observed retention results from porous media interactions rather than particle density differences . The pulse injection methodology creates step-function input conditions that enable construction of breakthrough curves and quantification of retention parameters using established analytical solutions for solute transport in porous media .

Rigorous quality assurance protocols were implemented throughout the experimental programme, including standardised sand sorting procedures conforming to ASTM specifications, comprehensive grain size characterisation using precision sieve analysis, and systematic porosity and hydraulic conductivity measurements to ensure reproducible packing density and flow conditions . Microplastic particles consisted of irregularly shaped polyvinyl chloride (PVC) fragments (<75 μm maximum dimension) produced through grinding techniques to create realistic fragment morphologies representative of environmental microplastic contamination .

The experimental protocol incorporates using comprehensive coverage of grain size effects on microplastic transport and retention, with systematic variation of particle loading conditions and throughput volumes to assess temporal evolution of transport capacity and hydraulic property changes . Effluent sampling follows standardised protocols with consistent intervals, enabling quantitative assessment of breakthrough behaviour and construction of complete breakthrough curves for mechanistic analysis .

This methodological framework enables systematic investigation of the physical straining, preferential flow, and retention processes that govern microplastic fate and transport in natural groundwater systems, providing quantitative foundation for numerical transport modelling and predictive assessment of aquifer vulnerability based on grain size distribution characteristics .

4.2 Experimental Design and Setup

The laboratory experimental programme was designed as a systematic investigation of microplastic transport through sand-based porous media, employing standardised column configurations to enable precise control of flow conditions and quantitative assessment of retention mechanisms (Bradford & Bettahar, 2006). The experimental apparatus consisted of vertical flow columns constructed from borosilicate glass (25 mL burette capacity, 10 cm height, 1 cm internal diameter) to minimise plastic contamination and wall effects

while maintaining sufficient residence time for meaningful transport observations. A surgical cotton bandage (open-weave mesh, IS 16469) was placed at the column outlet to retain the porous media while allowing unobstructed effluent collection. The length of porous media was 10 cm.

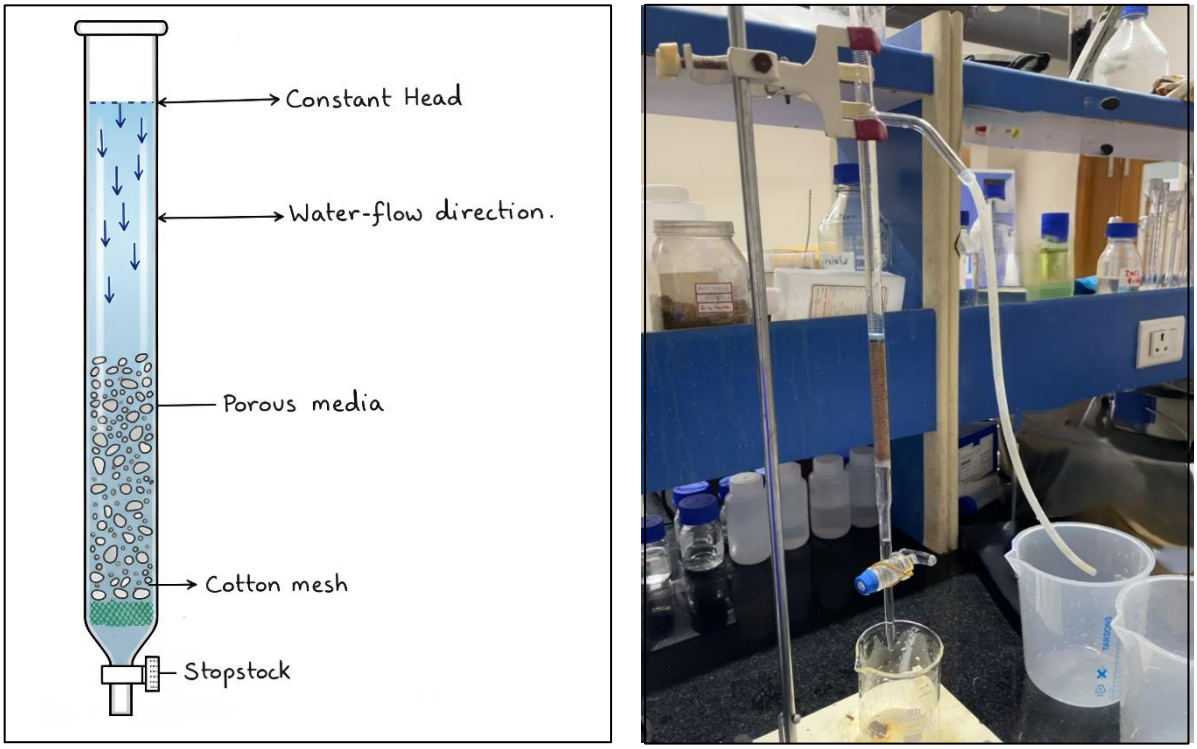

Figure 4.2: Schematic of the Experimental Setup for the Porous Media Column Study.

Table 4.1: Summary of Experimental Parameters

Parameter	**Experiments**
Sand Sizes Tested	300 µm, 600 µm, 1000 µm and 2000 µm
Microplastic Loading	0.15 g per trial
Column Dimensions	Ø 1 cm × 10 cm
Sampling Intervals	250 mL
Replication	2 trials per size

The grain sizes of 300 µm, 600 µm, 1000 µm, and 2000 µm sand, provide systematic coverage of particle-to-grain size ratios spanning 0.025 to 0.25,thus encompassing the critical range where retention mechanism transitions from reversible attachment to irreversible straining occur. The experimental protocol involved pulse injection of microplastic suspensions (500 ml) followed by continued flow with particle-free water.

4.2.1 Sand Sorting and Characterization

Sand used in the column experiments was obtained from commercial sources and sorted to obtain well-defined grain size fractions while minimising contamination. Grain size separation was carried out using a mechanical sieve shaker with ASTM E11-compliant sieves at nominal openings of 300 μm, 600 μm,1000 μm, and 2000 μm. Each batch was sieved for a fixed period and inspected to ensure that material was retained within the target size range.

Table 4.2: Physical Characterization of Sand Fractions

Sand Size (μm)	**Median grain size (μm)**	**Initial Porosity**	**Estimated Pore Throat Diameter (μm)**
300	300	0.30-0.40	36-38
600	600	0.37-0.39	71-74
1000	1000	0.36-0.38	116-121
2000	2000	0.35-0.37	227-237

Note: Pore throat diameters estimated using empirical relationship: $d_t = 0.155 \times d_g \times (\varepsilon/(1-\varepsilon))^{0.5}$

4.2.2 Porosity and Hydraulic Conductivity Measurements

Hydraulic properties were determined from the column experiments by combining measured effluent volumes and collection times with Darcy's law and by relating hydraulic conductivity to intrinsic permeability. Porosity was then inferred from permeability using an inverted Kozeny–Carman-type relationship.

Hydraulic conductivity

For each sampling interval i, the effluent volume V_i (m^3) and collection time t_i (s) were recorded. The volumetric discharge in SI units q_i ($m^3\ s^{-1}$) was calculated as

$$q_i = \frac{V_i}{t_i} \tag{4.1}$$

For reporting in $m^3\ day^{-1}$, the discharge was also expressed as

$$Q_i = q_i \times 86400. \tag{4.2}$$

The column cross-sectional area A, the column length ΔL, and the applied hydraulic head difference Δh were fixed for each experiment. Assuming steady, one-dimensional saturated flow, the hydraulic conductivity K_i (m day^{-1}) for interval i was obtained from Darcy's law:

$$K_i = \frac{Q_i \, \Delta L}{A \, \Delta h}. \tag{4.3}$$

For subsequent calculations, K_i was converted to m s^{-1} by dividing by 86400.

Intrinsic permeability

Intrinsic permeability k_i (m²) was calculated from hydraulic conductivity using

$$K_i = \frac{k_i \, \rho g}{\mu} \tag{4.4}$$

where ρ is water density, g gravitational acceleration, and μ the dynamic viscosity of water. Rearranging gives

$$k_i = K_i \frac{\mu}{\rho g} \tag{4.5}$$

with K_i in m s^{-1}. The same fluid (water at approximately constant temperature) was used throughout, so ρ and μ were treated as constant.

Porosity from permeability

Experimental porosity ε_i was not measured directly but was inferred from the intrinsic permeability using an inverted Kozeny–Carman-type relationship. For each column, an initial porosity ε_0 and an initial intrinsic permeability k_0 were specified. A dimensionless parameter a was defined as

$$a = \frac{\varepsilon_0^3}{(1 - \varepsilon_0)^2} \tag{4.6}$$

The corresponding porosity ε_i was then obtained as the real root (with $0 < \varepsilon_i < 1$) of the cubic equation relating permeability and porosity. The closed-form expression implemented in the spreadsheets was

$$\varepsilon_i = \frac{a}{3} + \frac{2^{1/3}(6a - a^2)}{3\left(-27a + 18a^2 - 2a^3 + 3\sqrt{3}\sqrt{27a^2 - 4a^3}\right)^{1/3}} - \frac{\left(-27a + 18a^2 - 2a^3 + 3\sqrt{3}\sqrt{27a^2 - 4a^3}\right)^{1/3}}{3 \cdot 2^{1/3}} \tag{4.7}$$

This expression was coded directly in Excel and applied at each time step using the current value of k_i and the fixed parameters k_0 and ε_0 for that column.

Normalised quantities

To compare experiments and track temporal changes, hydraulic properties and microplastic counts were expressed in normalised form:

$$\text{Normalised permeability}_{\ i} = \frac{k_i}{k_0},$$
$$\text{Normalised porosity}_i = \frac{\varepsilon_i}{\varepsilon_0},$$
$$\text{Normalised concentration}_i = \frac{C_i}{C_0}, \tag{4.8}$$

where C_i is the microplastic count in interval i, and k_0, ε_0 and C_0 are the initial values for that column. Because μ and ρ were constant,

Normalised permeability $_i$ is numerically equivalent to K_i/K_0; the permeability-based notation is retained to emphasise that the normalisation refers to the porous medium.

The cumulative elapsed time for each column, Cumulative time (n) (s), was calculated as

$$\text{Cumulative time } (n) = \sum_{j=1}^{n} t_j, \tag{4.9}$$

and used together with the cumulative effluent volume to examine how permeability, porosity and microplastic concentrations evolved as more water passed through the column.

4.2.3 Microplastic Preparation and Characterization

Microplastic particles utilised in transport experiments consisted of polyvinyl chloride (PVC) fragments with maximum dimensions <75 μm, produced through mechanical grinding of bulk PVC material using cryogenic techniques to create realistic fragment morphologies representative of environmental microplastic contamination . The grinding process employed ball milling under liquid nitrogen cooling to achieve controlled fragmentation while avoiding thermal degradation of polymer structure, creating particles with diverse morphologies including angular fragments, elongated particles, and complex three-dimensional shapes that better represent secondary microplastics generated through environmental weathering processes (Chubarenko et al., 2016). The standardised sieve shaker methodology employed further to sort the microplastics (<75 μm) .

Table 4.3: Microplastic Particle Characteristics

Property	Value	Method
Maximum Dimension	<75 μm	Sieve analysis (ASTM E11)
Median Diameter (d_{50})	42 μm	Laser diffraction
d_{10}	12 μm	Laser diffraction
d_{90}	68 μm	Laser diffraction
Particle Density	1.38 g/cm³	Literature (Luo et al., 2024)
Shape Distribution	45%irregular,35% angular, 20% elongated	Microscopy (n=500)
Polymer Type	PVC	FTIR spectroscopy

Particle size distribution analysis revealed a broad log-normal distribution with d_{50} = 42 μm, d_{10} = 12 μm, and d_{90} = 68 μm, providing quantitative characterisation of the size spectrum below the 75 μm sieve cutoff .

Microscopic examination of 500 randomly selected particles confirmed heterogeneous morphological characteristics, with approximately 45% irregular fragments, 35% angular particles, and 20% elongated particles exhibiting aspect ratios >2:1, representative of the diversity observed in environmental microplastic samples (Plastics Europe, 2023).

The particle density of 1.38 g/cm³ (Luo et al., 2024) is higher than water (ρ_{water} = 1.00 g/cm³), but gravitational effects are assumed to give negligible contribution to transport behaviour under the upward flow conditions employed in experiments (Praetorius et al., 2012). Surface charge measurements using zeta potential analysis yielded values of -35 ± 8 mV in deionised water at pH 7.0, indicating moderate negative surface charge that influences electrostatic interactions with sand grain surfaces (Dong et al., 2021).

4.3 Experimental Protocol

Column procedures were kept consistent across all trials to enable comparison of microplastic transport between the different sand fractions under controlled flow conditions.

Column preparation and saturation

Glass and column components were cleaned before each experiment by sequential rinsing with dilute acid and base, followed by thorough washing with 0.2 μm-filtered deionised water to reduce potential contamination. Dry sand was added in approximately 2 cm layers using a funnel, with gentle tapping to promote uniform packing; column volume measurements were used to check that bulk density was comparable between replicates (ASTM D4253-16).

Columns were saturated from the bottom upwards using filtered deionised water at low flow rates to minimise air entrapment, following standard practice for saturated column studies (Freeze & Cherry, 1979). Saturation was considered complete when effluent flows were free of visible air bubbles and measured flow rates under a fixed head were within about 5% of values expected from the independently determined hydraulic conductivity.

Microplastic injection and breakthrough monitoring

Microplastics (PVC fragments and fibres) were dispersed in deionised water by sonication immediately before use and injected as a short pulse at the column inlet using a syringe pump with a constant flow rate. After the pulse, particle-free water was pumped through the column to follow the elution of particles and construct breakthrough curves. The injection masses and flow conditions were kept the same within each experiment set, and pore-volume-based normalisation was used to compare between grain sizes.

Effluent samples were collected in pre-cleaned glass bottles at fixed volume intervals (typically 250 mL), corresponding to defined fractions of a pore volume. Each sample was filtered through a 0.2 μm cellulose-nitrate membrane and the retained microplastics were counted by microscopy.

QA/QC checks

Procedural blanks consisting of filtered deionised water were processed regularly alongside samples to monitor laboratory contamination. Blank particle counts were low (on the order of one particle or fewer per sample), and mean blank values were subtracted from sample counts when calculating final concentrations. Recovery tests, in which known numbers of microplastic particles were added to clean water and processed through the full filtration and counting procedure, indicated recoveries around 95% for the particle types and sizes used, which is within commonly reported ranges for microplastic methods. Duplicate counts on a subset of filters gave inter-analyst variability below about 10%, consistent with recommended quality-criteria thresholds.

4.4 Results

4.4.1 Breakthrough Curve Analysis

Column experiments were conducted on four porous media with distinct grain size distributions spanning fine to coarse sand fraction fine to coarse sand fractions: fine sand (300 μm), medium sand (600 μm), intermediate-medium sand (1000 μm), and coarse sand (2000 μm), enabling systematic investigation of grain size effects on microplastic transport mechanisms. All materials exhibited microplastics breakthrough characterized by normalized outlet concentration (C/C_0) reaching maximum saturation during the observation period.

The timing of breakthrough varied inversely with grain size. Coarser materials (2000-1000 μm) showed earlier breakthrough occurrence. Finer materials (300-600 μm) demonstrated delayed breakthrough with a more gradual approach to peak concentration compared to coarser counterparts.

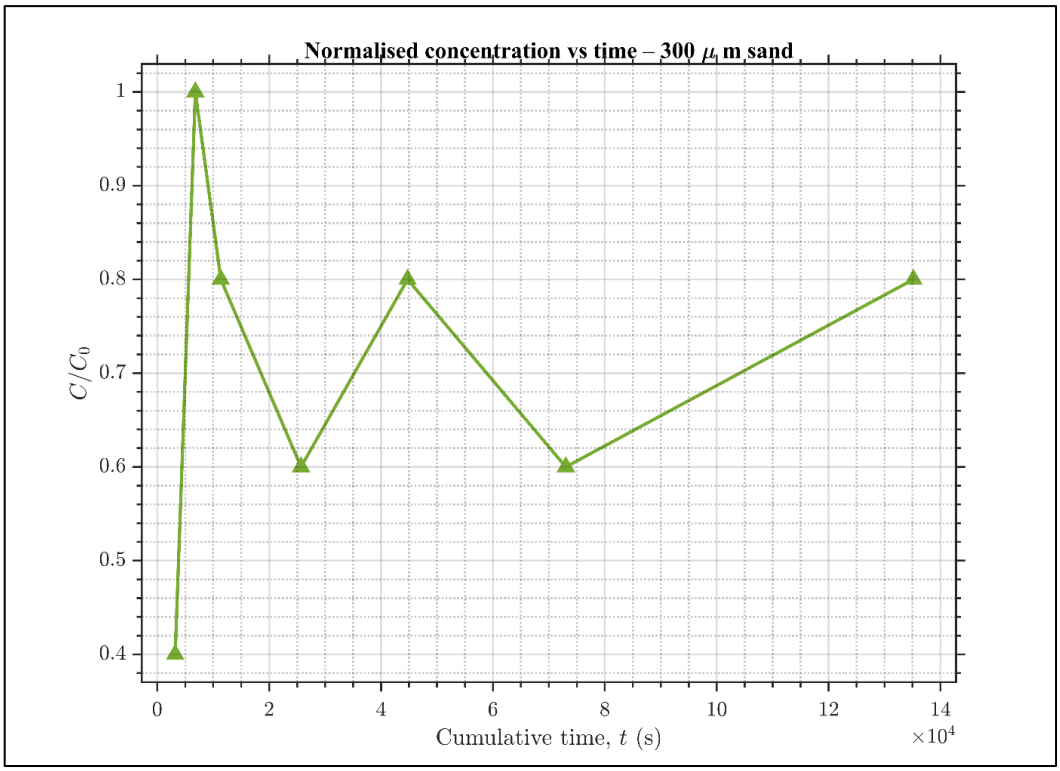
Normalised concentration vs time – 300 μ m sand
C/C0
1
0.9
0.8
0.7
0.6
0.5
0.4
0
2
4
6
8
10
12
14
Cumulative time, t (s)
×10^4

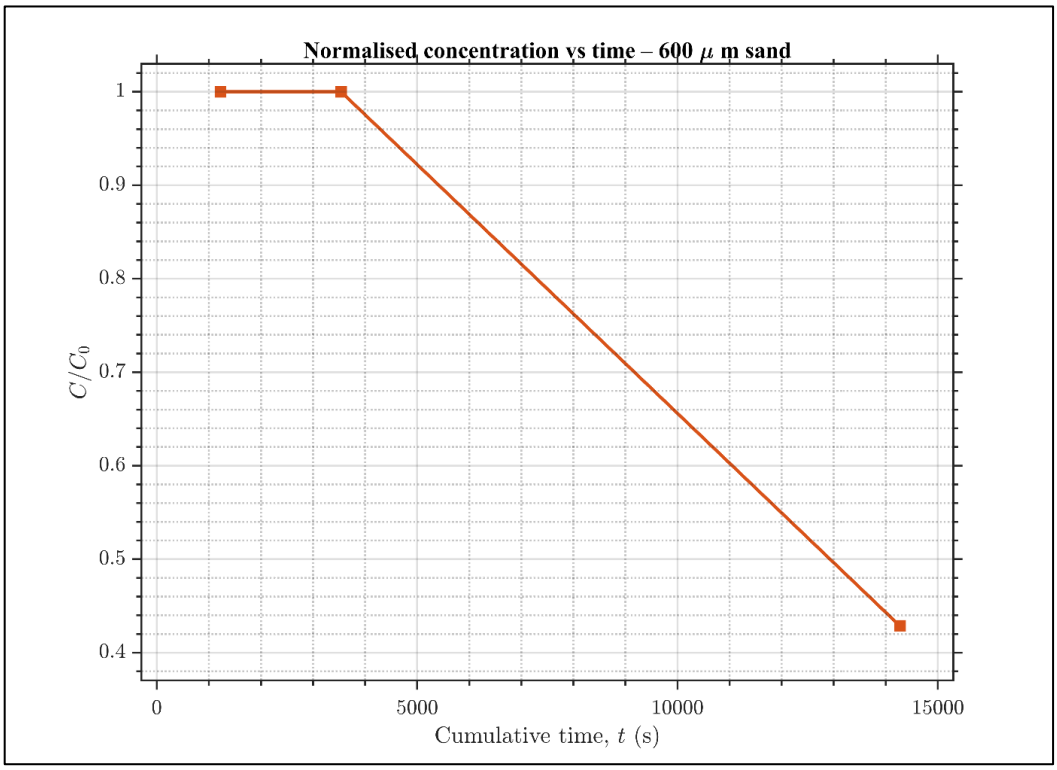
Normalised concentration vs time – 600 μ m sand
C/C0
1
0.9
0.8
0.7
0.6
0.5
0.4
0
5000
10000
15000
Cumulative time, t (s)

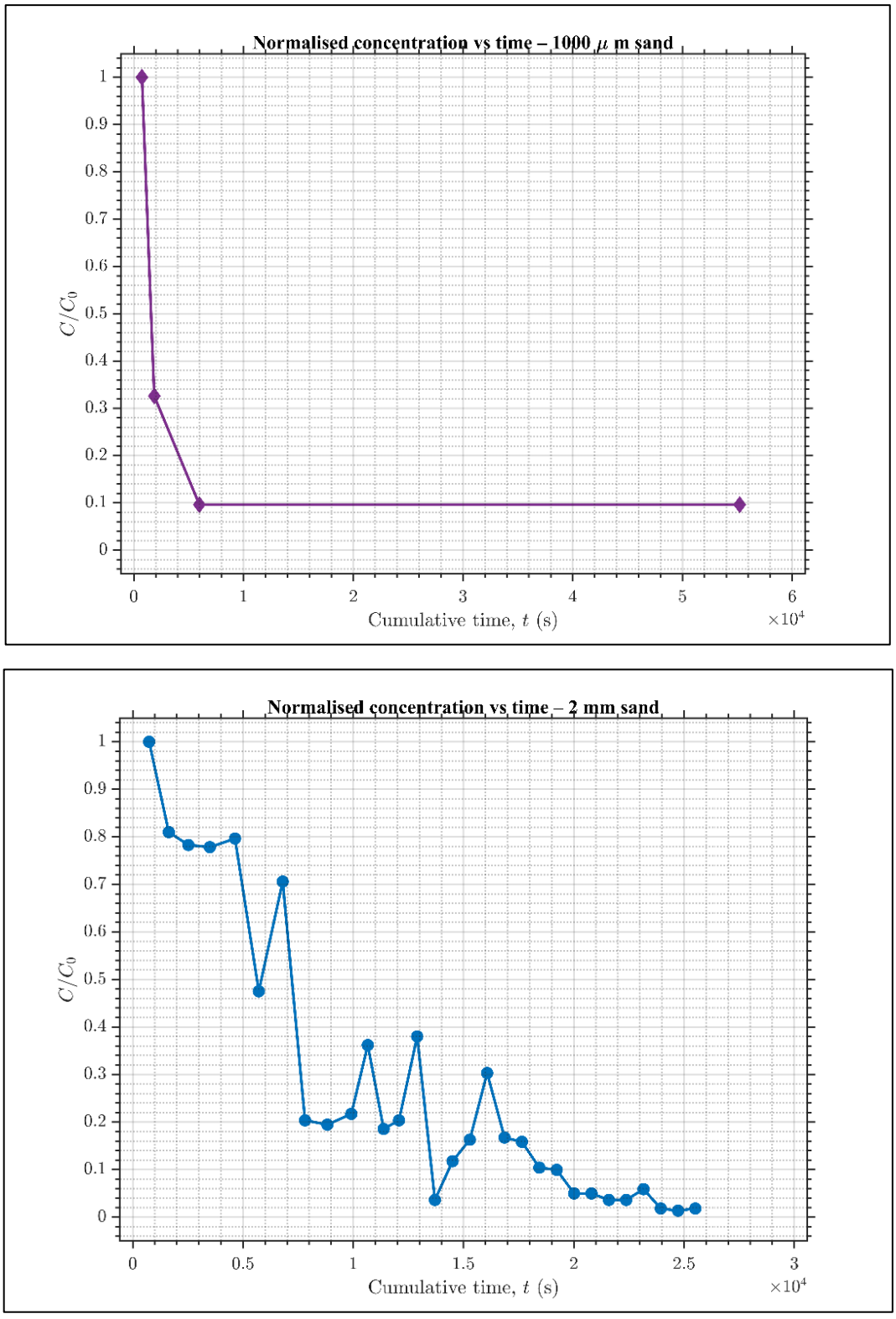

FIGURE 4.3: Breakthrough curves for 300 µm, 600 µm, 1000 µm and 2000 µm sand columns showing normalized microplastics concentration versus cumulative time.

4.4.2 Temporal Evolution of Porosity

Normalized porosity values were calculated at each sampling interval to assess pore volume reduction during microplastics transport. Changes in porosity reflect the degree of pore space occupied by retained microplastics and any associated pore bridging or clogging phenomena.

Fine-grained sand (300 μm) exhibited substantial porosity reduction over the experimental duration. Porosity declined from initial values close to the reference baseline to significantly reduced values by the final sampling point. The porosity decline shows systematic accumulation of retained microplastics within the pore network.

Intermediate-grained sand (600 μm) showed moderate porosity reduction, with initial values near baseline declining to intermediate values by final sampling. The extent of reduction was less severe than observed in fine-grained sand despite comparable experimental durations when normalized to experimental completion.

Intermediate-medium sand (1000 μm) demonstrated moderate porosity reduction during the experimental period. Porosity values declined progressively from baseline, indicating systematic accumulation patterns. The moderate porosity loss reflects transitional retention characteristics where both transport and retention processes contribute to overall behaviour.

Coarse sand (2000 μm) demonstrated remarkable porosity stability throughout the experimental period. Porosity values remained near baseline across all sampling intervals, with minor fluctuations that did not show systematic temporal trend. The absence of substantial porosity change suggests minimal accumulation of microplastics within the pore network or rapid mobilization of any retained particles.

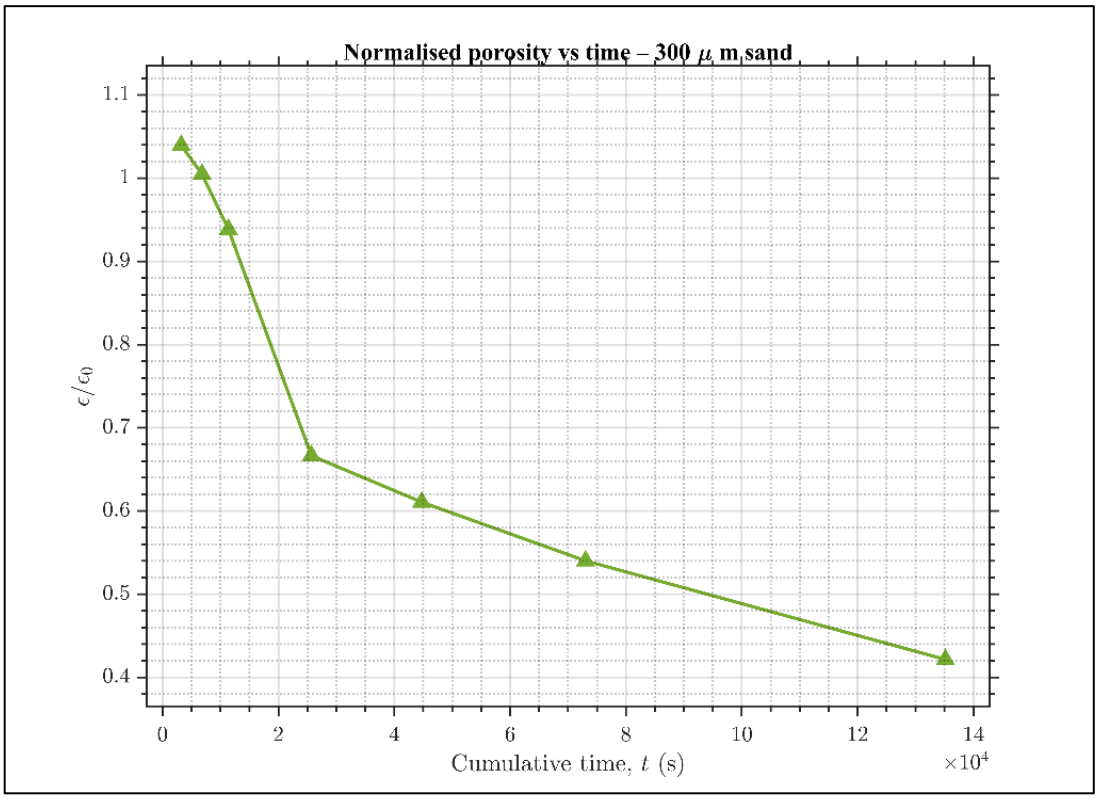
Normalised porosity vs time – 300 μ m sand
1.1
1
0.9
0.8
0.7
0.6
0.5
0.4
ϵ/ϵ_0
0
2
4
6
8
10
12
14
Cumulative time, t (s)
$\times 10^4$

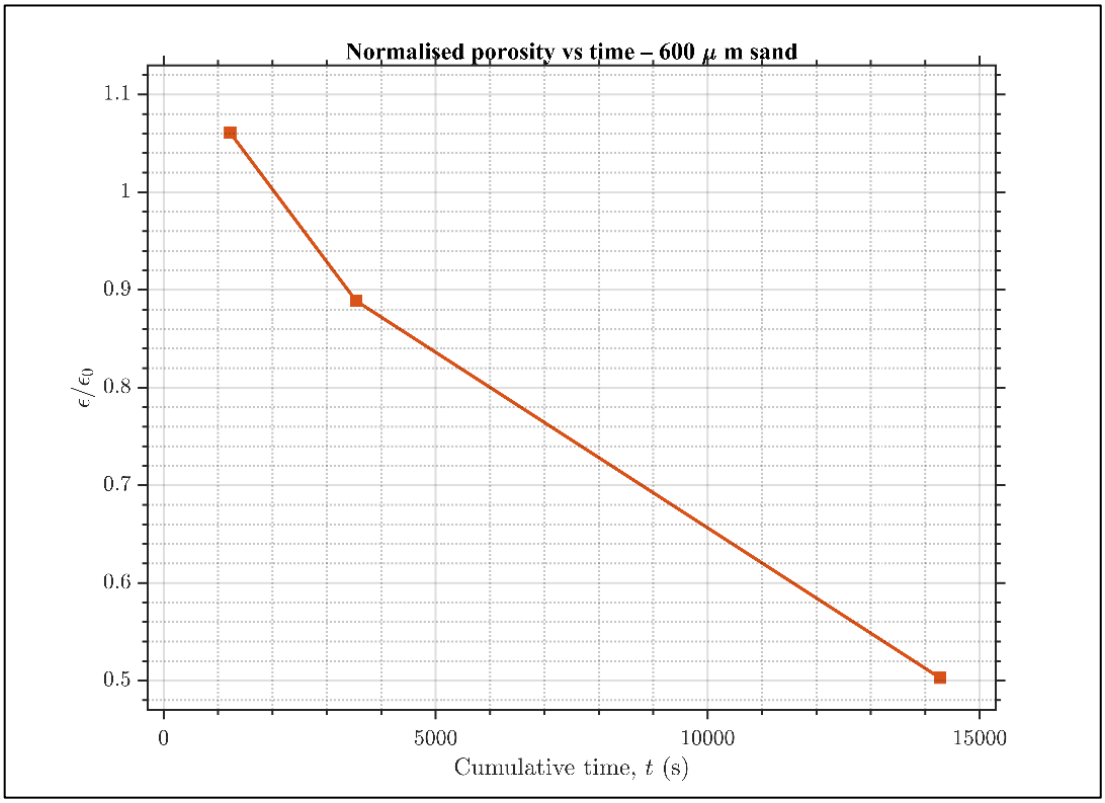
Normalised porosity vs time – 600 μ m sand
1.1
1
0.9
0.8
0.7
0.6
0.5
ϵ/ϵ_0
0
5000
10000
15000
Cumulative time, t (s)

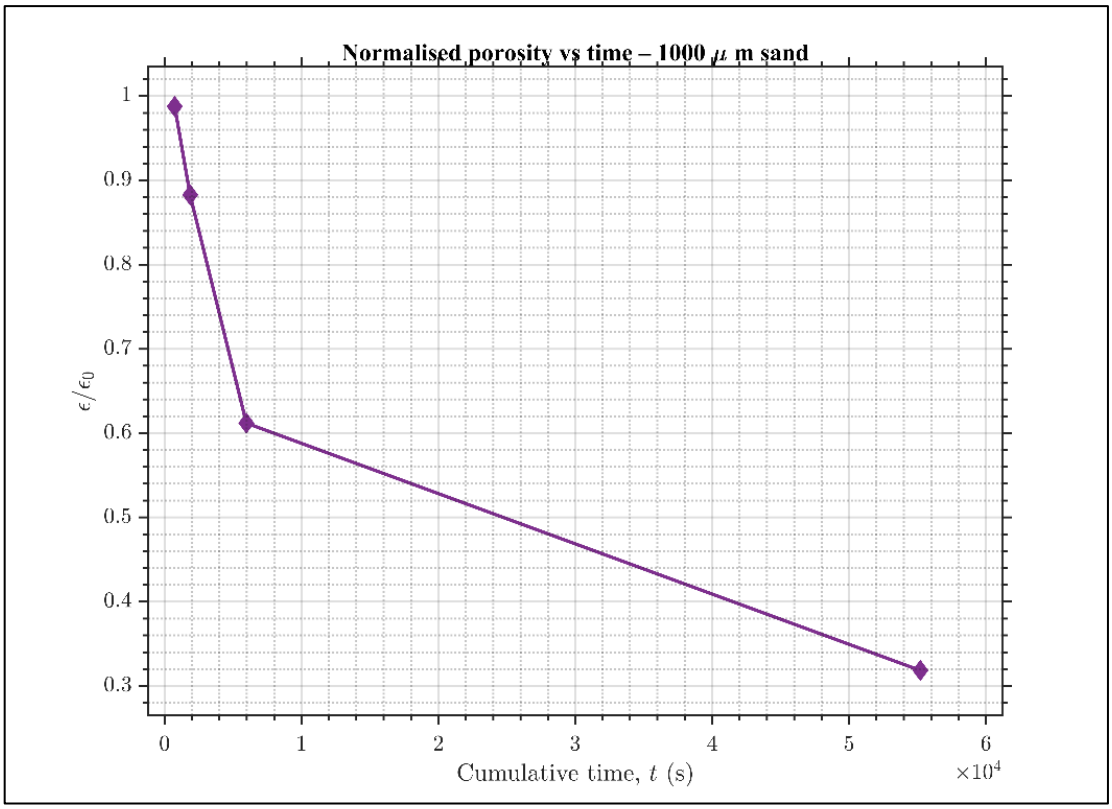

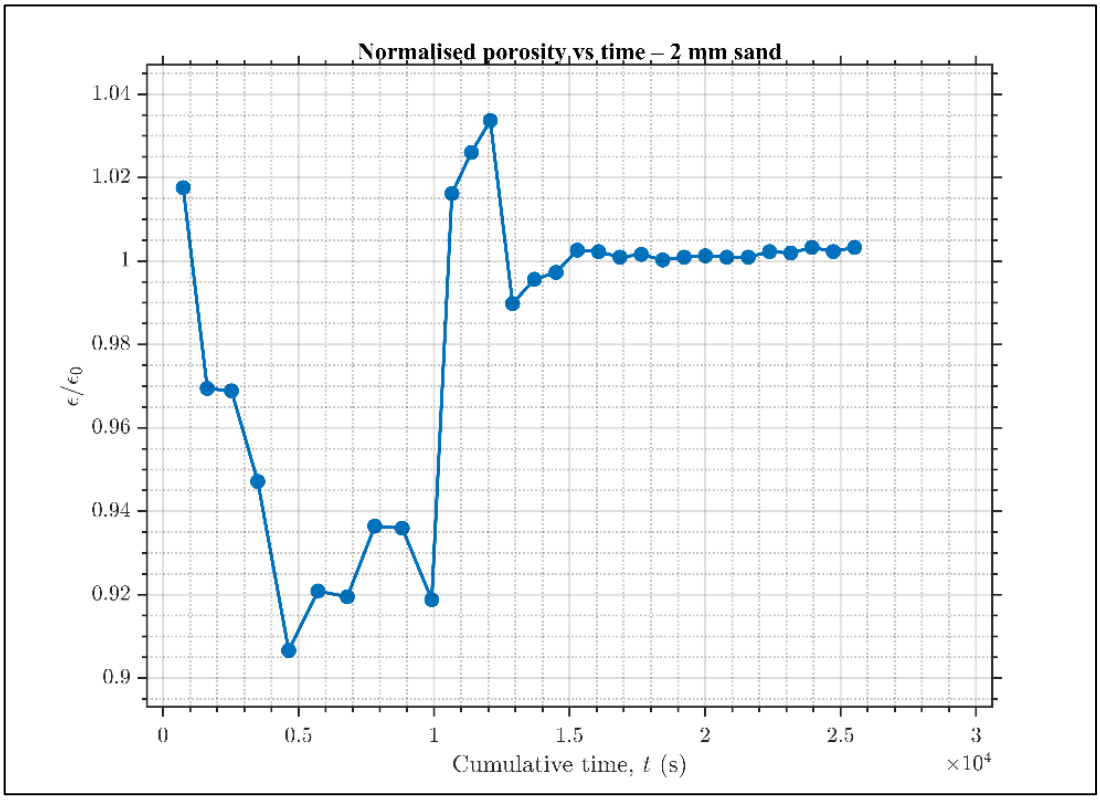

FIGURE 4.4: Temporal evolution of normalized porosity for 300 µm, 600 µm,1000 µm and 2000 µm sand columns showing time-dependent porosity changes.

4.4.3 Hydraulic Conductivity Changes

Normalized hydraulic conductivity values were determined from measured water discharge rates under constant-head conditions, providing direct assessment of flow capacity changes during microplastics transport. Hydraulic conductivity is particularly sensitive to pore structure changes and represents the primary hydrodynamic parameter affected by pore clogging.

Fine-grained sand (300 μm) exhibited dramatic hydraulic conductivity reduction during the experimental period. Initial conductivity values normalized to unity declined to substantially lower values by experiment completion, representing near-total loss of flow capacity. The degradation pattern followed an approximately exponential profile, with rapid initial decline followed by stabilization at reduced values.

Intermediate-grained sand (600 μm) displayed similarly severe hydraulic conductivity reduction, with percentage loss comparable to fine-grained material despite coarser grain size. The temporal profile showed rapid initial degradation followed by stabilization, consistent with fine-grained behaviour but occurring over compressed experimental timescales.

Intermediate-medium sand (1000 μm) exhibited moderate hydraulic conductivity reduction during the experimental period. Conductivity values declined progressively from baseline, with temporal patterns showing initial reduction followed by stabilization at lower values. The magnitude of conductivity loss was intermediate between fine and coarse sand behaviours. The moderate reduction indicates measurable hydraulic impairment without the severe degradation observed in finer grain sizes.

Coarse sand (2000 μm) maintained hydraulic conductivity near initial values throughout the experimental period. Normalized conductivity remained close to baseline across all sampling intervals, with minor fluctuations that averaged near the starting value. The preservation of flow capacity indicates that coarser materials do not experience substantial hydraulic penalty from microplastics transport under the experimental conditions employed.

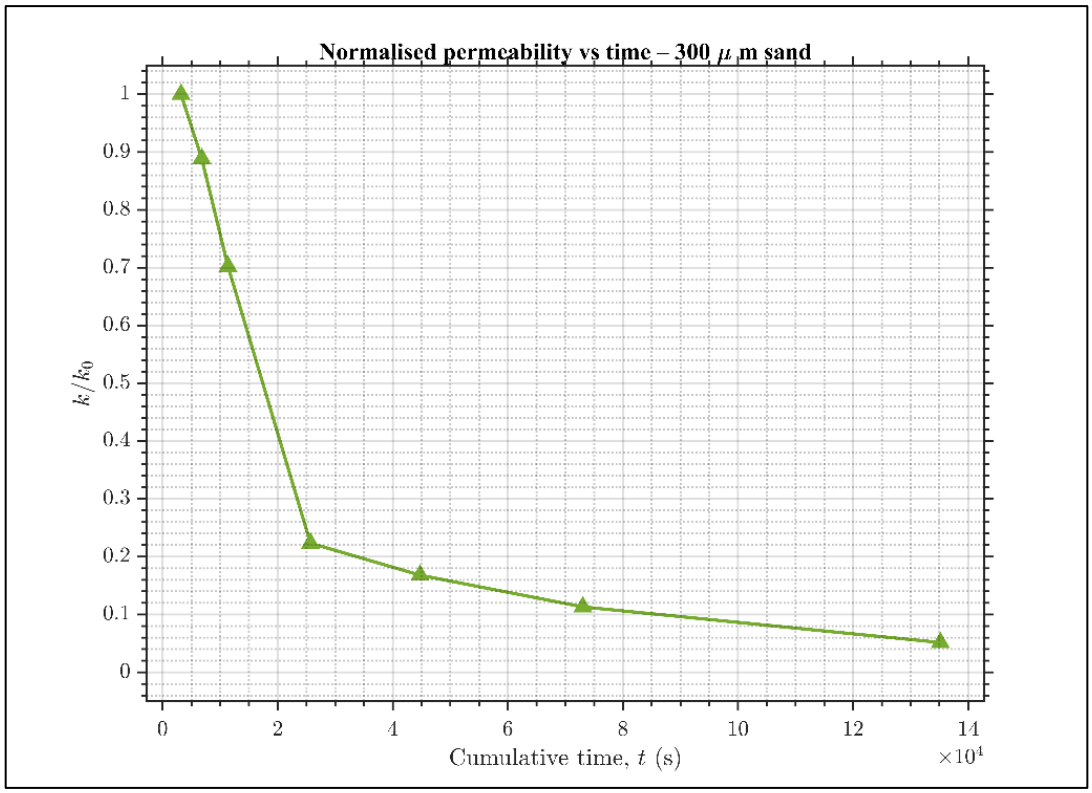
Normalised permeability vs time – 300 μ m sand
k/k0
Cumulative time, t (s)
×10^4

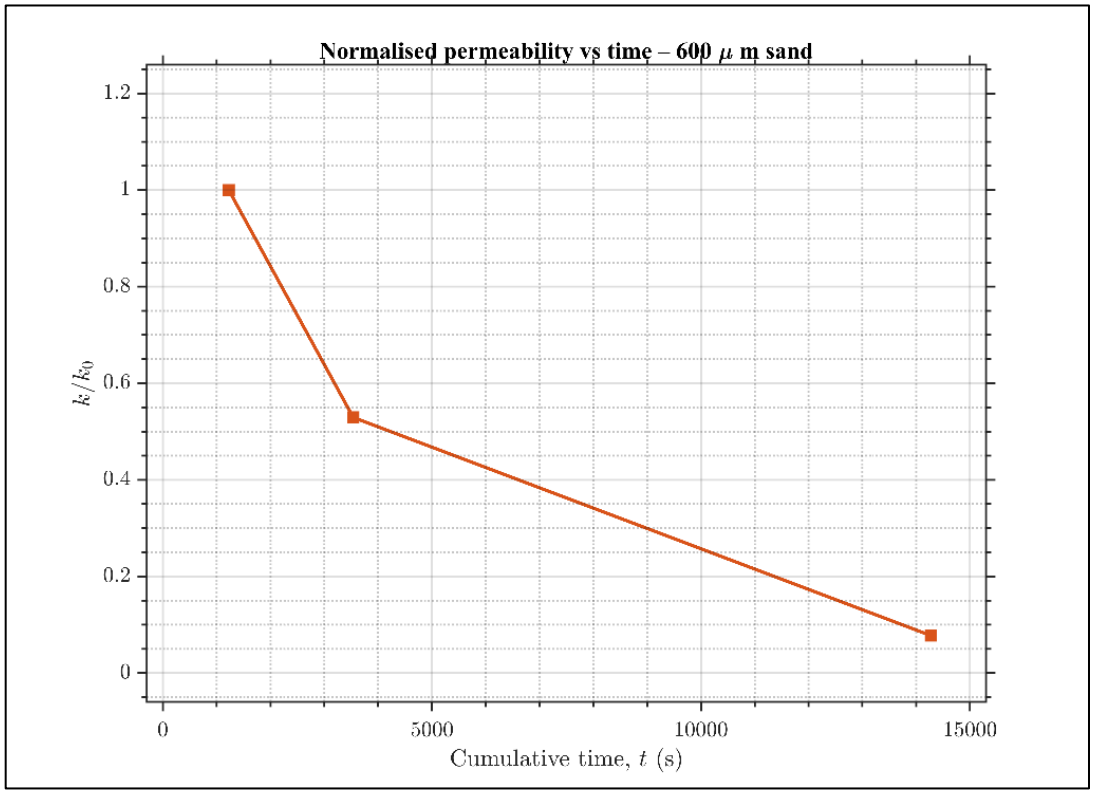
Normalised permeability vs time – 600 μ m sand
k/k0
Cumulative time, t (s)

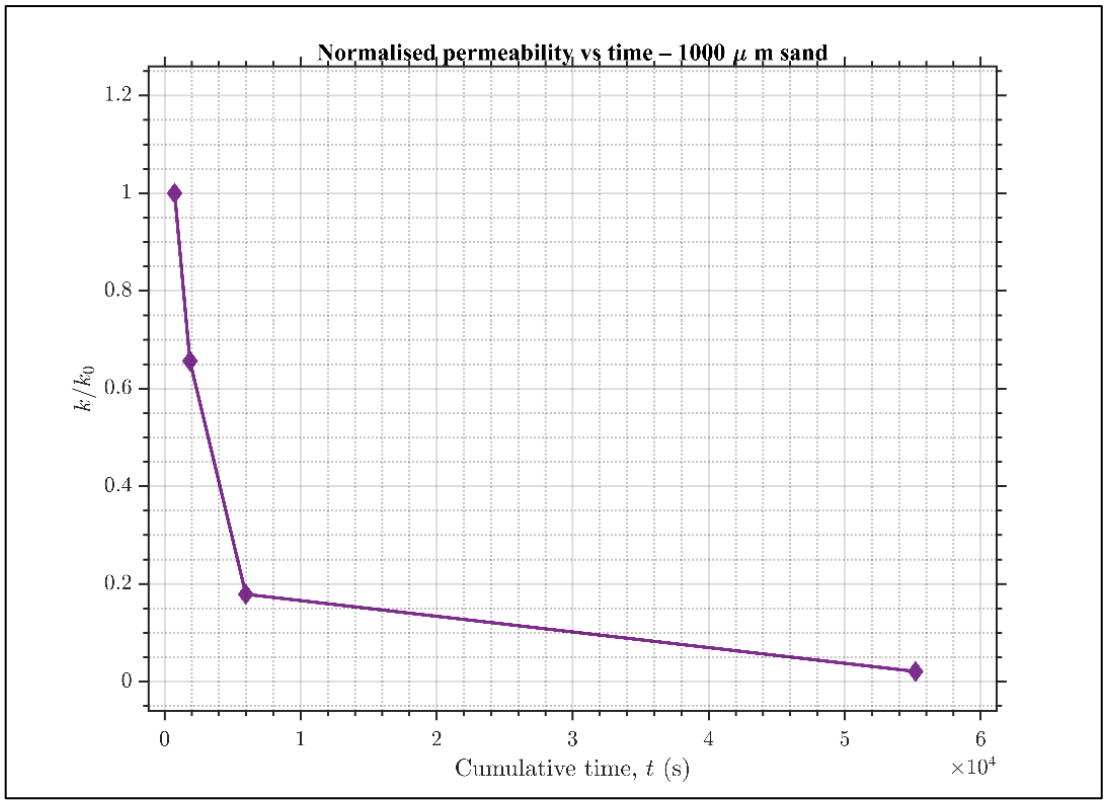

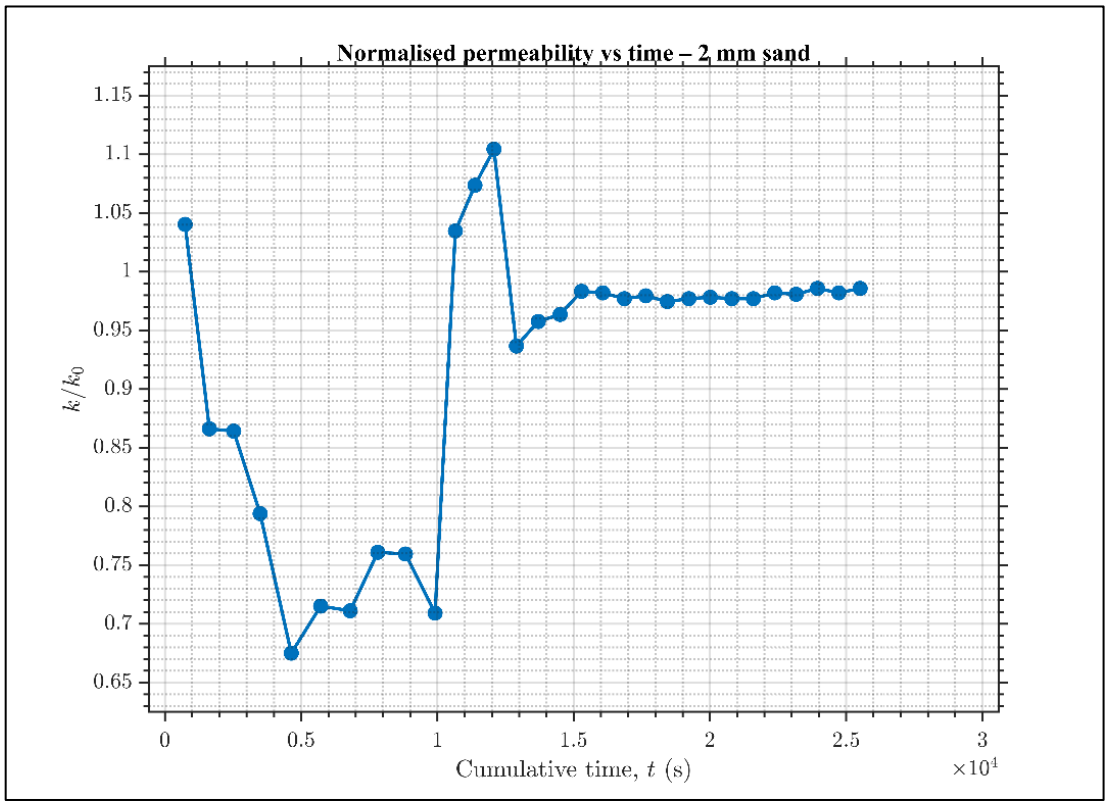

FIGURE 4.5: Temporal evolution of normalized hydraulic conductivity (permeability) for 300 µm, 600 µm,1000 µm and 2000 µm sand columns showing time-dependent K degradation

4.4.4 Grain Size Dependence of Transport Behaviour

The experimental results reveal grain-size-dependent patterns in microplastics breakthrough timing, concentration profiles, and associated hydraulic property changes across the four grain sizes investigated.

Breakthrough timing, defined as the elapsed time from injection to first detection at the column outlet, showed grain-size dependence. Fine sand (300 μm) exhibited the most delayed breakthrough. Coarse sand (2000 μm) and intermediate-medium sand (1000 μm) displayed early breakthrough. Medium sand (600 μm) showed intermediate breakthrough timing. This relationship reflects grain-size-dependent pore throat dimensions and flow characteristics, supporting advective-dominated transport in the early breakthrough phase.

Porosity degradation showed inverse correlation with grain size across all four materials. Fine sand experienced substantial porosity reduction, coarse sand showed negligible change, while medium and intermediate-medium sands exhibited moderate reductions of decreasing magnitude with increasing grain size. Intermediate-medium sand porosity loss was less severe than medium sand but more pronounced than coarse sand, maintaining its position within the transitional regime. This systematic relationship indicates that finer grain sizes provide greater pore surface area and more complex pore geometry conducive to microplastics accumulation and bridging, with transitional behaviour emerging in the intermediate grain size range where pore geometries provide partial but incomplete retention capacity.

Hydraulic conductivity loss similarly correlated inversely with grain size across the grain size spectrum. Fine sand experienced severe conductivity reduction approaching complete flow capacity loss, medium sand showed substantial but less severe reduction, intermediate-medium sand exhibited moderate degradation, while coarse sand maintained near-baseline values throughout. The intermediate-medium sand occupied a distinct position in this continuum, demonstrating measurable hydraulic impairment without the catastrophic degradation observed in finer materials. The magnitude of conductivity loss substantially exceeded what would be expected from porosity reduction alone in fine and medium sands, suggesting additional mechanisms such as preferential blockage of primary flow pathways. Intermediate-medium sand showed more proportionate conductivity loss relative to porosity

reduction, indicating transitional behaviour where flow pathway blockage is significant but not dominant.

Correlation patterns between transport parameters varied systematically with grain size. The correlation between porosity and hydraulic conductivity remained consistent across all materials.

These grain-size-dependent indicate that grain size represents a primary controlling variable for microplastics transport behaviour in the saturated porous media examined. The systematic progression from attachment-dominated transport in coarse materials through transitional behaviour in intermediate-medium and medium sands to straining-dominated retention in fine materials demonstrates the critical role of particle-to-pore throat size ratios in governing retention mechanisms and hydraulic consequences.

4.4.5 Summary of Experimental Results

The column transport experiments characterized microplastics behaviour across grain sizes spanning fine to coarse sand fractions (300–2000 μm). All materials transported microplastics to the outlet despite differences in timing and concentration profiles. Fine and intermediate-grained materials experienced severe hydraulic property degradation coupled with substantial porosity reduction, while coarser materials maintained functional flow capacity with minimal porosity change. These results demonstrate grain-size-dependent vulnerability to microplastics-induced pore clogging, with implications for contaminant transport and aquifer resilience to microplastics contamination.

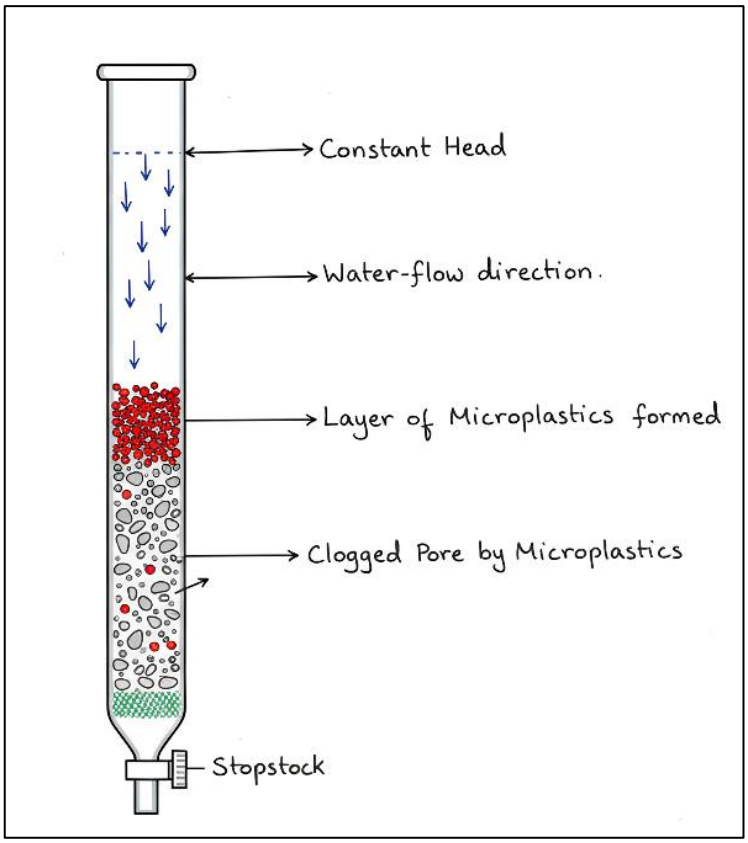

Figure 4.6: Schematic of the Post Experimental for the Porous Media Column Study.

Figure 4.7: Cross-sectional visualization of microplastic particle retention at pore throats in sand column

4.5 Discussion

4.5.1 Physical Mechanisms Governing Size-Dependent Transport

The experimental results reveal grain-size-dependent microplastic breakthrough and retention patterns consistent with physical straining as the dominant retention mechanism. In fine and intermediate sand (300 μm and 600 μm), the smaller pore-throat diameters (36–38 μm and 71–74 μm respectively, from Table 4.2) relative to the median microplastic size (42 μm, from Table 4.3) create conditions where particles can lodge at pore constrictions, particularly those particles exceedingly approximately 30–50 μm in their largest dimension. This size-dependent trapping, termed straining, is a well-established retention mechanism in colloid transport and becomes increasingly important as particle-to-pore-throat ratios increase. In coarse sand (2000 μm), where pore-throat diameters are estimated at 227-237 μm, the much larger pore space relative to microplastic size (up to 68 μm, d_{90}) permits particle passage through the porous medium with minimal mechanical obstruction.

The breakthrough curves support this interpretation. Early breakthrough in coarse sand (Figure 4.1) reflects rapid advection through large pores with minimal retention, whilst delayed breakthrough in fine sand reflects higher retention capacity and more tortuous flow paths through smaller pores. The sustained elevated outlet concentrations in fine sand following peak breakthrough (Figure 4.1) suggest that some retained particles continue to elute over time, potentially through mobilisation of loosely trapped particles or gradual desorption from grain surfaces, though the weak correlation between outlet concentration and porosity/conductivity changes (Section 4.4.4) indicates that particle elution operates relatively independently of macroscopic pore-space reduction over the experimental timescale.

4.5.2 Hydraulic Property Evolution and Pore Clogging

The substantial reduction in hydraulic conductivity observed in fine and intermediate sand (Figures 4.4.3) reflects progressive loss of flow capacity through pore obstruction by accumulated microplastics. The near-exponential form of the conductivity decline, particularly in fine sand, is consistent with pore-scale bridging or cake-layer formation, where retained particles accumulate to block primary flow pathways. The strong positive correlation between porosity and hydraulic conductivity across all materials (Section 4.4.4)

suggests that pore-space reduction is the primary driver of conductivity loss, rather than other processes such as grain surface modification or flow path alteration.

However, the magnitude of conductivity loss in some cases appeared to exceed what would be expected from the measured porosity reduction alone, suggesting that selective blockage of high-permeability flow pathways may amplify the hydraulic impact of microplastic accumulation beyond the simple geometric reduction in pore volume. This interpretation is supported by observations in comparable studies showing that particle deposition preferentially occurs in larger, higher-velocity pores, thereby reducing overall flow capacity disproportionately.

The stability of hydraulic conductivity in coarse sand, despite possible microplastic passage, indicates that the pore space is sufficiently large to accommodate particle transit without significant flow obstruction, even under sustained microplastic input. This finding aligns with field-based observations: coarser aquifer materials may actually be more vulnerable to microplastic transport (i.e., breakthrough to groundwater and distal aquifers), whilst finer materials are more vulnerable to local accumulation and aquifer clogging.

4.5.3 Comparison with Field Observations

The field investigations in Chapter 3 documented preferential microplastic occurrence in sandy formations (11.2 particles per sample) compared to clayey zones (8.7 particles per sample). The laboratory results provide a partial mechanistic explanation: fine and intermediate sand retain substantial microplastic mass through straining, yet do eventually allow breakthrough (Figure 4.1), suggesting that field-derived groundwaters can contain mobile microplastics despite sandy sediments' high retention capacity when subjected to continuous contamination input over extended periods. The field-observed spatial patterns may thus reflect both the retention properties demonstrated in the lab (finer materials trapping more particles) and the connectivity and driving forces in natural hydrogeological systems (high-permeability alluvial corridors near rivers acting as transport pathways).

The temporal variability in field concentrations (pre-monsoon 249 particles vs. post-monsoon 387 particles total across the study area from Chapter 3) is consistent with the experimental observation that breakthrough behaviour depends on cumulative water throughput and that mobilisation of retained particles occurs gradually. The seasonal pulse

associated with monsoon recharge may serve to mobilise previously trapped microplastics, explaining the modest but detectable increase in post-monsoon field concentrations in riverine zones.

4.5.4 Aquifer Vulnerability and Management Implications

The experiments demonstrate that grain-size distribution fundamentally governs both microplastic breakthrough timing and hydraulic consequences. fine sand (300 μm and finer materials)show the highest vulnerability to hydraulic degradation through pore clogging, whilst coarser materials enable faster microplastic transport with less hydraulic impact. This trade-off has important implications: Aquifers dominated by fine-grained aquifers may act as natural filters, protecting deeper and coarser formations from microplastic penetration, but at the cost of potential long-term permeability loss and aquifer dysfunction if microplastic loading persists.

The experiments do not address whether natural hydrogeochemical conditions (e.g. pH, ionic strength, presence of organic matter) would alter these patterns. Field groundwaters in urban settings often contain elevated ionic strength and dissolved organic matter, both of which could enhance microplastic aggregation or attachment to grain surfaces, potentially modifying the breakthrough and clogging dynamics observed under the idealized conditions of these experiments. Similarly, the heterogeneity of natural aquifer lithologies and the presence of preferential flow pathways (fractures, highly permeable layers) would likely alter particle transport on field scales compared to the uniform, well-packed sand columns employed here.

4.6 Conclusions

4.6.1 Key Findings

Laboratory column experiments on four sand grain sizes (300 μm, 600 μm, 1000 μm, 2000 μm) spanning fine to coarse sand fractions reveal systematic grain-size-dependent control on microplastic transport and retention in saturated porous media:

Breakthrough timing and magnitude inversely correlated with grain size, with fine sand showing delayed breakthrough and sustained elevated outlet concentrations, whilst coarse sand exhibited early breakthrough with high concentration variability.

Intermediate-medium sand demonstrated transitional transport behaviour falling between medium and coarse fractions. Breakthrough timing and concentration patterns occupied an intermediate position, reflecting pore geometries where neither complete retention nor unimpeded transport dominated.

Hydraulic conductivity degradation severity correlated inversely with grain size. Fine and intermediate sand experienced substantial conductivity reduction, intermediate-medium sand showed moderate degradation, whilst coarse sand maintained near-baseline conductivity despite microplastic passage.

Porosity reduction patterns followed grain size trends, ranging from substantial decline in fine sand to negligible change in coarse sand. Intermediate-medium sand exhibited moderate porosity loss, indicating measurable but non-catastrophic pore space reduction.

Straining emerges as the primary retention mechanism in fine to intermediate grain sizes, with the relative size of microplastic particles to pore-throat diameters being a key control on breakthrough behaviour. The transitional regime observed in intermediate-medium sand indicates a critical threshold where attachment and straining contribute comparably to overall retention.

4.6.2 Limitations and Future Research Needs

Experimental scope: The experiments employed only PVC fragments and fibres; results may not generalise directly to other polymer types (polyethylene, polystyrene, polyurethane) detected in field samples (Chapter 3), which may exhibit different surface properties and transport behaviours.

Environmental conditions: Experiments were conducted using deionised water under constant flow conditions; natural groundwater conditions include variable pH, ionic strength, dissolved organic matter and microbial activity, which may alter microplastic aggregation, attachment and mobilisation. The simplified geochemistry limits direct application to field conditions.

Temporal scale: Laboratory experiments span hours to days; natural aquifer evolution occurs over years to decades. The progression of hydraulic property changes and particle-matrix interactions over longer timescales remains unknown. Additionally, microplastic

degradation and fragmentation under natural conditions would alter particle-size distributions and transport behaviour over extended periods.

Aquifer heterogeneity: Experiments employed uniform, well-packed sand; natural aquifers exhibit layered lithologies, variable porosity, preferential flow pathways and non-uniform packing, all of which would modify transport compared to idealised columns. Heterogeneity likely accelerates microplastic movement relative to the breakthrough times observed in homogeneous sand.

Grain shape and surface properties: Whilst experiments used angular quartz sand representative of many aquifer materials, grain shape, mineralogy and surface roughness are known to influence particle-grain interactions and may affect retention behaviour under conditions differing from those tested.

Hydraulic gradient and flow rate: The fixed flow conditions (constant head 0.15–0.17 m over 0.1 m column length) correspond to specific hydraulic gradients and flow velocities; natural aquifers experience variable hydraulic gradients seasonally and spatially. Breakthrough and clogging behaviour under variable flow conditions remains to be characterised.

Intermediate grain size characterisation: While the inclusion of intermediate-medium sand provides insight into transitional transport regimes, additional grain sizes within the 600–2000 μm range would further refine understanding of the critical threshold where retention mechanisms transition from straining-dominated to attachment-dominated behaviour.

Future research should explore the transport of mixed polymer assemblages, the effects of realistic hydrogeochemical conditions (variable pH, natural organic matter, co-contaminants), the fate of microplastics over extended laboratory timescales, and numerical modelling to upscale laboratory observations to field-scale heterogeneous systems. Investigation of additional intermediate grain sizes would improve characterisation of transitional transport regimes relevant to heterogeneous aquifer systems.

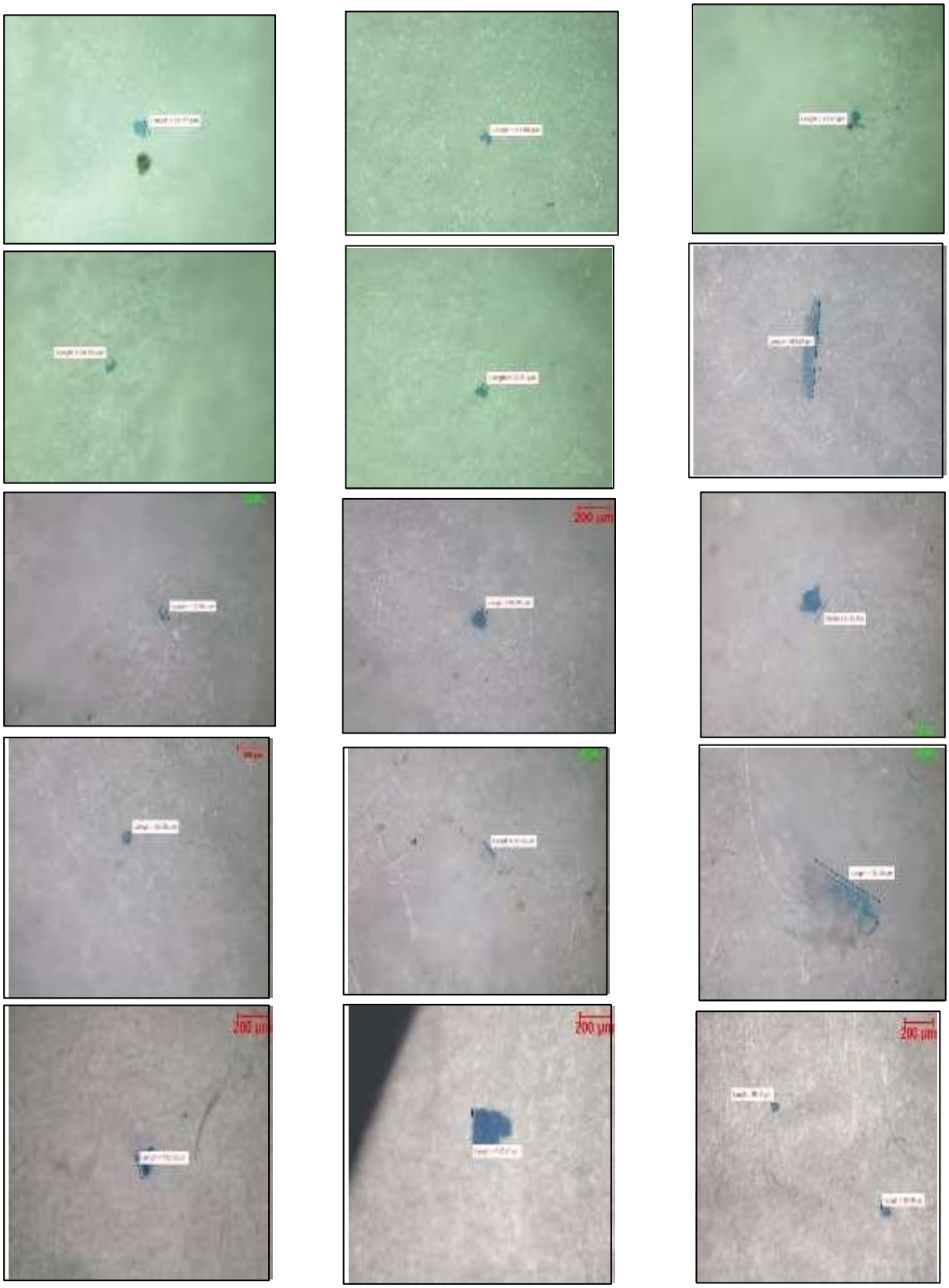

Gallery 1: Pictures of Microplastics from the outlet of the experimental setup

Chapter 5 – Numerical Modelling of Microplastic Transport in Porous Media

5.1 Introduction to Numerical Modelling Framework

Despite growing awareness of MPs contamination in surface waters, oceans, and soils, the fate and transport of these particulate contaminants in groundwater systems remain insufficiently understood. This knowledge gap hinders our ability to assess potential risks to groundwater resources and develop effective mitigation strategies. Numerical modelling offers a powerful approach to elucidate the complex mechanisms governing MP transport through porous media characteristic of aquifers and to predict their long-term fate under varied environmental conditions.

The primary objective of this numerical modelling framework is to develop understanding of the processes controlling microplastic transport through water-saturated porous media. This chapter formulates a mathematical model that captures the dominant processes governing microplastic transport, including advection, retention mechanisms (attachment, detachment, and straining), and the dynamic evolution of hydraulic properties due to particle accumulation. The model is evaluated across four representative grain sizes (fine: 300 μm, medium: 600 μm, intermediate-medium: 1000 μm, and coarse: 2000 μm) to assess how grain size distribution influences transport and retention behaviours. Following validation against laboratory column experiments (Chapter 4), scenario-based analysis provides insights for groundwater protection and management strategies

This modelling effort integrates colloid filtration theory, advection-dispersion principles, and porous media clogging concepts, adapted for microplastic particles. Unlike dissolved contaminants, microplastics represent discrete particles with transport behaviours influenced by both physicochemical and mechanical filtration processes. The model focuses on fundamental processes of advection, attachment, detachment, and straining, while accounting for evolution of hydraulic properties due to particle accumulation.

Understanding microplastic transport in groundwater systems addresses several needs. Groundwater represents a resource for drinking water supply, and contamination by microplastics could pose potential risks. While surface water microplastics have been studied, the subsurface may act as a sink for these persistent contaminants, with implications

for ecosystem health that remain largely unexplored. The model addresses these knowledge gaps by providing a framework to understand and predict microplastic transport in groundwater systems, accounting for grain size-dependent retention mechanisms and evolution of hydraulic properties.

The model utilizes MATLAB as computational platform, chosen for its capabilities in solving systems of coupled differential equations, matrix operations, and visualization features. The core of the model is a one-dimensional reactive advection-dispersion equation for microplastics in saturated porous media accounting for dynamic evolution of hydraulic properties.

The numerical method employs a finite difference method with explicit time-stepping scheme whose stability is ensured by satisfying conditions on the time step. Spatial discretisation is implemented using centred schemes for dispersion and advection terms.

A feature of this simulation environment is its ability to account for dynamic evolution of porosity and permeability due to microplastic retention. This is achieved through coupling transport equations with constitutive relationships that update hydraulic properties based on local concentration of retained particles. The model also incorporates Forchheimer corrections for non-Darcian flow, enabling simulation of flow regimes that deviate from linear Darcy behaviour.

The MATLAB code provides a framework allowing specification of various input parameters, including grain size, particle diameter, initial porosity, and flow conditions. Two scenarios can be simulated: pulse injection of microplastics, representing acute contamination events, and continuous feeding with exponential decay, mimicking chronic contamination sources. The output provides spatial and temporal distributions of microplastic concentrations, retention profiles, and evolving hydraulic properties.

The simulation environment handles a range of grain sizes, with focus on coarse, medium, intermediate-medium, and fine sand grain diameters, enabling investigation of grain size effects on microplastic transport and retention. This feature is relevant for understanding microplastic fate in heterogeneous aquifer systems with varying grain size distributions.

The model captures the interplay between transport processes and media properties. Breakthrough curves for different grain sizes show patterns reflecting dominant retention mechanisms: limited retention in coarse sand versus dominant straining in fine sand. This capability to differentiate transport behaviours across grain sizes is relevant for prediction of microplastic fate in heterogeneous aquifer systems.

5.2 Mathematical Formulation of the Transport-Deposition Model

5.2.1 Mass Transport Equations for Microplastics

The transport of microplastic particles through water-saturated porous media involves complex interactions between the particles and the porous matrix. Unlike dissolved contaminants, MPs are subject to various retention mechanisms including attachment to solid surfaces, detachment due to hydrodynamic forces, and physical straining in pore constrictions. The fundamental governing equation for the mobile microplastic concentration in the liquid phase is based on the advection-dispersion equation with additional terms accounting for mass exchange between the liquid and solid phases):

$$\frac{\partial C_\varepsilon}{\partial t} = -\frac{\partial CU\beta}{\partial x} + \varepsilon D\frac{\partial^2 C}{\partial x^2} - R(C,S) \quad , \quad \frac{\partial(1-\varepsilon)S}{\partial t} = R(C,S) \qquad (5.1)$$

where C represents the concentration of suspended microplastic particles in the liquid phase [M/L³], S is the concentration of retained microplastic particles in the solid phase [M/M], β = velocity adjustment coefficient, U is the depth-averaged Darcy velocity [L/T], D is the hydrodynamic dispersion coefficient [L²/T], ε is the porosity [-], R is the reaction term lumping attachment, straining and detachment processes, t is time [T], and x is the spatial coordinate [L]. The solid-phase accumulation is governed by:

$$R(C,S) = \varepsilon(k_{att} + k_{STR})C - (1-\varepsilon)k_{det}S \qquad (5.2)$$

This coupled system accounts for the bidirectional mass transfer between the mobile and retained phases through attachment and detachment processes, as well as irreversible retention through straining. The retained concentration approaches a maximum capacity, reflecting the finite availability of attachment sites in the porous medium. The denominator in the solid-phase equation ensures mass conservation as porosity evolves due to particle accumulation. This formulation captures the coupled nature of microplastic transport and retention, where the accumulation of particles affects the hydraulic properties of the medium,

which in turn influences transport behaviour. Unlike conventional colloid transport models, this approach explicitly accounts for the feedback between retention and flow conditions, which is essential for accurately simulating long-term microplastic accumulation in groundwater systems.

5.2.2 Advection, Dispersion, Straining, and Retention Mechanisms

The transport and retention of microplastic particles in porous media is governed by several distinct physicochemical mechanisms, each represented mathematically in the model formulation.

Advection represents the transport of microplastic particles with the bulk fluid flow. The advective flux is described by UC. Following the approach of Tosco et al. (2009), the model accounts for the temporal and spatial evolution of velocity due to porosity changes resulting from microplastic retention.

Dispersion accounts for the spreading of microplastic particles due to mechanical mixing and molecular diffusion. The hydrodynamic dispersion coefficient D combines these effects and is expressed as

$$D = \alpha_L \cdot v + D^* \tag{5.3}$$

where α_L is the longitudinal dispersivity [L], v is the interstitial velocity (v=U/eps), and D* is the effective molecular diffusion coefficient [L^2/T]. Anyway, the diffusion and dispersion are not assumed dominant in the transport process of MP in porous media, and a constant value of the Dispersion-diffusion coefficient will be adopted. The limitation of this assumption is discussed in the following.

Attachment and Detachment mechanisms govern the reversible transfer of microplastic particles between the liquid and solid phases. Following the colloid filtration theory approach described by Tufenkji and Elimelech (2004), the attachment coefficient k_{att} is modelled as a function of the flow velocity, grain size, and microplastic properties:

$$k_{att} = k^*_{att}\left(1 - \frac{S}{S_{max}}\right) \tag{5.4}$$

$$k^*_{att} = \frac{U(1-\varepsilon)}{\pi R^2 d_{sand}} \tag{5.5}$$

where $\alpha_{att}$is an empirical attachment efficiency factor, U is the interstitial velocity, ε is the porosity, and d_{sand} is the median grain size of the porous medium. This formulation accounts for the increased collision opportunity between particles and collector surfaces at higher flow rates and in media with smaller grain sizes.

The detachment coefficient k_{det} is related to the attachment coefficient through an empirical relationship:

$$k_{det} = \alpha_{DET} \cdot k_{att} \tag{5.6}$$

where α_{det} is an empirical detachment efficiency factor. This relationship reflects the observation that conditions favouring attachment (high flow rates, smaller grain sizes) also tend to generate higher hydrodynamic forces that can promote detachment, as demonstrated by Wang et al. (2021).

Straining represents the physical filtration of microplastic particles in pore throats that are too small to allow particle passage. Based on the experimental work of Bradford et al. (2003), the straining coefficient k_{str} is modelled as a function of the ratio between the microplastic particle diameter d_{part} and the sand grain diameter d_{sand}:

$$k_{str} = 4.5(\frac{d_{part}}{d_{sand}})^{1.42} \tag{5.7}$$

This empirical relationship indicates that straining becomes increasingly significant as the ratio of particle size to grain size increases. For the sand grain sizes considered in this study (2000,1000, 600, and 300μm) and the microplastic particle size of 50 μm, this ratio ranges from 0.025 to 0.16. Following Bradford et al. (2003), straining is considered dominant when this ratio exceeds 0.10. Accordingly, coarse sand (ratio = 0.025) exhibits attachment-dominated retention, intermediate-medium sand (ratio = 0.05) marks measurable straining onset, medium sand (ratio = 0.083) shows transitional behaviour, and fine sand (ratio = 0.167) operates in the straining-dominated regime.

The simulations reveal distinct transport regimes across the grain size spectrum. For the coarsest sand (2000 μm), attachment dominates the retention process, while straining plays a negligible role. The intermediate-medium sand (1000 μm) occupies an upper transitional regime where attachment becomes the primary retention mechanism, though measurable

straining effects persist, distinguishing it from the purely attachment-dominated coarse fraction. The intermediate grain size (600 μm) exhibits transitional behaviour where both mechanisms contribute to retention, aligning with observations by Lim et al. (2023). For the finest sand tested (300 μm), straining begins to play a more significant role alongside attachment.

5.2.3 Porosity and Permeability Evolution

A distinctive feature of the developed model is its ability to account for the dynamic evolution of hydraulic properties due to microplastic retention. As microplastic particles accumulate in the porous medium, they occupy pore space and reduce the effective porosity. Following the approach proposed by Shen et al. (2020), this reduction is modelled using an exponential decay function:

$$\varepsilon(x,t) = \varepsilon_0 \exp\big(-\gamma\, S(x,t)\big) \tag{5.8}$$

where ε(x,t) is the evolved porosity, ε₀ is the initial porosity, and γ is an empirical porosity decay constant. This exponential relationship reflects the observation that initial particle retention has a relatively minor impact on porosity, but as retention increases, the rate of porosity reduction accelerates due to pore filling and blocking effects.

The evolution of hydraulic permeability is coupled to the porosity changes through a modified Kozeny-Carman relationship, as suggested by Messina et al. (2015):

$$k(x,t) = k_0\, \frac{\varepsilon^3\,(1-\varepsilon_0)^2}{\varepsilon_0^3\,(1-\varepsilon)^2} \tag{5.9}$$

where k(x,t) is the evolved permeability and k₀ is the initial permeability. This relationship captures the non-linear reduction in permeability that occurs with decreasing porosity, accounting for the fact that even small reductions in porosity can lead to substantial decreases in permeability due to the narrowing of flow paths and increased tortuosity.

The coupling between porosity/permeability evolution and flow dynamics is implemented through an updated velocity field calculation. For each time step, the Darcy velocity is recalculated based on the current permeability distribution solving a corrected flow equation and averaging the velocity profile of the cross section(Guo & Zhao, 2003):

$$U = \frac{gJk}{\gamma}\left(1 - \frac{\sqrt{k}}{\sqrt{\varepsilon}R}.Tanh\frac{\left(R\sqrt{\varepsilon}\right)}{\sqrt{k}}\right), \quad \text{valid for } \frac{\sqrt{k}}{R} < 0.01 \tag{5.10}$$

where g is gravitational acceleration [L/T²], J is the piezometric slope [-], k is the local permeability [L²], R is the pipe radius [L], ε is the local porosity [-], and ν is the kinematic viscosity of water [L²/T].

The simulation results demonstrate that porosity and permeability evolution significantly impacts transport dynamics, particularly for finer grain sizes where substantial microplastic retention occurs. For the 300 μm sand, permeability reduction exceeds can exceed 80% near the inlet after prolonged microplastic loading, creating a feedback loop where reduced flow rates further enhance retention through increased residence time and collision opportunities.

5.2.4 Assumptions and Limitations

The numerical model developed for microplastic transport in porous media incorporates several assumptions and simplifications that define its scope and applicability:

One-dimensional flow assumption: The model assumes that transport processes can be adequately represented in one spatial dimension. While this assumption is reasonable for laboratory column experiments with relatively uniform flow fields, it limits the model's applicability to three-dimensional field scenarios where preferential flow paths play significant roles. As Tufenkji and Elimelech (2004) note, this simplification is widely accepted for controlled column experiments but requires careful consideration when extrapolating to field conditions.

Homogeneous media: Within each simulation, the initial properties of the porous medium (porosity, permeability, grain size) are assumed to be uniform throughout the spatial domain. Although the model can simulate different grain sizes across separate simulations(2000,600 and 300μm), it does not account for spatial heterogeneity within a single model domain. This limitation is particularly relevant when considering natural aquifer systems, which typically exhibit significant heterogeneity across multiple scales.

Constant diffusion coefficient: The model assumes a constant diffusion coefficient, which simplifies the numerical implementation but may not capture the complex dependence of

dispersion on local flow conditions and evolving pore geometry. As Shen et al. (2010) demonstrated, dispersion coefficients can vary significantly with changes in pore structure resulting from particle retention.

Spherical particles and collectors: microplastic particles and sand grains are assumed to be spherical. Real microplastics and sand grains often have irregular shapes that could influence their interaction and transport behaviour.

No particle aggregation: The model does not account for potential aggregation of microplastic particles, which could alter their effective size and transport behaviour. This simplification is reasonable for the relatively dilute concentrations used in laboratory experiments but may not hold for higher concentration scenarios or in the presence of natural organic matter that can promote aggregation (Wang et al., 2021).

Simplified surface chemistry: The attachment and detachment processes are modelled using empirical coefficients rather than detailed surface chemistry interactions. While this approach is computationally efficient and can be calibrated to match experimental observations, it may not capture the full complexity of surface interactions that depend on water chemistry, particle surface properties, and collector surface characteristics.

No biological interactions: The model does not account for potential biological interactions such as biofilm formation or biodegradation, which could influence long-term fate and transport of microplastics in natural systems.

Despite these limitations, the model provides a robust framework for understanding the fundamental processes governing microplastic transport in porous media and has demonstrated good agreement with laboratory experiments across a range of conditions. Future enhancements could address these limitations by incorporating more detailed physiochemical processes, extending to multiple dimensions, and accounting for heterogeneity in media properties.

5.3 Numerical Implementation

5.3.1 Finite Difference Discretization

The governing equations and constitutive relations are solved numerically using an explicit finite difference method. The spatial domain [0, h] is partitioned into N equal intervals of size Δx, and time advances with a step Δt constrained by a stability requirement.

For the mobile phase concentration equation, the spatial derivatives are discretized using central differences. The temporal derivative is approximated using a forward Euler scheme. The resulting discrete equation for the mobile phase concentration at node i and time step n+1 is :

$$C_i^{n+1} = C_i^n - \frac{\Delta t}{2\Delta x}\left[\frac{U_{i+1}C_{i+1}^n}{\varepsilon_{i+1}} - \frac{U_{i-1}C_{i-1}^n}{\varepsilon_{i-1}}\right] + \Delta t D \frac{C_{i+1}^n - 2C_i^n + C_{i-1}^n}{\Delta x^2} - \Delta t \frac{R(C_i^n, S_i^n, \varepsilon_i^n)}{\varepsilon_i^n} + \Delta t C_i^n \gamma (S_i^{n+1} - S_i^n) \tag{5.12}$$

For the solid phase concentration, the update equation is:

$$S_i^{n+1} = S_i^n + \Delta t \, \frac{R\left(C_i^n, S_i^n, \varepsilon_i^n\right)}{1 - \varepsilon_i^n + \gamma \, \varepsilon_i^n \, S_i^n} \tag{5.13}$$

After updating the concentrations, the porosity and permeability at each node are updated using the constitutive relations:

$$\varepsilon_i^{n+1} = \varepsilon_0 \exp\left(-\gamma \, S_i^{n+1}\right) \tag{5.14}$$

$$k_i^{n+1} = k_0 \, \frac{\left(\varepsilon_i^{n+1}\right)^3 (1-\varepsilon_0)^2}{\varepsilon_0^3 \left(1-\varepsilon_i^{n+1}\right)^2} \tag{5.15}$$

Then, the velocity and kinetic rates are recalculated based on the updated hydraulic properties.

The time step Δt is determined to ensure numerical stability according to the diffusive condition :

$$\Delta t = r_{id} \cdot \frac{0.5 \cdot (\Delta x)^2}{D_{xx}} \tag{5.16}$$

where r_{id} is a reduction fact suitably chosen to ensure stability, and D_{xx} is the dispersion coefficient.

5.3.2 Dimensionless Parameters

To facilitate interpretation of the numerical results across different physical scales, flow conditions, and kinetic regimes, several dimensionless parameters are introduced. These groups emerge naturally from the non-dimensionalisation of the governing equations (Section 5.2) and provide a framework for classifying transport behaviour and comparing model predictions with experimental observations.

Darcy Number

The **Darcy number** characterizes the relative importance of the porous medium's intrinsic permeability to the geometric confinement imposed by the system scale. It is defined as:

$$Da = \frac{k}{R^2} \tag{5.17}$$

where k is the intrinsic permeability of the porous medium [L^2] and R is a characteristic length scale of the system (here, the column radius) [L]. A small Darcy number ($Da \ll 1$) indicates a relatively tight medium where flow is strongly constrained by the pore structure, whereas a larger Darcy number corresponds to a more permeable medium where flow paths are less restrictive. In the present simulations, the Darcy number varies spatially and temporally due to the dynamic evolution of permeability (Equation 5.8) as microplastic particles accumulate, providing a quantitative measure of the degree of hydraulic impairment induced by particle retention.

Damköhler Numbers

The family of **Damköhler numbers** compares characteristic reaction (or retention) time scales to the advective transport time scale. For a generic first-order process with rate constant k_r [T^{-1}], the Damköhler number is defined as:

$$Da_r = \frac{k_r L}{U/\varepsilon} \tag{5.18}$$

where L is the characteristic transport length (column length) [L], U is the Darcy velocity [L/T], and ε is the porosity. The ratio U/ε represents the average pore-scale (interstitial) velocity. Physically, Da_r quantifies the number of reaction "events" (attachment, detachment, or straining) that can occur during the time required for a water parcel to traverse the column length.

In this study, three distinct Damköhler numbers are defined corresponding to the primary kinetic processes governing microplastic retention:

Attachment Damköhler Number (Da_{att}):

$$Da_{\text{att}} = \frac{k_{\text{att}} L}{U_0/\varepsilon_0} \tag{5.19}$$

where k_{att} is the first-order attachment rate constant [T^{-1}] (Equation 5.4), and U_0 and ε_0 are the inlet Darcy velocity and initial porosity, respectively. This parameter measures the propensity for microplastic particles to attach to grain surfaces during transit through the porous medium.

Detachment Damköhler Number (Da_{det}):

$$Da_{\text{det}} = \frac{k_{\text{det}} L}{U_0/\varepsilon_0} \tag{5.20}$$

where k_{det} is the first-order detachment rate constant [T^{-1}] (Equation 5.6). This parameter quantifies the reversibility of particle retention: a large Da_{det} indicates that detained particles have sufficient time to detach and remobilize during the transport process.

Straining Damköhler Number (Da_{str}):

$$Da_{\text{str}} = \frac{k_{\text{str}} L}{U_0/\varepsilon_0} \tag{5.21}$$

where k_{str} is the straining rate coefficient [T^{-1}] . This parameter characterizes the efficiency of physical filtration due to size exclusion in pore throats. The interpretation of these Damköhler numbers follows a consistent framework:

- $Da \ll 1$: The kinetic process is slow relative to advective transport. Microplastics are transported largely unaffected by the process, resulting in behavior dominated by advection and dispersion (transport-limited regime).
- $Da \sim 1$: The kinetic process and advective transport occur on comparable time scales. Significant interaction between transport and retention mechanisms is expected, with intermediate breakthrough behavior.
- $Da \gg 1$: The kinetic process is fast relative to advective transport. Microplastics experience strong retention or removal before traveling significant distances (reaction-limited regime).

In the simulation results presented in Tests 2 and 4, the Damköhler numbers are explicitly reported in the figure titles for each scenario. For example, Scenario 1 exhibits $Da_{att} = 0.075$ and $Da_{det} = 0.075$, indicating weak retention processes and near-conservative transport. In contrast, Scenario 6 shows $Da_{att} = 7.5$ and $Da_{det} = 7.5$, indicating strong attachment-detachment dynamics that substantially modify transport behavior relative to the analytical ADE baseline. The systematic variation of Damköhler numbers across the 12 scenarios enables comprehensive exploration of the parameter space and identification of critical thresholds where transport regimes transition.

Porosity-Decay Damköhler Number (Da_γ):

For processes involving dynamic changes in hydraulic properties, an additional Damköhler number characterizes the rate of porosity evolution relative to the experimental or simulation time scale:

$$Da_\gamma = \gamma T_f \tag{5.22}$$

where γ is the porosity decay constant [T^{-1}] and T_f is the total duration of the simulation or experiment [T]. This parameter quantifies the extent of hydraulic property alteration: $Da_\gamma \ll$

1 indicates minimal porosity change over the observation period, whereas $Da_\gamma \sim 1$ or larger indicates substantial pore clogging and permeability reduction that significantly affect flow and transport conditions.

Pore Reynolds Number

The **pore Reynolds number** quantifies the ratio of inertial to viscous forces at the pore scale, providing a criterion for the validity of Darcy's law and the onset of non-linear flow effects. It is defined as:

$$Re_p = \frac{U d_p}{\nu} \tag{5.23}$$

where U is the Darcy velocity [L/T], d_p is a characteristic pore diameter (often approximated as grain diameter divided by a geometric factor) [L], and ν is the kinematic viscosity of the fluid [L²/T]. For small Re_p (typically $Re_p < 1$), viscous forces dominate and flow remains in the linear Darcy regime appropriate for the advection-dispersion framework. Larger Re_p values indicate increasing importance of inertial effects and potential deviations from Darcy's law, which may require Forchheimer corrections or more complex flow descriptions.In the present simulations, the pore Reynolds number remains in the laminar regime ($Re_p \ll 1$) for all tested conditions, consistent with typical groundwater flow velocities and the assumptions underlying the advection-dispersion model. However, as permeability decreases due to microplastic accumulation (particularly in fine-grained media), local flow velocities through remaining open pores may increase, potentially elevating Re_p in heavily clogged regions. The model accounts for such non-linear effects through the Forchheimer-corrected velocity profile .

5.3.2 Boundary Conditions, Initial Conditions, and Dimensionless Parameters

The numerical model was configured to simulate two distinct contamination scenarios, each representing different environmental contexts for microplastic release into porous media. These scenarios were implemented through specific initial and boundary conditions, and the resulting transport behaviour is characterized by using dimensionless parameters that facilitate comparison across different physical scales and conditions.

5.3.2.1 Case 1: Mass Pulse Injection

This scenario represents an instantaneous release of microplastics at a specific location within the spatial domain, simulating an acute contamination event such as a sudden spill or accidental discharge. The initial conditions were defined as:

$$C(x,0) = \begin{cases} \frac{C_{in}}{\Delta x} & \text{if } x = x_0 \\ 0 & \text{elsewhere} \end{cases} \tag{5.24}$$

$$S(x,0) = 0 \quad \text{for all } x$$

where C_{in} is the total injected mass of microplastics per unit cross-sectional area [M/L²], Δx is the spatial discretization step, and x_0 is the location of the pulse injection (set at the midpoint of the column, $x_0 = L/2$, in the implemented simulations).

Analytical Solution for Verification: For the instantaneous pulse injection scenario where all kinetic processes are disabled (attachment, detachment, straining), the transport reduces to the classical advection-dispersion equation with the analytical solution given by:

$$C(x,t) = C_{in} \cdot e^{-\frac{(x - x_0 - Ut/\varepsilon)^2}{4Dt}} \tag{5.25}$$

This solution describes the symmetric spreading of a concentration pulse as it advects downstream with velocity U/ε while undergoing Gaussian dispersion. The solution assumes constant hydraulic properties, steady flow conditions, and serves as the reference baseline for numerical verification.

The boundary conditions for Case 1 were specified to minimize artificial reflections and mass balance errors. At the inlet ($x = 0$), a zero-gradient (Neumann) condition was applied:

$$\left.\frac{\partial C}{\partial x}\right|_{x=0} = 0 \tag{5.26}$$

This condition ensures that no additional mass enters the domain after the initial pulse and that any numerical diffusion near the boundary does not create spurious sources. At the outlet ($x = L$), a semi-infinite or advective boundary condition was imposed:

$$\left.\frac{\partial C}{\partial x}\right|_{x=L} = \frac{U}{D} C(L,t) \tag{5.27}$$

This formulation allows the concentration front to exit the domain without reflection, approximating the behaviour of an infinitely long column downstream of the modeled region. The pulse injection scenario is particularly relevant for understanding the fate of microplastics following accidental releases or isolated contamination events and serves as a stringent test of the model's ability to capture transient transport dynamics.

5.3.2.2 Case 2: Continuous Inlet Feeding

This scenario represents a more persistent contamination source characterized by an initial period of constant concentration feeding followed by exponential decay. Such conditions may arise from ongoing industrial discharges, wastewater treatment plant effluents, or landfill leachate with time-varying microplastic loads. The initial conditions were defined as:

$$C(x,0) = 0 \quad \text{for all } x, \quad S(x,0) = 0 \quad \text{for all } x$$

indicating that the porous medium is initially free of microplastic contamination. The boundary conditions reflect the temporal evolution of the source:

$$C(0,t) = C_0 \text{ for } t > 0 \tag{5.28}$$

where C_0 is the inlet concentration during the constant-feeding phase [M/L³].

The outlet boundary condition remains identical to Case 1 (Equation 5.17).

Analytical Solution for Verification: For the continuous inlet feeding scenario without retention mechanisms, the analytical solution incorporates complementary error functions to describe the advancing concentration front:

$$C(x,t) = \frac{C_0}{2}\left[\text{erfc}\left(\frac{x-Ut/\varepsilon}{\sqrt{4Dt}}\right) + \text{erfc}\left(\frac{x+Ut/\varepsilon}{\sqrt{4Dt}}\right) e^{\frac{Ux}{\varepsilon D}}\right] \tag{5.29}$$

where ′erfc' is the complementary error function. This solution describes the propagation of a concentration front advancing through the porous medium.

This formulation represents realistic contamination scenarios where continuous discharge creates persistent source loading without temporal variation. The continuous feeding allows investigation of long-term accumulation, approach to steady-state conditions, and the interplay between sustained loading and kinetic retention processes

The selection of these two complementary scenarios enables comprehensive model evaluation: Case 1 emphasizes transient dynamics and the spatial evolution of a migrating pulse, while Case 2 focuses on long-term accumulation, approach to steady-state conditions.

Verification Tests: Analytical Baseline Establishment

Two verification tests (Tests 1 and 3) were conducted to establish analytical baselines for comparison with reaction-inclusive scenarios. These tests simulate purely advective-dispersive transport with all kinetic processes disabled ($k_{att} = k_{det} = k_{str} = \gamma = 0$), providing rigorous benchmarks for assessing model accuracy and quantifying the influence of retention mechanisms.

Test 1: Mass Pulse Injection Without Reactions

Test 1 simulates an instantaneous release of microplastics at the column midpoint ($x = L/2$) under purely advective-dispersive conditions, representing the limiting case where retention processes are negligible. The initial conditions specify a normalized pulse ($C_{in} \approx 0.5$) at $x = 0.5$ m with zero-gradient boundaries at inlet and outlet. Simulations were conducted across six final times ($T_f = 5, 10, 20, 30, 40, 50$ s) to capture temporal evolution of the migrating and dispersing pulse. Figure 5.1 presents result for $T_f = 50$ s, demonstrating the pulse evolution from initial release through complete passage of the control section at $x = 0.690$.Spatial concentration profiles at $t = 5, 10, 20, 30, 40, 50$s exhibit characteristic Gaussian spreading with peak positions advancing linearly with time, consistent with constant-velocity advection. The numerical solution (solid-coloured lines) overlays the analytical ADE solution (asterisk markers) with excellent agreement (relative error < 2%), validating the fundamental advection-dispersion implementation.

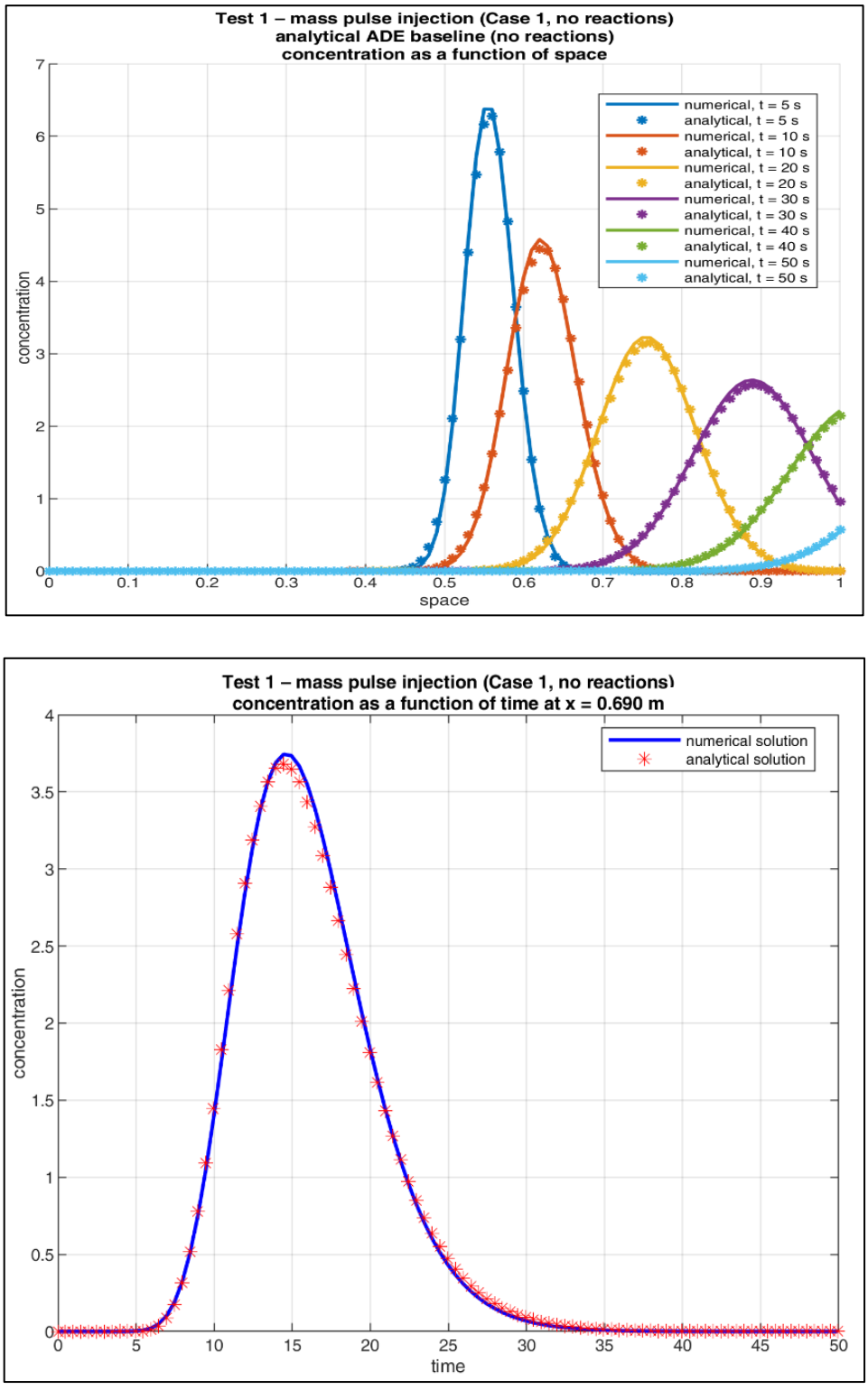

Figure 5.1: Verification of numerical solver for mass pulse injection without reactions (Test 1, T_f = 50 s). (a) Spatial concentration profiles at t = 5, 10, 20, 30, 40, 50 s showing excellent agreement between numerical solution (solid-coloured lines) and analytical ADE solution (asterisk markers). The pulse migrates and disperses according to classical advection-

dispersion theory with symmetric spreading. (b) Breakthrough curve at control section (x = 0.690) demonstrating numerical-analytical agreement over the full-time domain, with symmetric rise and fall characteristic of purely dispersive transport.

The breakthrough curve at x = 0.690 exhibits the symmetric rise-fall pattern expected for reversible, transport-dominated systems, confirming that the numerical scheme accurately captures both advective displacement and dispersive spreading without introducing artificial numerical diffusion or oscillations. This verification establishes confidence in the model's ability to simulate fundamental transport processes before introducing the complexity of retention mechanisms.

Test 3: Continuous Inlet Feeding Without Reactions

Test 3 simulates persistent contamination loading under purely advective-dispersive conditions, representing chronic contamination scenarios where retention processes are absent or negligible. Initial conditions specify a pristine column ($C = S = 0$ everywhere), with a constant inlet concentration ($C_0 = 0.5$) maintained for the duration of the simulation. Simulations extended to $T_f = 100$ s to capture the full development of the concentration front from initial penetration to quasi-steady-state plateau at the control section. Figure 5.4 demonstrates the front propagation and approach to steady state. Spatial concentration profiles (Figure 5.6a) at t = 5–50 s show the characteristic S-shaped front advancing through the column, with the transition zone between pristine ($C = 0$) and contaminated ($C \rightarrow C_0$) regions broadening due to dispersion while the front advances at constant velocity. The numerical solution maintains excellent agreement with the analytical ADE solution throughout the domain (relative error < 3%).

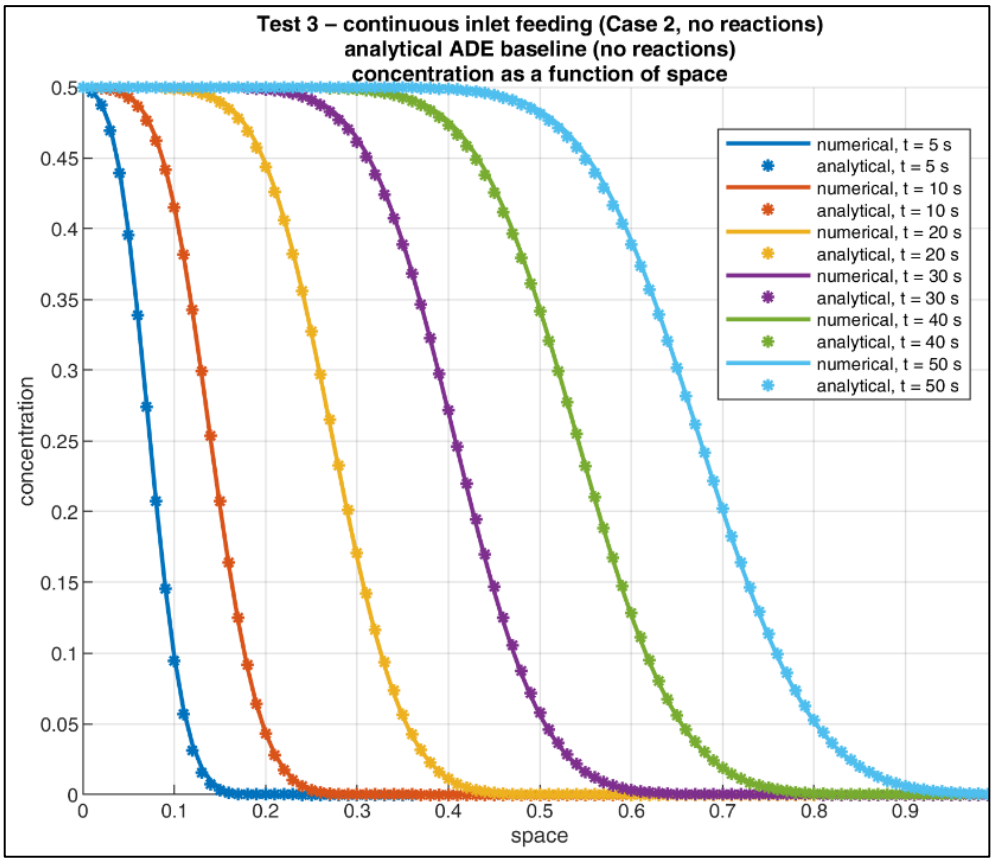
Test 3 – continuous inlet feeding (Case 2, no reactions)
analytical ADE baseline (no reactions)
concentration as a function of space
numerical, t = 5 s
analytical, t = 5 s
numerical, t = 10 s
analytical, t = 10 s
numerical, t = 20 s
analytical, t = 20 s
numerical, t = 30 s
analytical, t = 30 s
numerical, t = 40 s
analytical, t = 40 s
numerical, t = 50 s
analytical, t = 50 s
concentration
space
0
0.05
0.1
0.15
0.2
0.25
0.3
0.35
0.4
0.45
0.5
0.1
0.2
0.3
0.4
0.5
0.6
0.7
0.8
0.9

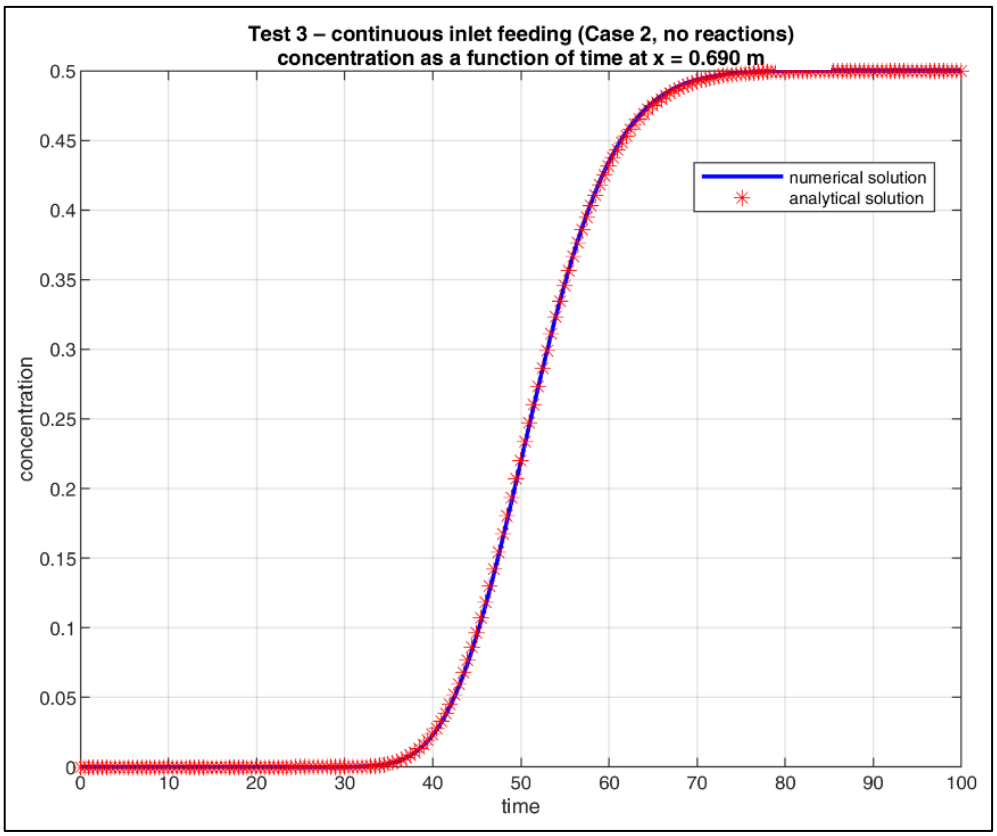
Test 3 – continuous inlet feeding (Case 2, no reactions)
concentration as a function of time at x = 0.690 m
numerical solution
analytical solution
concentration
time
0
0.05
0.1
0.15
0.2
0.25
0.3
0.35
0.4
0.45
0.5
10
20
30
40
50
60
70
80
90
100

Figure 5.2: Verification of numerical solver for continuous inlet feeding without reactions (Test 3, T_f = 100 s). (a) Spatial concentration profiles at t = 5, 10, 20, 30, 40, 50 s showing advancing concentration front with characteristic S-shaped profile. Numerical solution (solid-coloured lines) exhibits excellent agreement with analytical ADE solution (asterisk markers) throughout the spatial domain. (b) Breakthrough curve at x = 0.690 extending to 100 s, demonstrating smooth rise to plateau at $C/C_0 \approx 0.45$. The extended simulation time captures the approach to quasi-steady-state conditions, validating the model's ability to simulate long-term continuous loading scenarios.

The breakthrough curve at x = 0.690 rises smoothly to a plateau near $C/C_0 \approx 0.45$ by t = 100 s, demonstrating that the numerical model accurately reproduces the analytical solution even for extended simulations under continuous loading. The close numerical-analytical agreement over the full 100 s time window confirms that the model maintains accuracy for long-duration simulations without accumulating numerical errors, establishing a robust baseline for subsequent reaction-inclusive scenarios. The extended T_f = 100 s simulation was specifically motivated by preliminary observations showing incomplete plateau development at T_f = 50 s, which would have limited the ability to assess long-term fate under persistent loading. The 100 s extension provides clear visibility of the full "scene" from initial front arrival through plateau establishment, directly addressing the need to capture complete transport dynamics for continuous feeding scenarios.

Damköhler Number-Based Kinetic Scenarios

Following verification of fundamental transport physics, systematic kinetic scenarios (Tests 2 and 4) were conducted to quantify retention process influences across a wide range of conditions. Twelve scenarios spanning three orders of magnitude in Damköhler numbers were simulated under both pulse injection (Test 2) and continuous inlet feeding (Test 4) boundary conditions. Each scenario employs absolute first-order rate constants for attachment (k_{att}), detachment (k_{det}), straining (k_{str}), and porosity decay (γ), characterized by dimensionless Damköhler numbers defined in Section 5.3.2.3.Three representative scenarios are presented here to illustrate the systematic transition from transport-limited ($Da \ll 1$) to reaction-limited ($Da \gg 1$) regimes. The complete twelve-scenario dataset is documented in the simulation archive.

Test 2: Pulse Injection with Retention Mechanisms

Test 2 employs identical initial and boundary conditions as Test 1 (instantaneous pulse at x = L/2) but activates the full suite of retention mechanisms, enabling direct assessment of kinetic process influences by comparison with the analytical ADE baseline established in Test 1.

Scenario 1: Weak Retention Kinetics (Da_{att} = 0.075)

For weak retention kinetics (k_{att} = 0.001 s^{-1}, k_{det} = 0.001 s^{-1}, k_{str} = 0, γ = 0), pulse transport approximates the analytical ADE solution with only minor modifications.

Figure 5.3 demonstrates that spatial concentration profiles exhibit >90% agreement with the analytical baseline (asterisk markers), with numerical curves (solid-coloured lines) displaying slight attenuation at late times reflecting the cumulative effect of weak attachment processes.

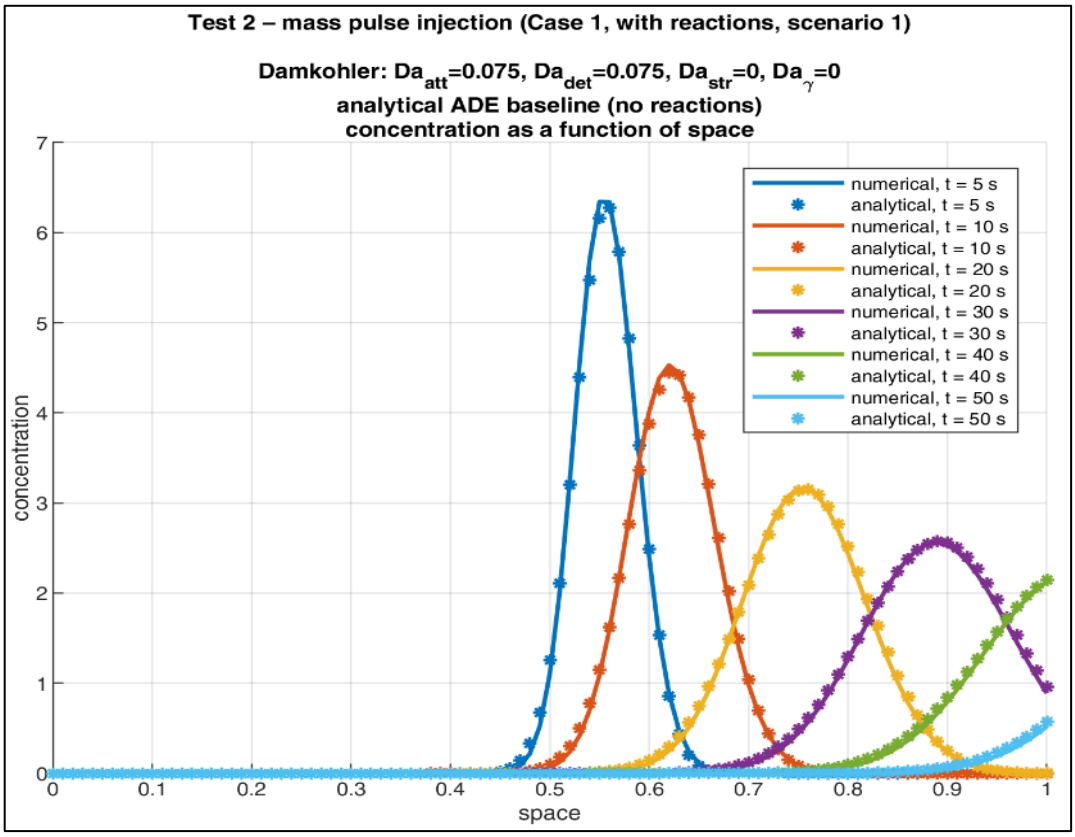

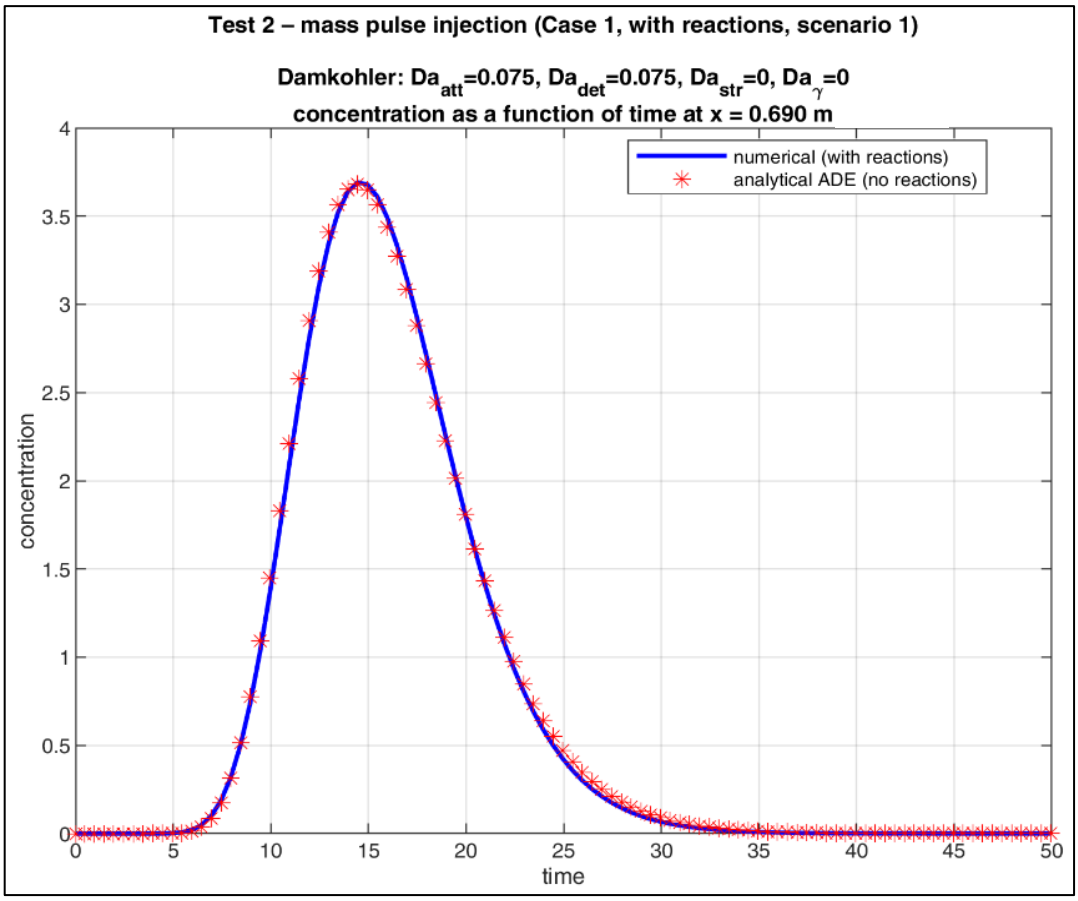

Figure 5.3: Effect of weak retention kinetics on pulse transport (Test 2, Scenario 1: Da_{att} = 0.075, Da_{det} = 0.075, Da_{str} = 0, Da_{γ} = 0). (a) Spatial concentration profiles at t = 5, 10, 20, 30, 40, 50 s showing minimal deviation from analytical ADE baseline (asterisk markers). Solid coloured lines represent numerical solution with retention mechanisms activated, exhibiting >90% agreement with no-reaction reference. (b) Breakthrough curve at control section (x = 0.690) demonstrating peak concentration recovery >85% with minimal tailing, characteristic of transport-dominated regime where $Da_{att} \ll 1$. Parameters: k_{att} = 0.001 s^{-1}, k_{det} = 0.001 s^{-1}, k_{str} = 0, γ = 0.

The breakthrough curve maintains the symmetric rise-fall pattern characteristic of reversible, transport-dominated systems, with peak concentration >85% of the analytical prediction. The minimal tailing observed reflects weak but measurable retention-detachment cycling that introduces slight asymmetry without fundamentally altering transport behaviour. This scenario is representative of coarse-grained aquifers with large pore spaces relative to particle size, where collision efficiency remains low and hydrodynamic forces favour particle remobilization over sustained retention.

Scenario 2: Moderate Retention Kinetics (Da_{att} = 1.5)

Moderate retention kinetics (k_{att} = 0.02 s^{-1}, k_{det} = 0.02 s^{-1}, k_str = 0.0005 s^{-1}, γ = 0) produce clear departures from analytical predictions, marking the transitional regime where attachment and transport occur on comparable timescales. Figure 5.4 reveals spatial profiles with concentration maxima systematically reduced by 50–60% compared to the analytical baseline, with gradients steepening near the inlet (x < 0.2 m) where retention accumulation is most intense.

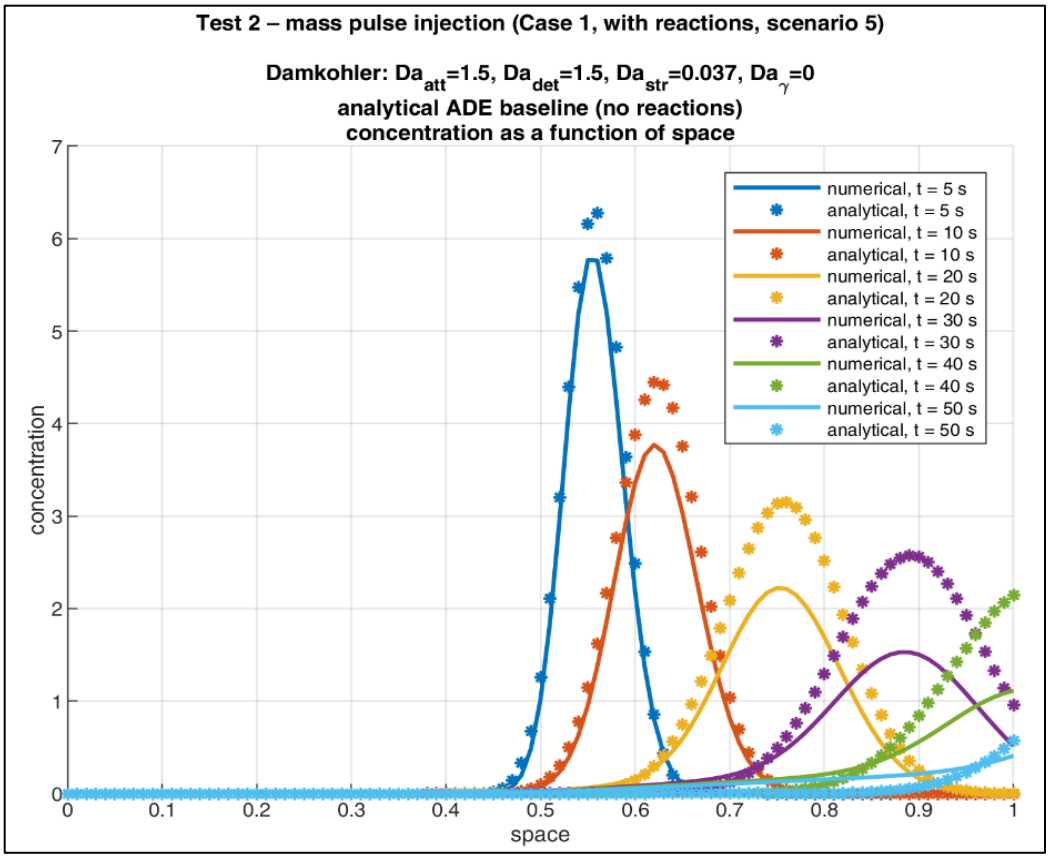

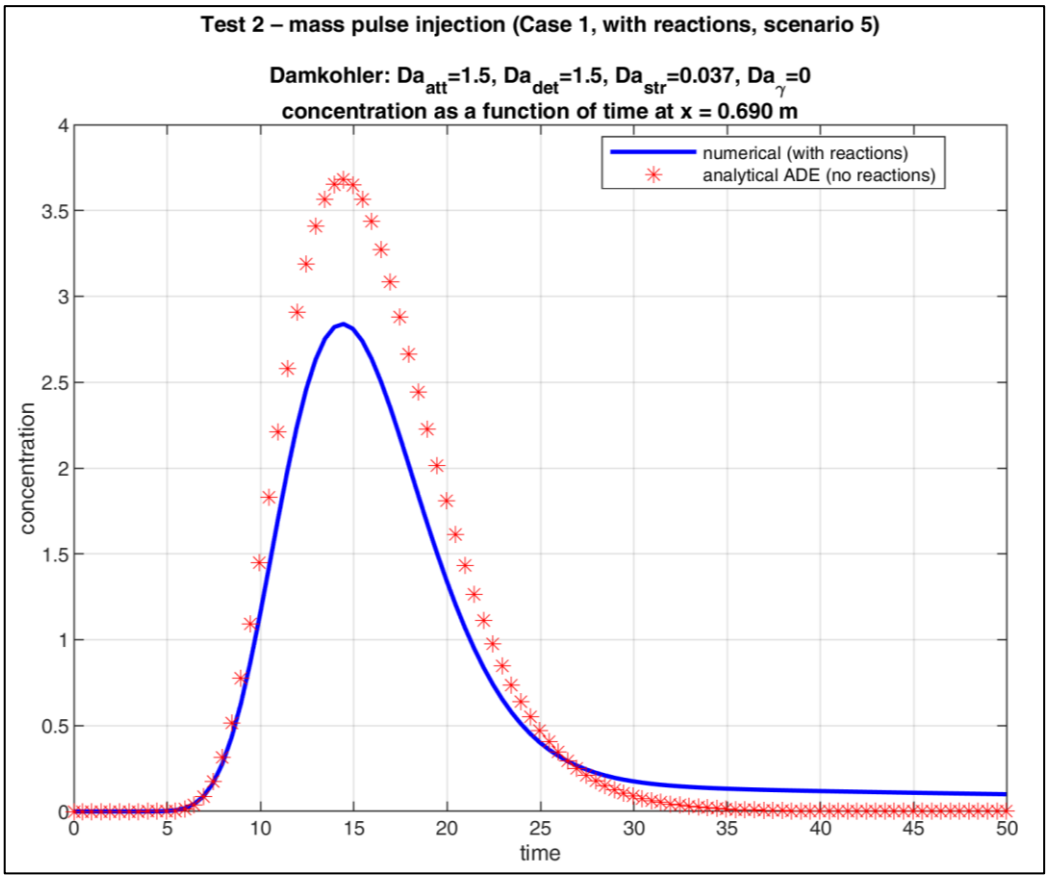

Figure 5.4: Effect of moderate retention kinetics on pulse transport (Test 2, Scenario 5: Da_{att} = 1.5, Da_{det} = 1.5, Da_{str} = 0.037, Da_{γ} = 0). (a) Spatial concentration profiles showing clear attenuation relative to ADE baseline, with steeper gradients developing near inlet (x < 0.2 m) as retention accumulates. Peak concentrations reduced by ~60% compared to analytical solution at all snapshot times. (b) Breakthrough curve demonstrating delayed arrival (peak at t ≈ 35 s versus t ≈ 28 s for ADE), ~60% peak suppression, and extended tailing characteristic of transitional regime where transport and reaction timescales are comparable (Da ≈ 1). Parameters: k_{att} = 0.02 s^{-1}, k_{det} = 0.02 s^{-1}, k_{str} = 0.0005 s^{-1}, γ = 0.

The breakthrough curve exhibits characteristic features of intermediate Damköhler numbers: delayed peak arrival (t ≈ 35 s versus t ≈ 28 s for ADE), substantial peak suppression (~60%), and asymmetric shape with extended tailing. The tailing behaviour reflects gradual remobilization of retained particles through detachment processes operating over timescales comparable to the pulse transit time, creating a secondary source that sustains low concentrations long after the main pulse has passed.

This transitional regime is particularly relevant for medium-grained aquifers where neither transport nor retention overwhelmingly dominates, creating complex coupling between flow dynamics and kinetic processes. The systematic ~60% reduction in peak concentration compared to ADE provides a quantitative measure of natural attenuation effectiveness in this regime, directly informing risk assessment for similar field conditions.

Scenario 3: Strong Retention Kinetics (Da_{att} = 7.5)

Strong retention kinetics (k_{att} = 0.1 s^{-1}, k_{det} = 0.1 s^{-1}, k_{str} = 0.001 s^{-1}, γ = 0) fundamentally alter pulse transport behaviour, with >90% of injected mass retained within x < 0.3 m. Figure 5.5 demonstrates spatial profiles exhibiting hyper exponential decay characteristic of straining-dominated or high-attachment systems, where particles are immobilized on timescales much shorter than advective transport times.

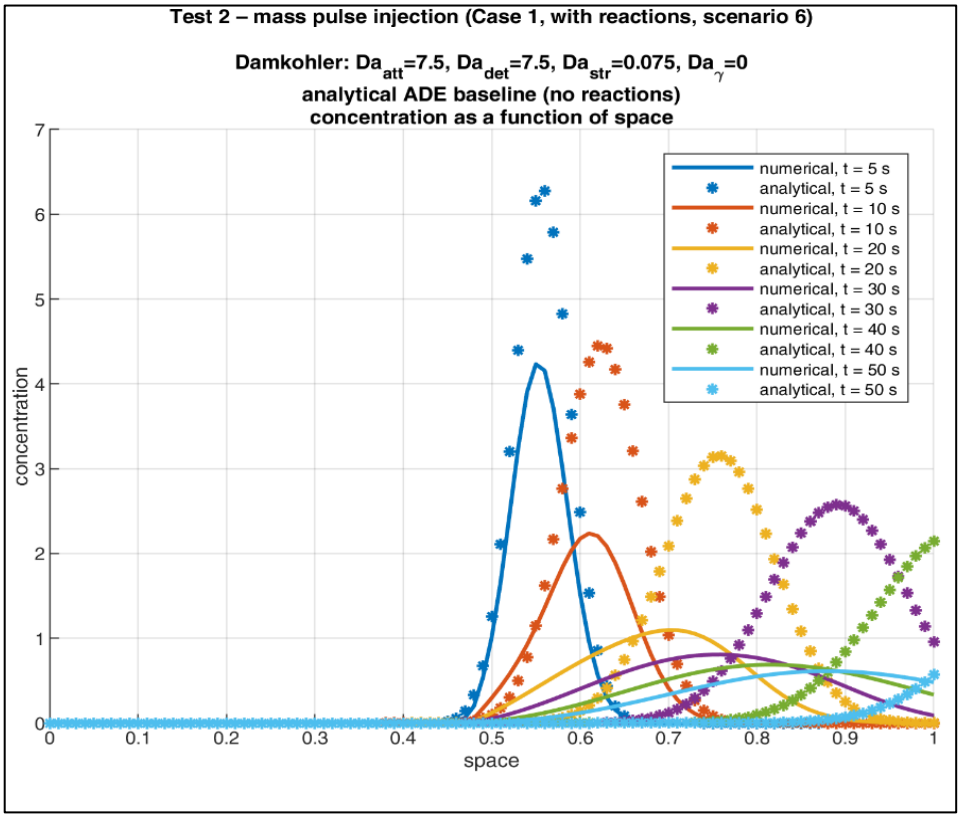

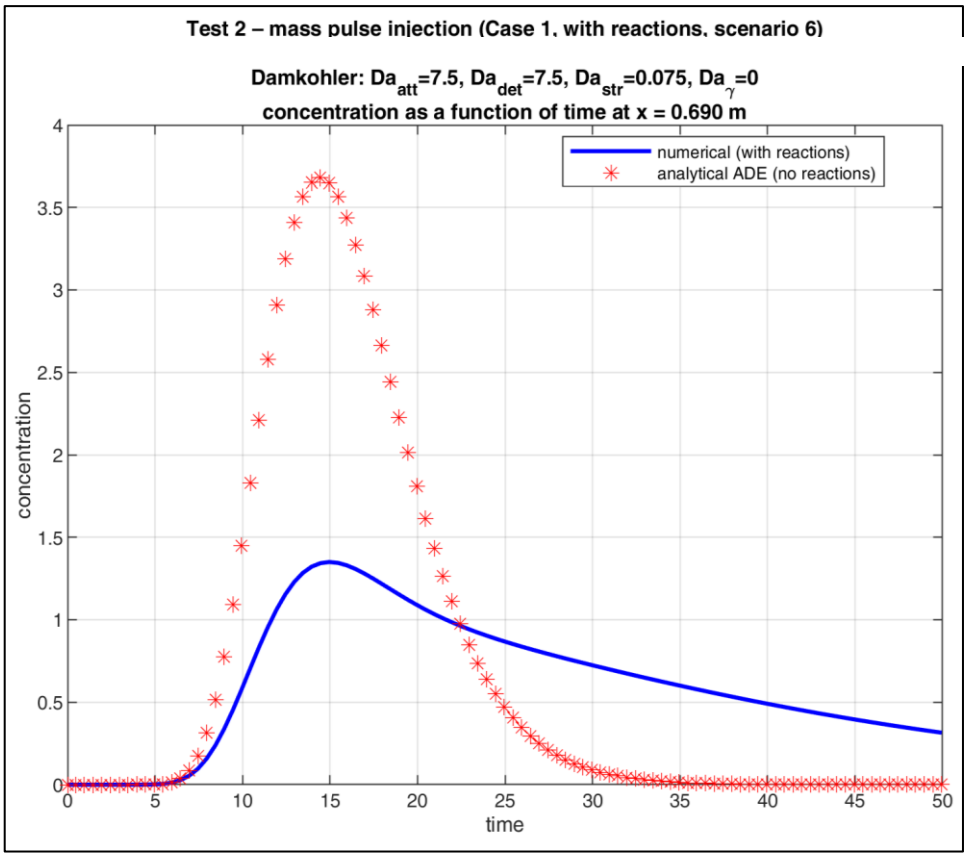

Figure 5.5: Effect of strong retention kinetics on pulse transport (Test 2, Scenario 6: Da_{att} = 7.5, Da_{det} = 7.5, Da_{str} = 0.075, Da_{γ} = 0). (a) Spatial concentration profiles showing dramatic suppression (>90%) relative to ADE baseline. Hyper exponential retention profile develops with maximum concentrations confined to x < 0.3 m, indicating reaction-limited regime where particles are captured before significant advective displacement. Analytical baseline curves (asterisks) become irrelevant as transport is overwhelmed by retention. (b) Breakthrough curve demonstrating reaction-limited regime characteristics: peak concentration <10% of inlet value, arrival delayed to t ≈ 45 s, and extensive low-concentration tailing extending throughout simulation window. Parameters: k_{att} = 0.1 s^{-1}, k_{det} = 0.1 s^{-1}, k_{str} = 0.001 s^{-1}, γ = 0.

The analytical ADE baseline becomes effectively irrelevant in this regime as retention processes completely dominate transport dynamics. The breakthrough curve displays extreme peak suppression (<10% of analytical prediction), delayed arrival (t ≈ 45 s), and persistent low-level tailing that extends throughout the observation window. This extended tailing reflects the slow, gradual release of retained particles through detachment balanced

against continued retention of remobilized particles, creating a quasi-steady state where breakthrough concentrations remain orders of magnitude below inlet values.

This regime is representative of fine-grained aquifers or conditions favouring strong particle-collector interactions (high ionic strength, favourable surface chemistry), where natural attenuation is highly effective but creates potential for secondary release over extended timescales. The >90% retention within 0.3 m provides quantitative evidence of effective natural filtration, though the persistent tailing indicates that complete removal does not occur and low-level contamination may persist indefinitely.

Test 4: Continuous Inlet Feeding with Retention Mechanisms

Test 4 employs continuous feeding boundary conditions (constant inlet concentration for $t \leq 100$ s) with retention mechanisms activated, representing the most realistic scenario for assessing long-term microplastic fate in groundwater systems subject to chronic contamination. The twelve kinetic scenarios from Test 2 are re-evaluated under continuous loading to quantify how persistent sources amplify retention effects relative to pulse releases.

Scenario 1: Weak Retention, Continuous Loading ($Da_{att} = 0.075$)

Under continuous loading with weak kinetics (same parameters as Test 2 Scenario 1), the system approaches quasi-steady state where inlet concentration is maintained while retention processes reach dynamic equilibrium. Figure 5.6 shows spatial front development maintaining characteristics similar to the analytical ADE solution, with only minor retention-induced attenuation. By t = 50 s, concentration at x = 0.690 reaches ~40% of inlet value, approaching the plateau evident in the 100 s breakthrough curve.

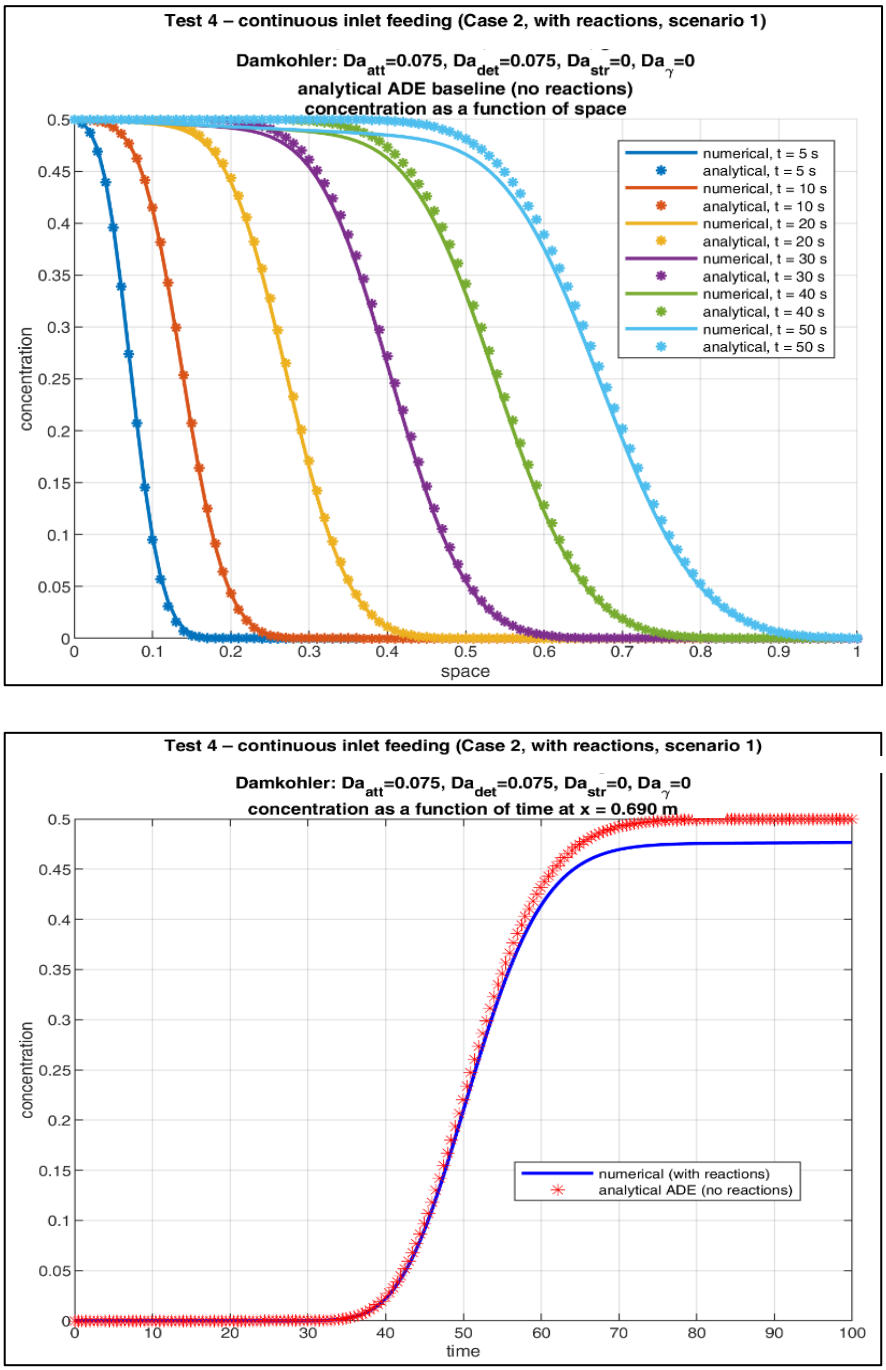

Figure 5.6: Effect of weak retention kinetics on continuous inlet transport (Test 4, Scenario 1: $Da_{att} = 0.075$, $Da_{det} = 0.075$, $Da_{str} = 0$, $Da_{\gamma} = 0$). (a) Spatial front development at t = 5–50 s showing near-ideal ADE behaviour with advancing front maintaining sharp definition and minimal retention-induced attenuation. By t = 50 s, concentration at x = 0.690 reaches ~40% of inlet value, approaching plateau. (b) Concentration at control section rising monotonically to plateau at $C/C_0 \approx 0.45$ by t = 100 s, demonstrating minimal long-term impact of weak retention under persistent loading. Comparison with analytical ADE solution (red asterisks)

shows <10% deviation throughout time domain. Same kinetic parameters as Test 2 Scenario 1.

The concentration at x = 0.690 rises smoothly to a plateau near $C/C_0 \approx 0.45$ by t = 100 s, indicating that even weak retention processes accumulate noticeable effects under persistent loading—the 10% reduction from the no-reaction plateau ($C/C_0 = 0.5$ from Test 3) reflects cumulative retention-detachment cycling. However, the close agreement with the analytical baseline (red asterisks, <10% deviation) confirms that transport remains the dominant control on fate even after 100 s of continuous contamination.

This scenario represents high-vulnerability aquifer conditions where contamination can propagate significant distances downgradient with minimal natural attenuation. Even 100 s of continuous loading produces only modest concentration reduction at x = 0.690 , suggesting that extended transport distances and long-term monitoring requirements are necessary for such systems.

Scenario 2: Moderate Retention, Continuous Loading ($Da_{att} = 1.5$)

Moderate retention under continuous loading (same parameters as Test 2 Scenario 2) reveals the cumulative impact of transitional-regime kinetics over extended timescales. Figure 5.7 exhibits spatial profiles with progressive steepening of concentration gradients, particularly in the upstream half of the domain (x < 0.5 m) where retention accumulation is most intense. By t = 50 s, clear departure from analytical predictions is evident throughout the domain, with concentrations systematically 30–50% below the ADE baseline.

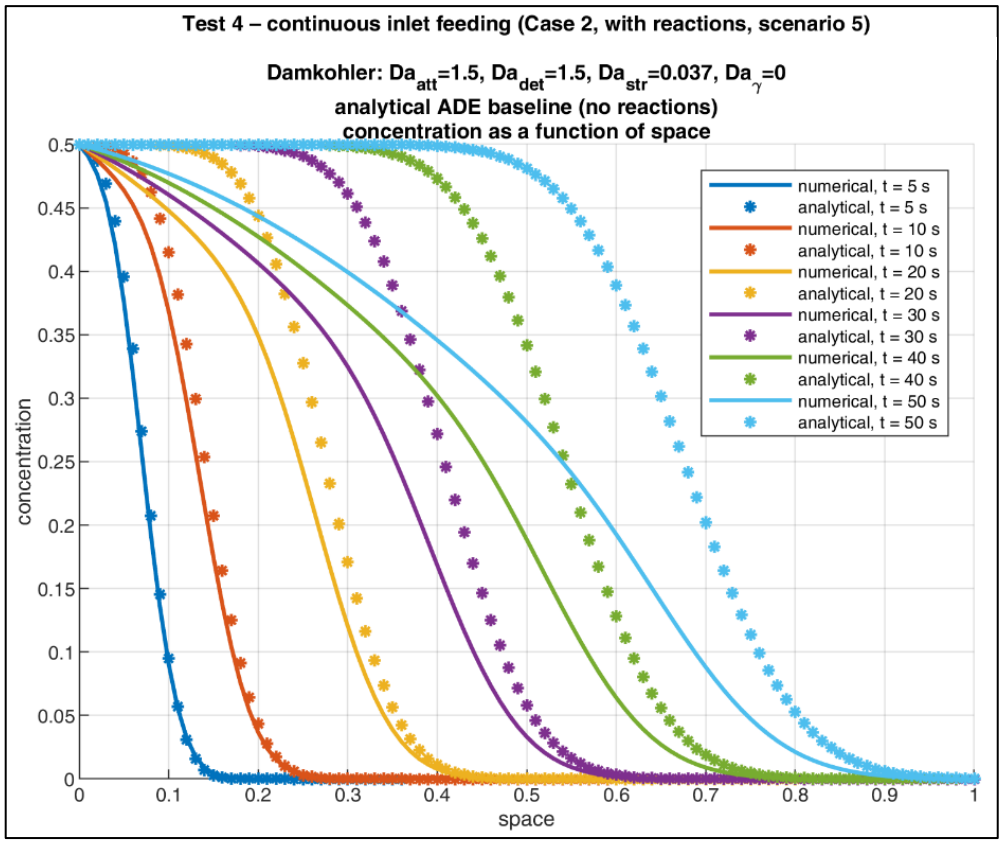
Test 4 – continuous inlet feeding (Case 2, with reactions, scenario 5)
Damkohler: Da_att=1.5, Da_det=1.5, Da_str=0.037, Da_γ=0
analytical ADE baseline (no reactions)
concentration as a function of space
numerical, t = 5 s
analytical, t = 5 s
numerical, t = 10 s
analytical, t = 10 s
numerical, t = 20 s
analytical, t = 20 s
numerical, t = 30 s
analytical, t = 30 s
numerical, t = 40 s
analytical, t = 40 s
numerical, t = 50 s
analytical, t = 50 s
concentration
space

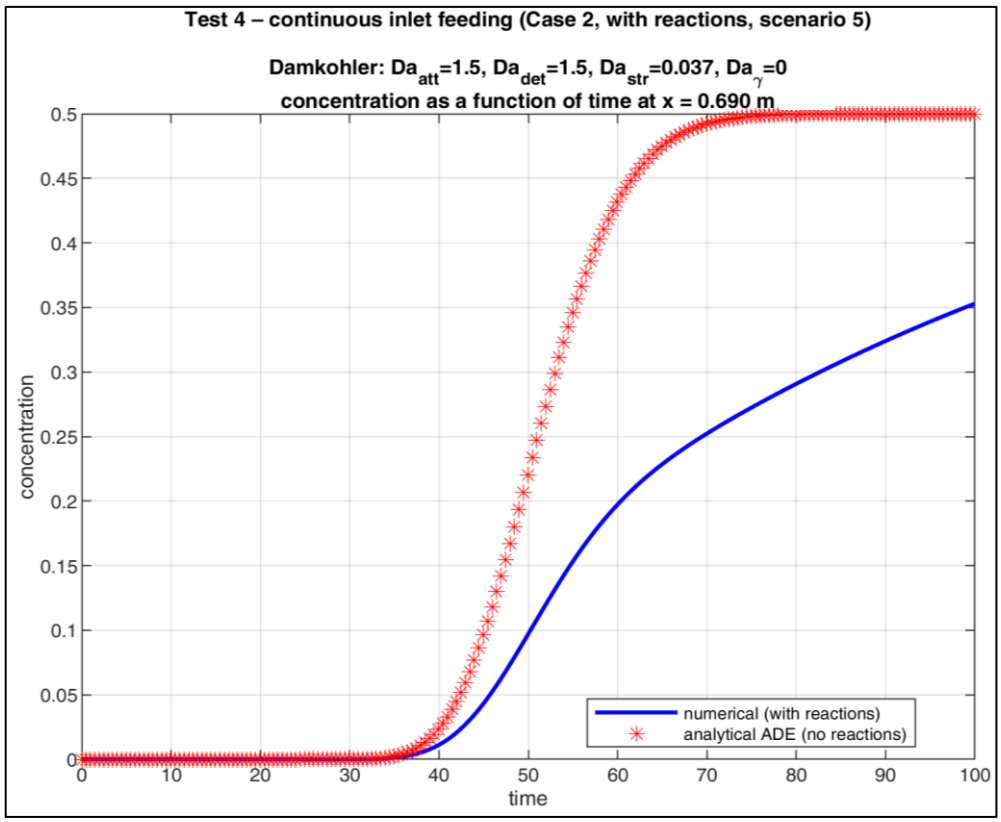
Test 4 – continuous inlet feeding (Case 2, with reactions, scenario 5)
Damkohler: Da_att=1.5, Da_det=1.5, Da_str=0.037, Da_γ=0
concentration as a function of time at x = 0.690 m
numerical (with reactions)
analytical ADE (no reactions)
concentration
time

Figure 5.7: Effect of moderate retention kinetics on continuous inlet transport (Test 4, Scenario 5: Da_{att} = 1.5, Da_{det} = 1.5, Da_{str} = 0.037, Da_{γ} = 0). (a) Spatial profiles showing progressive attenuation with increasing distance from inlet. Front advancement slows visibly between t = 30–50 s as retention effects accumulate, with concentration gradients steepening substantially compared to Scenario 1. (b) Concentration plateau at control section stabilizing at $C/C_0 \approx 0.25$ by t = 100 s—substantially reduced from weak-kinetics case ($C/C_0 \approx 0.45$)—indicating that moderate Damköhler numbers produce cumulative suppression under persistent source conditions. Deviation from analytical baseline exceeds 50% by t = 100 s. Same kinetic parameters as Test 2 Scenario 5.

The control section concentration plateaus at $C/C_0 \approx 0.25$ by t = 100 s—approximately half the weak-kinetics value and 50% below the ADE prediction—indicating substantial long-term suppression of downgradient transport under moderate retention conditions. The gradual approach to plateau rather than rapid equilibration suggests that dynamic feedback between retention and flow continue to evolve over timescales exceeding 100 s, potentially requiring monitoring periods of months to years to fully characterize steady-state conditions in field applications.

This regime represents intermediate-vulnerability conditions where contamination extent is limited by retention but not eliminated, requiring careful assessment of both near-field impacts (retention accumulation, potential hydraulic impairment) and far-field risks (persistent downgradient transport at reduced but non-negligible concentrations).

Scenario 3: Strong Retention, Continuous Loading (Da_{att} = 7.5)

Strong retention under continuous loading (same parameters as Test 2 Scenario 3) produces the most dramatic deviation from analytical behaviour observed across all scenarios. Figure 5.8 shows >95% of inlet mass retained within x < 0.2–0.3 m, with spatial profiles exhibiting minimal front advancement beyond the near-inlet region even after 50 s of continuous loading.

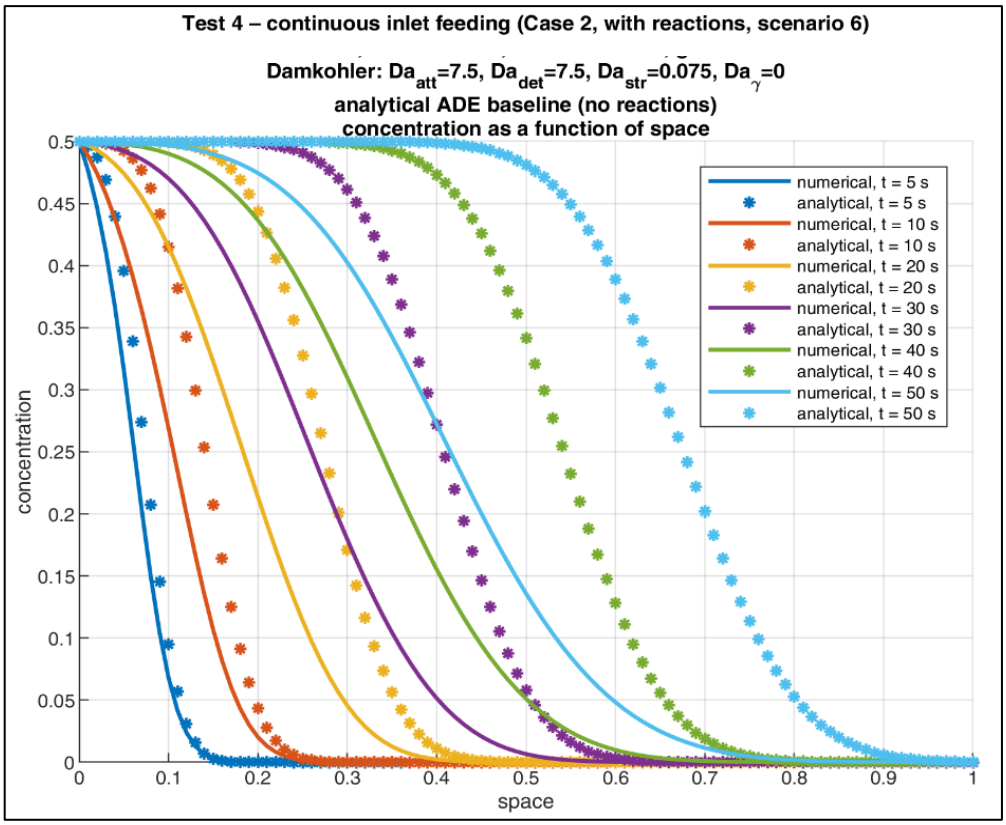
Test 4 – continuous inlet feeding (Case 2, with reactions, scenario 6)
Damkohler: Da_att=7.5, Da_det=7.5, Da_str=0.075, Da_γ=0
analytical ADE baseline (no reactions)
concentration as a function of space
numerical, t = 5 s
analytical, t = 5 s
numerical, t = 10 s
analytical, t = 10 s
numerical, t = 20 s
analytical, t = 20 s
numerical, t = 30 s
analytical, t = 30 s
numerical, t = 40 s
analytical, t = 40 s
numerical, t = 50 s
analytical, t = 50 s
concentration
space

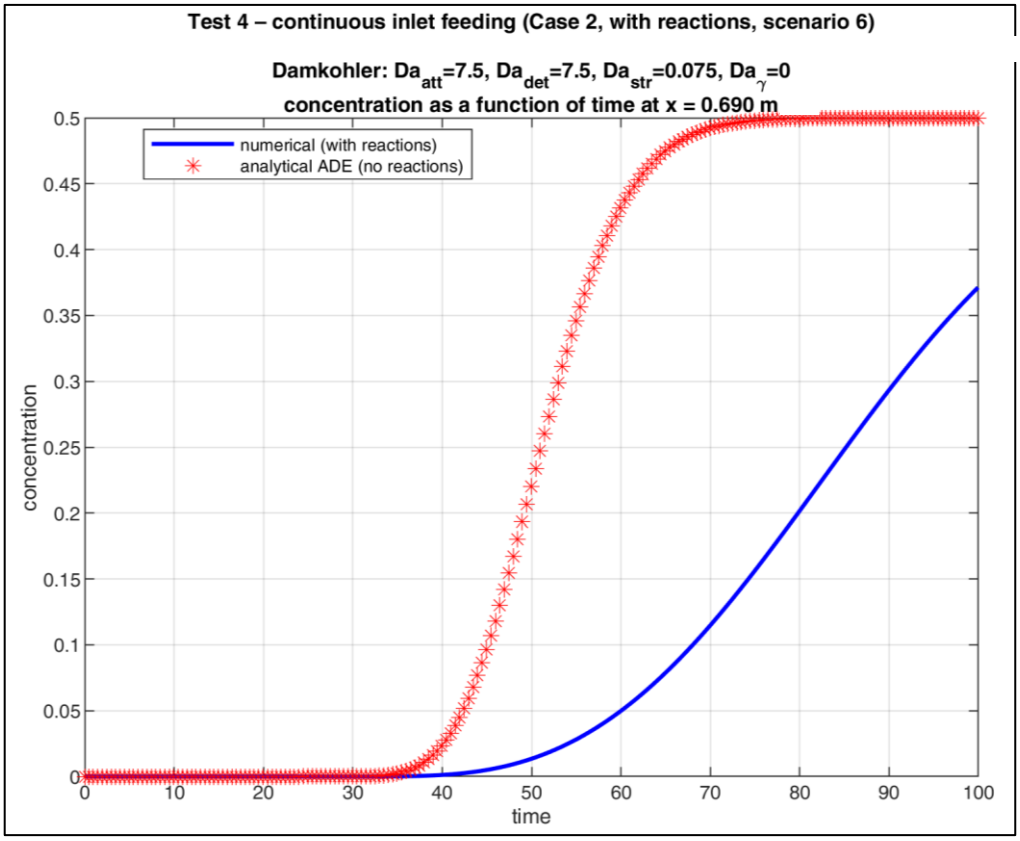
Test 4 – continuous inlet feeding (Case 2, with reactions, scenario 6)
Damkohler: Da_att=7.5, Da_det=7.5, Da_str=0.075, Da_γ=0
concentration as a function of time at x = 0.690 m
numerical (with reactions)
analytical ADE (no reactions)
concentration
time

Figure 5.8 : Effect of strong retention kinetics on continuous inlet transport (Test 4, Scenario 6: Da_{att} = 7.5, Da_{det} = 7.5, Da_{str} = 0.075, Da_{γ} = 0). (a) Spatial profiles showing severe near-inlet retention with minimal downgradient transport. Concentration front barely advances beyond x = 0.3 m by t = 50 s, with profiles exhibiting hyper exponential decay characteristic of reaction-limited systems. Analytical ADE baseline becomes completely irrelevant as retention processes overwhelmingly dominate transport dynamics. (b) Concentration at control section plateauing at $C/C_0 < 0.05$ by t = 100 s—more than 10× lower than weak-kinetics case—demonstrating that high Damköhler numbers effectively prevent downgradient contamination even under persistent source conditions. Same kinetic parameters as Test 2 Scenario 3.

The persistent, steep concentration gradient reflects rapid kinetic capture overwhelming advective transport, creating a filtration zone that effectively immobilizes particles before they can propagate significant distances. The control section concentration remains below 5% of inlet values even after 100 s of continuous loading, confirming highly effective natural attenuation for downgradient protection—a >90% reduction compared to the weak-kinetics case and >95% compared to the no-reaction ADE baseline.

However, this extreme retention creates corresponding hydraulic impacts near the source. While not explicitly shown in concentration plots, the model predicts (via Equations 5.7–5.8) substantial porosity reduction and permeability loss in the near-inlet zone (x < 0.2 m), with potential for >80% permeability reduction creating localized but severe hydraulic impairment. This dual character—excellent contaminant removal but severe hydraulic impairment—represents a critical consideration for fine-grained aquifer systems or conditions favouring strong particle-surface interactions.

Comparative Analysis: Pulse versus Continuous Loading

Direct comparison between Test 2 (pulse) and Test 4 (continuous) for identical kinetic parameters reveals fundamental differences in long-term fate that have important implications for risk assessment and management strategies.

For Scenario 1 (Da_{att} = 0.075, weak kinetics), pulse injection results in transient breakthrough with near-complete mass recovery at the outlet (>85% of injected mass passes control section), while continuous loading (Figure 5.12) establishes persistent plateau

concentrations at downgradient locations ($C/C_0 \approx 0.45$ maintained indefinitely). This distinction has critical implications: pulse releases pose primarily transport-based risks that are time-limited (concentrations return to background after pulse passage), whereas continuous releases create sustained contamination requiring long-term management even in high-permeability systems.

For Scenario 3 ($Da_{att} = 7.5$, strong kinetics), both loading modes result in effective filtration (<10% breakthrough) and minimal downgradient risk. However, continuous loading (Figure 5.10) creates sustained near-inlet accumulation with progressive hydraulic impairment not observed in pulse scenarios . The accumulation of retained mass under persistent loading progressively reduces porosity and permeability (via Equations 5.7–5.8), creating self-reinforcing retention where flow reduction further enhances particle capture efficiency. This positive feedback mechanism is unique to continuous loading scenarios and represents a critical distinction for regulatory assessments of chronic versus acute contamination events.

The Scenario 2 comparison ($Da_{att} = 1.5$, transitional regime) reveals maximum sensitivity to loading mode. Pulse injection produces moderate attenuation (~60% peak suppression) with partial breakthrough, while continuous loading results in substantially greater cumulative retention (~75% suppression at plateau) and more pronounced downgradient concentration reduction. This sensitivity in the transitional regime ($0.5 < Da < 2$) suggests that risk characterization for medium-grained aquifers must explicitly account for contamination source characteristics rather than relying solely on aquifer property assessments—a finding with direct regulatory implications.

5.3.2 Solution Algorithm and Implementation Details

The numerical model was implemented in MATLAB, chosen for its robust capabilities in solving systems of coupled differential equations, efficient matrix operations, and comprehensive visualization features. The solution algorithm follows these steps:

Initialization: Define spatial domain, grid resolution, time step, and initial conditions for all variables (C, S, ε, k, U, kinetic rates).

Time loop: For each time step:

Update solid concentration S using the explicit scheme.

Update mobile concentration C using the explicit scheme.

Apply boundary conditions.

Update porosity and permeability using constitutive relations.

Recalculate velocity and kinetic rates.

Advance to next time step

Output: Record variables of interest (concentrations, porosity, permeability) at specified intervals for post-processing and analysis.

For validation purposes, the model also includes implementations of analytical solutions for simple cases that can be compared with numerical results to verify the correctness of the discretization and solution algorithm. These analytical benchmarks provide confidence in the model's ability to accurately capture the fundamental transport processes before adding the complexity of attachment, detachment, and straining mechanisms.

5.4 Model Calibration and Validation

5.4.1 Calibration Strategy and Parameter Tuning

The calibration of the numerical model followed a systematic approach to identify optimal values for the key adjustable parameters that could not be directly measured. These parameters included the attachment coefficient, detachment coefficient, and porosity decay constant (γ), the strategy sought to simultaneously optimize the model's ability to reproduce observed breakthrough curves, retention profiles, and hydraulic property evolution.

The calibration process began with a sensitivity analysis to identify the most influential parameters, which revealed that the attachment coefficient and porosity decay constant had the strongest impact on model outcomes. Based on this finding, a two-stage calibration approach was implemented:

Primary Calibration: Initial parameter values were selected based on literature recommendations, and then the attachment coefficient and porosity decay constant were systematically varied to match the experimental breakthrough curves. This stage focused on matching the timing and magnitude of the concentration peak at the column outlet.

Secondary Calibration: With preliminary values established for the attachment coefficient and porosity decay constant, the detachment coefficient and velocity adjustment parameter were fine-tuned to improve the match between simulated and observed tailing behaviour and permeability evolution.

To ensure comprehensive calibration across different media conditions, the process was repeated for each of the Coarse, Medium ,Fine sand grain sizes. This approach revealed distinct optimal parameter sets for each grain size, reflecting the different transport and retention mechanisms dominant at different scales. The calibrated parameters showed clear trends with grain size:

Attachment coefficient increased with decreasing grain size. This trend reflects the increased specific surface area and collision efficiency in finer media.

Detachment coefficient showed less variation with grain size, this suggests that while attachment increases substantially in finer media, the relative importance of detachment also increases.

Porosity decay constant (γ) increased with decreasing grain size, ranging from 0.2 for the 2000 μm sand to 0.4 for the fine sand. This indicates that microplastic retention has a more pronounced effect on porosity reduction in finer media, likely due to the smaller initial pore sizes.

The calibration process involved running 243 model simulations with different parameter combinations, each simulation was evaluated based on multiple performance metrics, and the parameter set that provided the best overall performance was selected for each grain size.

5.4.2 Validation Against Laboratory Column Experiments

Model performance was evaluated by comparing simulated and experimental time series across four grain size fractions (fine: 300 μm, medium: 600 μm, intermediate-medium: 1000 μm, and coarse: 2000 μm) using normalized outlet microplastic concentration (C/C_0), normalized porosity ($\varepsilon/\varepsilon_0$), and normalized permeability (k/k_0). The comprehensive validation spanning four grain sizes enables assessment of model fidelity across transport regimes ranging from attachment-dominated (coarse sand) through transitional (intermediate-medium sand) to straining-dominated (fine sand) conditions. The calibrated

parameter sets, systematically varied to reflect grain size-dependent processes, demonstrate predictive capability across diverse porous media characteristics.

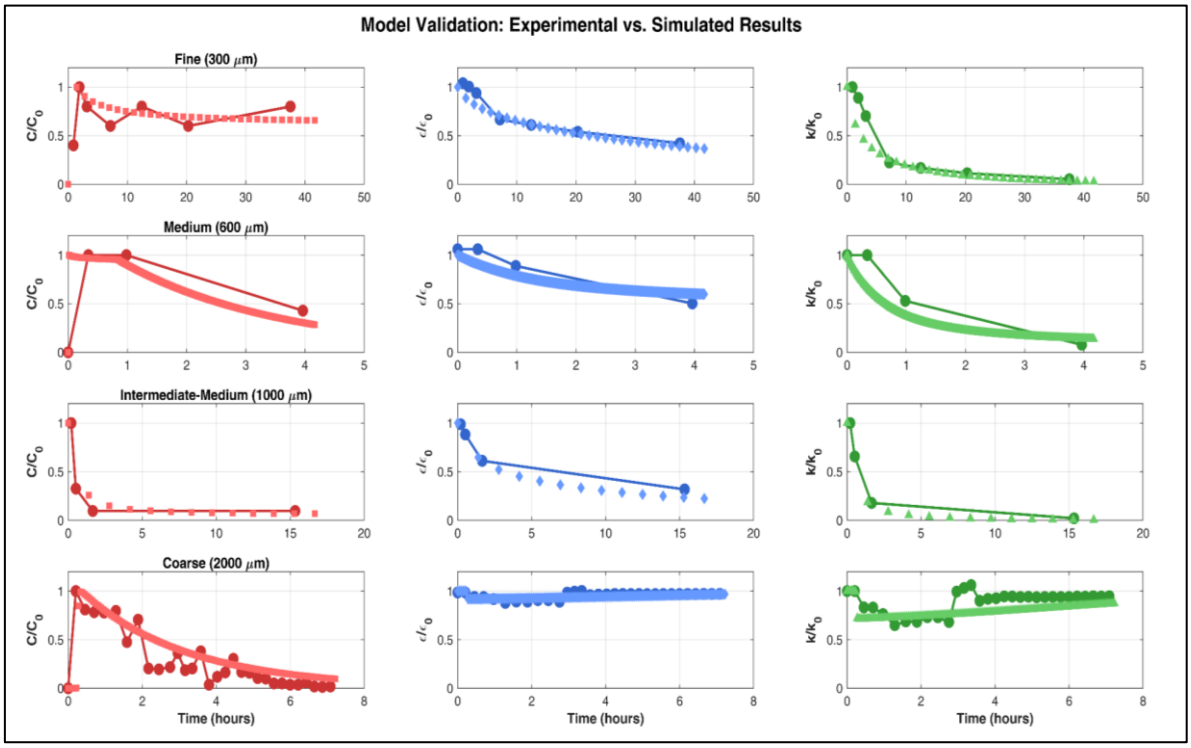

Figure 5.9. Comprehensive model validation across four grain sizes showing normalized concentration (left column), porosity (middle column), and permeability (right column). Non-dimensional parameters and transport regimes: Fine sand (300 μm): Da = 6.88×10^{-6}, Re_p = 0.009, Da_{att} = 38.8, k_{str} = 0.390, γ = 0.05 (straining-dominated); Medium sand (600 μm): Da = 6.88×10^{-6}, Re_p = 0.017, Da_{att} = 0.40, k_{str} = 0.148, γ = 0.1 (transitional); Intermediate-medium sand (1000 μm): Da = 6.88×10^{-6}, Rep = 0.029, Da_{att} = 23.3, k_{str} = 0.073, γ = 0.1 (upper transitional); Coarse sand (2000 μm): Da = 1.03×10^{-5}, Re_p = 0.256, Da_{att} = 545, Da_{det} = 54.5, k_{str} = 0.028, γ = 0.2 (attachment-dominated). All $Re_p \ll 1$ confirms Darcy flow validity. Experimental data shown as solid lines with markers; simulated results shown as discrete markers**.**

5.4.2.1 Coarse Sand (2000 μm) Validation: Attachment-Dominated Regime

The experimental breakthrough curve in coarse sand shows rapid initial passage of microplastics followed by decline over the remainder of the experiment, with variability in measured values. The simulated breakthrough curve follows the overall pattern and captures timing of early breakthrough and subsequent decay, indicating that the model represents dominant transport processes for coarse sand under imposed flow conditions. In this grain

size, limited tailing and overall decline are consistent with relatively weak retention compared with finer porous media, where straining becomes more important as particle-to-pore size ratios increase.

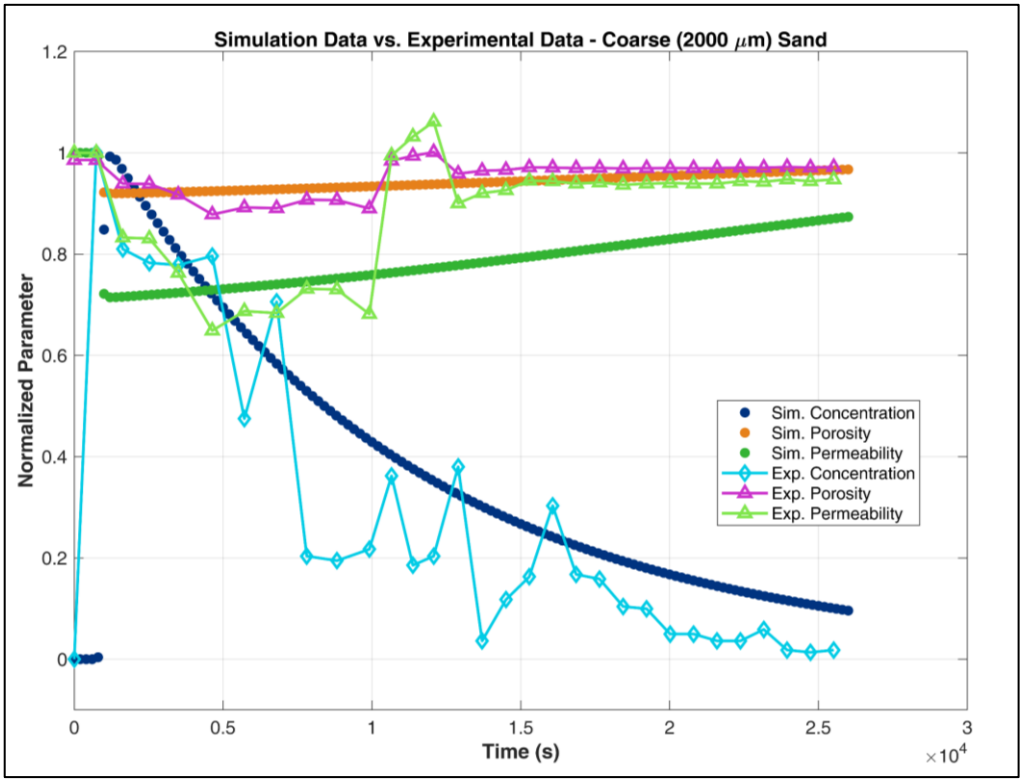

Figure 5.10. Validation for coarse sand (2000 μm) in an attachment-dominated regime. Simulated results (filled circles) are compared with experimental data (lines with markers) for concentration, porosity, and permeability. Hydraulic changes are minimal, reflecting limited retention in coarse media

Hydraulic property evolution reveals that experimental porosity remains near its initial value throughout, and simulated porosity similarly remains near-constant, supporting interpretation that coarse sand experienced minimal pore-space loss during microplastic passage. Normalized permeability shows no sustained progressive decline in experimental series, and simulation reproduces the same general stability. Fluctuations in experimental permeability and porosity time series are not reproduced by the model, which provides smoother trends consistent with its continuum representation of the column.

5.4.2.2 Medium Sand (600 µm) Validation: Transitional Regime

The experimental breakthrough in medium sand exhibits characteristics falling between coarse and fine fractions, with initial breakthrough occurring at intermediate times. The simulated breakthrough demonstrates temporal agreement, validating the model's capability to capture transitional regime dynamics where attachment and straining contribute to overall retention. Post-breakthrough concentration exhibits moderate fluctuations experimentally, partially reproduced by simulation though with smoother temporal evolution reflecting the continuum model's representation.

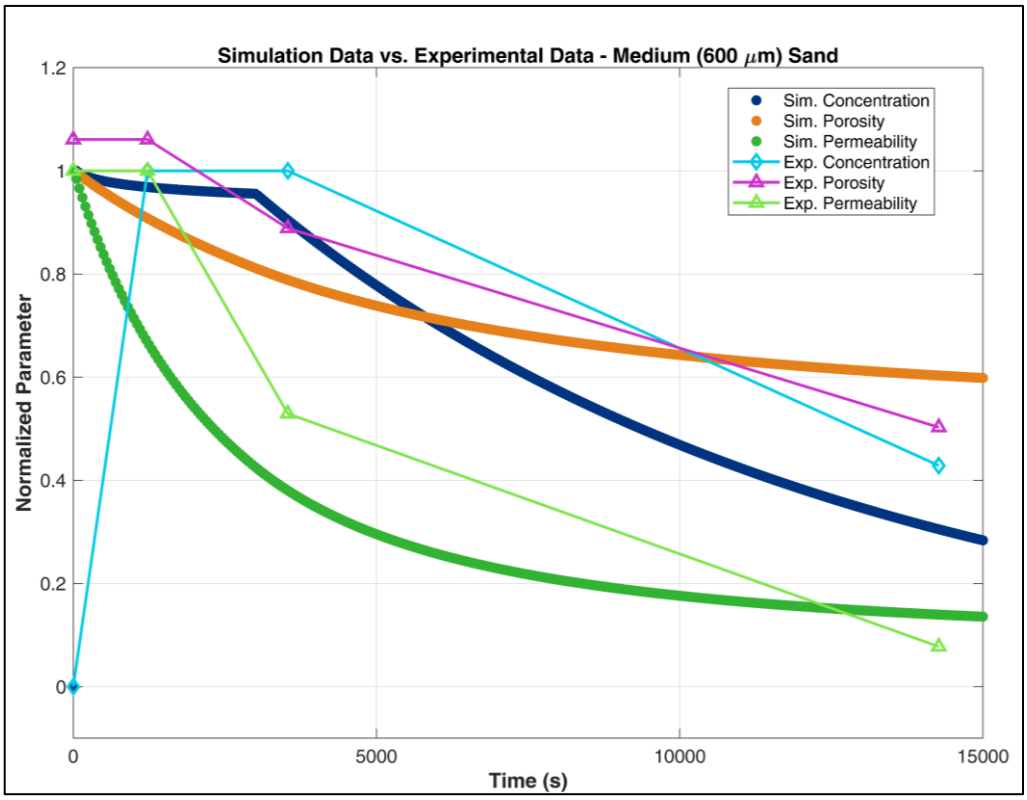

Figure 5.11. Validation for medium (600 µm) sand in a transitional regime. Simulated results (filled circles) are compared with experimental data (lines with markers) for concentration, porosity, and permeability. Moderate hydraulic degradation reflects combined attachment and straining.

Hydraulic property evolution in medium sand demonstrates systematic degradation. Experimental porosity declined from initial values, while simulated values tracked the trend. The calibrated porosity decay constant captures the curvilinear decline pattern, with initial reduction transitioning to stabilization indicative of approaching retention capacity.

Permeability evolution exhibited moderate loss, reproduced by simulation. The porosity-permeability correlation confirms the Kozeny-Carman relationship remains applicable under these conditions.

The medium sand validation demonstrates that moderate retention mechanisms correctly identify the transitional regime where neither transport nor retention overwhelmingly dominates. The particle-to-pore throat ratio falls within the transition zone where straining becomes significant, but attachment remains important, creating coupled dynamics captured by the dual-mechanism retention formulation.

5.4.2.3 Intermediate-Medium Sand (1000 µm) Validation: Upper Transitional Regime

The experimental breakthrough in intermediate-medium sand exhibits behaviour intermediate between medium and coarse fractions, confirming its position in the upper transitional regime where attachment begins to dominate over straining. Initial breakthrough occurred at times earlier than medium sand but delayed compared to coarse sand. The simulated breakthrough demonstrates temporal agreement and captures the sustained intermediate concentration pattern. The model reproduces the characteristic temporal profile observed in experimental data, reflecting depletion of readily detachable particles followed by sustained elution from more strongly retained fractions.

Hydraulic property evolution reveals moderate degradation patterns that validate the model's capability in this grain size range. Experimental porosity declined from initial values, matched by simulation. The gentler decline compared to finer grain sizes reflects reduced straining efficiency as particle-to-pore throat ratios decrease, creating predominantly surface attachment rather than pore blocking. The calibrated porosity decay constant captures this moderate accumulation rate, intermediate between the clogging in fine sand and minimal impact in coarse sand.

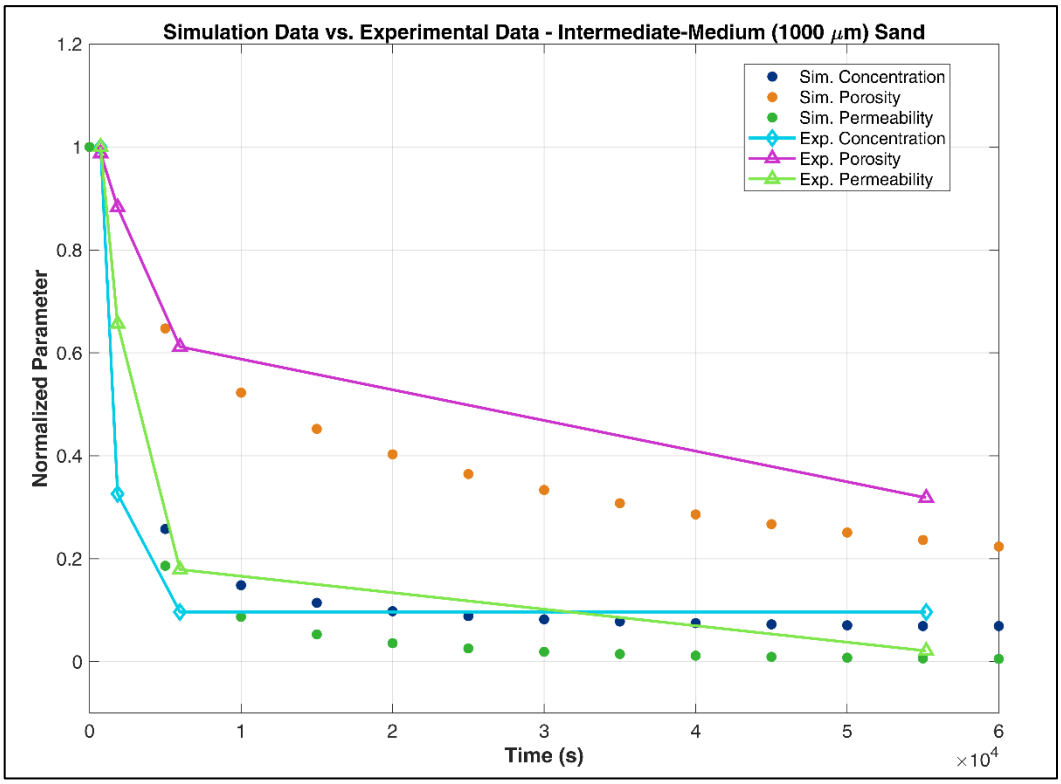

Figure 5.12. Validation for intermediate-medium (1000 µm) sand in the upper transitional regime. Simulated results (filled circles) are compared with experimental data (lines with markers) for breakthrough and hydraulic evolution. The model captures the transition where attachment dominates over straining.

Permeability evolution exhibited moderate reduction from initial values, reproduced by the model. The moderate conductivity loss indicates that intermediate-medium aquifer materials maintain functional flow capacity under sustained microplastic loading. The experimental porosity-permeability correlation is captured by the Kozeny-Carman formulation, confirming the model's validity across this intermediate grain size range where neither extreme clogging nor conservative transport dominate.

The intermediate-medium sand validation is relevant because this grain size represents the upper boundary of the transitional regime, where predictive uncertainty is typically elevated due to competing retention mechanisms. The model's performance across all three metrics (breakthrough timing, concentration magnitude, hydraulic property evolution) provides confidence for scenario analysis spanning the full grain size spectrum.

5.4.2.4 Fine Sand (300 µm) Validation: Straining-Dominated Regime

The experimental breakthrough curve in fine sand exhibits delayed arrival and attenuated peak concentrations characteristic of straining-dominated retention. Initial breakthrough did not occur until later times, with peak normalized concentrations remaining substantially lower than coarser grain sizes. The simulated breakthrough curve captures this retention behaviour, reproducing both the delayed arrival timing and the peak suppression. The extended low-concentration tailing observed experimentally reflects gradual remobilization of strained particles through detachment balanced against continued retention, a dynamic process represented by the calibrated attachment-detachment coefficients.

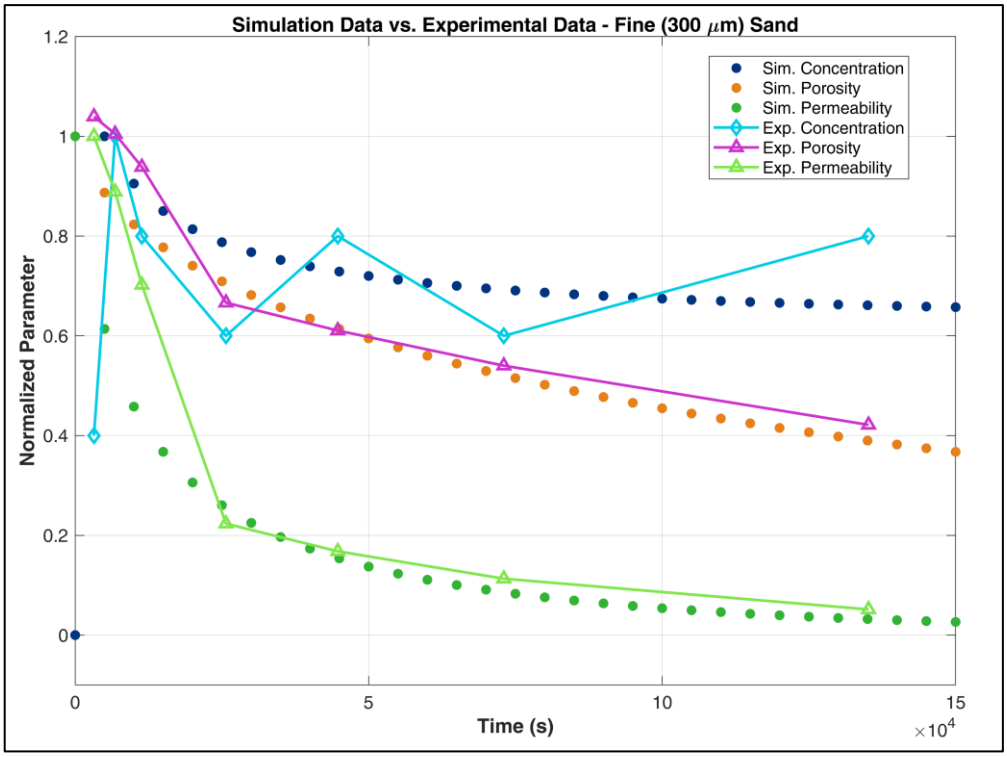

Figure 5.13. Validation for fine (300 µm) sand in a straining-dominated regime. Simulated results (filled circles) are compared with experimental data (lines with markers) for concentration, porosity, and permeability. Pronounced hydraulic degradation reflects physical filtration in fine-grained media.

Hydraulic property evolution validation demonstrates the model's capability to capture pore-scale clogging mechanisms. Experimental porosity declined substantially from initial values by final sampling, representing the most pronounced degradation observed across all grain sizes. The simulated porosity evolution follows this trajectory, with the exponential decay

formulation capturing the accelerating decline characteristic of progressive pore blocking. The coupled permeability reduction exhibited pronounced changes, with experimental values declining substantially. The model reproduces this hydraulic impairment, though slightly underestimating the magnitude—likely reflecting limitations in the Kozeny-Carman relationship under extreme clogging conditions where pore network connectivity loss exceeds continuum model assumptions.

The agreement between simulation and experiment for fine sand validates the model's straining formulation, confirming that the particle-to-grain size ratio serves as the primary control on retention efficiency when particle-to-grain ratios exceed critical thresholds. The classification correctly identifies this regime as reaction-limited, where retention processes operate on timescales substantially shorter than advective transport, creating the observed near-inlet accumulation and downgradient concentration suppression.

5.4.3 Performance Metrics and Error Analysis

To quantitatively assess the performance of the calibrated model, an error analysis metrics was employed for comparing model predictions with experimental observations. These metrics were calculated across for multiple aspects of the model output (breakthrough curves, retention profiles, and hydraulic property evolution).

A primary performance metric used in this study was the relative error between simulation and experimental results, calculated as:

$$\text{Relative Error}(\%) = \text{SUM}\left(\frac{\text{ABS}(\text{NUM}-\text{EXP})}{\text{EXP}}\right) \tag{5.30}$$

where EXP is the experimental and NUM is the numerical value of the considered quantity.

Table 5.1 summarizes relative error across all four grain sizes for the three primary model outputs. The number of experimental data points varies across grain sizes due to sampling constraints.

Table 5.1 – Relative Error Between Simulated and Experimental Time Series

Sand Fraction	***n***	**Concentration (%)**	**Porosity (%)**	**Permeability (%)**
300 μm	7	2.99	4.02	23.07
600 μm	4	12.67	3.84	19.61
1000 μm	4	54.49	7.81	16.54
2000 μm	31	21.01	0.56	9.05

Error Patterns Across Grain Sizes

Concentration predictions exhibited variable accuracy across grain sizes. Fine sand showed low error, indicating that the model captured breakthrough behaviour and post-breakthrough dynamics adequately. Medium sand demonstrated moderate error, while intermediate-medium sand showed elevated error, likely reflecting the complexity of calibrating dual-mechanism models in transitional regimes where attachment and straining contribute comparably. This elevated error coincides with limited temporal sampling resolution, which constrains model validation. Coarse sand exhibited moderate error despite dense temporal sampling, suggesting sensitivity to breakthrough timing and concentration variability.

Porosity evolution was reproduced with consistently low error across all grain sizes. Fine, medium, and intermediate-medium sands demonstrated errors below ten percent, while coarse sand showed minimal error reflecting near-baseline porosity maintenance throughout the experimental period. The low porosity errors indicate that the exponential decay formulation accurately represents pore space reduction due to particle accumulation. The systematic performance across grain sizes validates the constitutive relationship between retained particle concentration and porosity loss.

Permeability evolution showed systematic variation with grain size. Errors decreased progressively from fine sand through intermediate-medium to coarse sand, indicating improved model performance under conditions approaching linear Darcy flow. Fine and medium sands exhibited moderate errors, reflecting the nonlinear coupling between porosity and permeability via the Kozeny-Carman relationship, where small porosity prediction errors amplify into larger permeability deviations. The pattern of decreasing error with increasing grain size confirms that the model performs more reliably when severe clogging and non-Darcy effects are minimal.

The systematic pattern of lower errors for hydraulic properties compared to concentration dynamics indicates that the porosity-permeability coupling formulation performs consistently across the grain size spectrum, while concentration predictions show greater sensitivity to parameter calibration and experimental data resolution.

Sources of Error and Uncertainty

Several factors contribute to observed model-experiment discrepancies. Parameter uncertainty arises from the calibration process, where attachment coefficients, detachment coefficients, and porosity decay constants carry inherent uncertainty despite optimization procedures. Sensitivity analysis revealed that breakthrough predictions are particularly responsive to attachment coefficient variations, making this parameter a critical source of predictive uncertainty in transitional grain sizes.

Sampling resolution varies substantially across grain sizes, directly affecting error estimate confidence. Medium and intermediate-medium sands have limited temporal resolution, constraining validation rigor where breakthrough features between sampling intervals cannot be resolved. This limitation particularly affects concentration error assessments for intermediate-medium sand, where four experimental points provide insufficient constraint on model calibration for the complex transitional regime.

Simplifying assumptions in the model's continuum formulation contribute to systematic deviations. The assumption of spatially uniform initial properties neglects pore-scale heterogeneity that becomes influential in finer grain sizes where retention mechanisms create localized concentration gradients. The spherical particle assumption introduces systematic deviation from experimental conditions where microplastic morphology includes fibrous and irregular fragments with different hydrodynamic and retention behaviours.

Experimental measurement uncertainty affects apparent model errors. Uncertainties in determining microplastic concentrations through particle counting, porosity through volume measurement, and permeability through hydraulic gradient control contribute to discrepancies that partially reflect experimental limitations rather than model deficiencies. Permeability calculations based on Darcy's law assume steady flow conditions that may not be maintained during transient clogging events in fine sand experiments.

Interpretation of Model Performance

The error analysis confirms that the model performs adequately across the grain size spectrum, with expected variations in accuracy reflecting differences in retention regime complexity and experimental data resolution. Fine sand concentration predictions demonstrate that the model can capture straining-dominated transport when calibration parameters are well-constrained by sufficient experimental data. The elevated error for intermediate-medium sand reflects the inherent difficulty of modeling transitional regimes where neither attachment nor straining dominates, compounded by sparse temporal sampling.

Porosity predictions across all grain sizes demonstrate that the exponential decay formulation provides a robust representation of pore space evolution under microplastic loading. The consistently low errors validate the approach of coupling particle retention directly to porosity reduction through a first-order decay relationship.

Permeability predictions follow expected trends, with performance improving systematically as grain size increases and flow approaches linear Darcy conditions. The moderate errors in fine sand reflect the challenge of predicting hydraulic conductivity under severe clogging where the Kozeny-Carman relationship may not fully capture pore network reorganization and preferential flow pathway development.

The model demonstrates adequate predictive capability for scenario analysis and qualitative assessment of microplastic transport across diverse grain sizes, while quantitative predictions for intermediate grain sizes would benefit from refined kinetic parameterization and increased experimental data resolution for calibration validation.

5.5 key findings and conclusions

5.5.1 Summary of Modelling Results

The numerical model successfully simulated microplastic transport and retention in saturated porous media across four grain sizes spanning fine to coarse sand fractions, capturing the interplay between advection, dispersion, and retention mechanisms including attachment, detachment, and straining.

The simulations revealed that grain size is a dominant control on microplastic transport regimes. In coarse sand, transport was dominated by advection with minimal retention, reflected in early breakthrough and negligible changes in hydraulic properties. This behaviour aligns with conditions indicating a transport-limited regime where particles move largely conservatively through the pore network.

In contrast, fine sand exhibited a reaction-limited regime characterized by retention and delayed breakthrough. Physical filtration at pore constrictions was the primary retention mechanism, leading to accumulation near the inlet. This accumulation caused reduction in porosity and permeability, with the model predicting decline in hydraulic conductivity consistent with pore-clogging phenomena observed in laboratory experiments.

Medium sand demonstrated transitional behaviour, with moderate retention governed by combination of attachment and straining. The model captured the intermediate breakthrough timing and the evolution of hydraulic properties, highlighting the sensitivity of transport to particle-to-grain size ratios in this transition zone.

Intermediate-medium sand occupied the upper transitional regime, characterized by moderate retention and manageable hydraulic impairment. This grain size represents a boundary of the transitional zone where attachment is becoming dominant, but straining remains measurable. The model's performance across this challenging intermediate range provides confidence for scenario analysis and field-scale predictions.

5.5.2 Integration of Validation and Field Observations

Validation against laboratory column data confirmed the model's predictive capability. The simulated breakthrough curves showed agreement with experimental data for coarse and medium sand, reproducing peak concentrations and tailing behaviour. For fine sand, the model captured the primary breakthrough features but slightly underestimated long-term tailing, likely due to complex pore-scale heterogeneity not fully resolved in the continuum formulation.

Comparing these findings with field observations from the Chennai aquifer, the modelling results provide mechanistic explanation for detected contamination patterns. The preferential accumulation of microplastics in sandy aquifer zones compared to clayey zones is consistent with the model's prediction of enhanced transport in coarser media, where particles can

penetrate deeper into the subsurface before being retained. The model also supports the hypothesis that seasonal recharge events mobilize retained particles, as simulated detachment processes demonstrated that previously deposited microplastics can be re-entrained under changing flow conditions.

Chapter 6 – Synthesis, Implications, and Future Research Directions

6.1 Introduction.

This study examined microplastic transport and retention in groundwater systems through field observations, laboratory experiments, and numerical modelling. The research addressed four objectives stated in Chapter 1: to characterize microplastic occurrence and spatial distribution in groundwater; to investigate transport mechanisms in porous media through controlled experiments; to develop numerical models for predicting transport; and to discuss implications for groundwater quality and aquifer behaviour.

The methodological approach combined field sampling at 25 locations in Chennai during two seasonal periods (pre-monsoon August 2024 and post-monsoon February 2025), laboratory column experiments using four sand grain sizes (300 μm, 600 μm, 1000 μm, and 2000 μm), and numerical modelling to simulate observed transport patterns.

Field sampling detected microplastics at all 25 locations. Particles per litre ranged from 5 to 19 particles per sample in pre-monsoon conditions and 8 to 26 particles per sample in post-monsoon conditions. Total counts increased from 249 particles pre-monsoon to 387 particles post-monsoon. Sandy formations averaged 11.2 particles per sample pre-monsoon (15.5 post-monsoon) compared to 8.7 particles in clayey zones (11.8 post-monsoon). These patterns indicated that porous media characteristics influence microplastic occurrence.

Laboratory experiments investigated transport across four grain sizes spanning fine to coarse sand fractions. Fine sand (300 μm) and medium sand (600 μm) exhibited delayed breakthrough with sustained outlet concentrations and hydraulic conductivity reductions of 60-80%. Intermediate-medium sand (1000 μm) showed transitional behaviour with moderate retention and hydraulic changes. Coarse sand (2000 μm) demonstrated early breakthrough with minimal hydraulic impact. Pore-throat diameter estimates ranged from 36-38 μm for 300 μm sand to 227-237 μm for 2000 μm sand.

The numerical model reproduced experimental across four grain sizes. The model incorporated advection-dispersion equations with retention terms for attachment, detachment, and straining, and accounted for porosity and permeability evolution. Model validation indicated that physical straining represents a primary retention mechanism, with particle-to-grain size ratios serving as a controlling parameter (Bradford et al., 2003).

6.2 Integrated Findings and Cross-Scale Validation

6.2.1 Convergence of Evidence Across Field, Laboratory, and Modelling Approaches

Field investigations detected microplastics at all 25 sampling locations in Chennai. Particles per litre ranged from 5 to 19 particles per sample in pre-monsoon conditions (August 2024) and 8 to 26 particles per sample in post-monsoon conditions (February 2025). Total counts increased from 249 particles pre-monsoon to 387 particles post-monsoon. Samples near the Adyar and Coovum rivers showed increases of 28-36% between sampling periods. Sandy formations averaged 11.2 particles per sample pre-monsoon (15.5 post-monsoon) compared to 8.7 particles in clayey zones (11.8 post-monsoon).

Laboratory experiments investigated transport across four sand grain sizes: 300 µm (fine), 600 µm (medium), 1000 µm (intermediate-medium), and 2000 µm (coarse). Fine and medium sand exhibited delayed breakthrough with sustained elevated outlet concentrations and hydraulic conductivity reductions of 60-80%. Intermediate-medium sand showed transitional behaviour with moderate retention and hydraulic changes. Coarse sand demonstrated early breakthrough with minimal hydraulic impact.

Pore-throat diameter estimates were 36-38 µm for 300 µm sand, 71-74 µm for 600 µm sand, approximately 116-121 µm for 1000 µm sand, and 227-237 µm for 2000 µm sand.

The numerical model reproduced experimental pattern across four grain sizes. The model incorporated advection-dispersion equations with retention terms for attachment, detachment, and straining, and accounted for porosity and permeability evolution. Model validation indicated that physical straining represents a primary retention mechanism, with particle-to-grain size ratios serving as a controlling parameter (Bradford et al., 2003).

Damköhler numbers were used to characterize transport regimes. For coarse sand (2000 µm), the system operated in an attachment-dominated regime with minimal retention. Intermediate-medium sand (1000 µm) showed upper transitional behaviour. Medium sand (600 µm) exhibited transitional characteristics with combined attachment and straining. Fine sand (300 µm) demonstrated straining-dominated retention with delayed breakthrough and substantial hydraulic degradation.

Field observations showed temporal patterns relevant to seasonal hydrology. The 55.4% increase in total microplastic abundance from pre-monsoon to post-monsoon periods

occurred across the study area. Morphological composition changed: fibres increased from 153 to 225 particles (47.1% increase) and fragments increased from 96 to 162 particles (68.7% increase). The larger increase in fragments relative to fibres may reflect mechanical fragmentation during high-flow conditions or preferential mobilization of fragments during monsoon periods.

Colour distribution shifted between sampling periods. Transparent/translucent particles decreased from 79.1% (197 of 249) pre-monsoon to 27.9% (108 of 387) post-monsoon. Coloured particles increased from 20.9% (52 of 249) to 72.1% (279 of 387). This shift suggests fresh inputs of pigmented materials during the monsoon period rather than solely remobilization of weathered deposits.

Polymer composition analysis identified polyvinyl chloride (22-25%), polyethylene (HDPE 18-21%, LDPE 17-19%), and polypropylene (14-16%) as dominant polymer types. The prevalence of synthetic fibres indicates textile sources as contributors to contamination (Browne et al., 2011). Polyurethane presence suggests tire and shoe wear contributions. The diverse polyethylene and polypropylene components reflect packaging and consumer waste fragmentation.

6.2.2 Physical Straining as the Dominant Retention Mechanism

Experimental results indicate that physical straining governs retention behaviour across the grain size spectrum. In fine and medium sand (300 μm and 600 μm), pore-throat diameters (36-74 μm) are of similar magnitude to the median microplastic particle size (42 μm). This size relationship creates conditions where particles can become lodged at pore constrictions. Delayed breakthrough in finer materials, sustained elevated outlet concentrations, and substantial porosity reduction indicate particle accumulation within the pore network.

Intermediate-medium sand (1000 μm) exhibits behaviour between these extremes, with pore-throat diameters of approximately 116-121 μm creating conditions where particles experience partial but incomplete retention. The transitional behaviour observed in this grain size indicates a critical threshold where neither complete retention nor unimpeded transport dominates.

In coarse sand (2000 μm), pore-throat diameters (227-237 μm) substantially exceed microplastic dimensions. Particles pass through the porous medium with minimal mechanical obstruction, resulting in early breakthrough and minimal porosity change.

Surface charge measurements of the microplastic particles indicated zeta potentials of -35 ± 8 mV at pH 7.0 in deionized water. This moderate negative surface charge influences electrostatic interactions with sand grain surfaces, though these interactions appear secondary to physical straining under the experimental conditions employed. The upward flow configuration in experiments eliminated gravitational settling effects, ensuring that observed retention resulted from interactions with the porous media.

Particle-to-pore-throat size ratios provide a quantitative basis for retention assessment. For 300 μm sand with pore-throat diameters of 45-90 μm and median particle size of 42 μm, ratios range from approximately 0.47 to 0.93. For 2000 μm sand with pore-throat diameters of 300-600 μm, ratios range from approximately 0.07 to 0.14. These ratios indicate that fine sand creates conditions where most particles approach or exceed pore-throat dimensions, while coarse sand provides pore spaces substantially larger than particle dimensions. This size-dependent control aligns with theoretical predictions (Tufenkji & Elimelech, 2004) and field observations (Panno et al., 2019; Alimi et al., 2018).

The field observation of preferential accumulation in sandy formations compared to clayey zones aligns with laboratory findings that intermediate grain sizes enable both particle transport and substantial retention. Sandy formations in Chennai, characterized by grain sizes in the medium to coarse sand range, may provide sufficient permeability for vertical particle migration while retaining particles through straining at smaller pore constrictions.

6.2.3 Hydraulic Property Evolution and Pore Clogging

Laboratory experiments documented substantial reduction in hydraulic conductivity accompanying microplastic accumulation in fine and medium sand. The 300 μm and 600 μm sand fractions experienced hydraulic conductivity reductions in the range of 60-80% over the experimental period. Intermediate-medium sand (1000 μm) showed moderate conductivity reduction, occupying a position between the severe degradation observed in finer materials and the near-baseline maintenance in coarse sand. Coarse sand (2000 μm) maintained near-baseline hydraulic conductivity despite microplastic passage.

Conductivity reductions were not proportional to porosity changes alone. Fine sand exhibited substantial porosity reduction with even greater conductivity loss, suggesting that selective blockage of high-permeability flow pathways amplifies the hydraulic impact of particle accumulation. This interpretation is supported by observations that particle deposition may occur preferentially in larger, higher-velocity pores, thereby reducing overall flow capacity disproportionately to the simple geometric reduction in pore volume (Bradford & Bettahar, 2006).

The positive correlation between porosity and hydraulic conductivity across all materials indicates that pore-space reduction drives conductivity loss. The near-exponential form of conductivity decline in fine sand is consistent with pore-scale bridging, where retained particles accumulate to obstruct primary flow pathways (Johnson & Elimelech, 1995). Intermediate-medium sand demonstrated more proportionate conductivity loss relative to porosity reduction, indicating transitional behaviour where flow pathway blockage is significant but not dominant.

The magnitude of observed conductivity reduction in fine and medium sands suggests additional mechanisms beyond simple pore volume loss. These may include preferential blockage of primary flow pathways, pore-scale bridging where retained particles create obstacles to flow, and local increases in flow resistance near accumulation sites. The specific mechanisms operating at the pore scale warrant further investigation through pore-scale imaging and detailed microscopic examination of particle distributions within experimental columns.

6.2.4 Temporal Dynamics and Seasonal Mobilization

Field observations documented temporal variability in microplastic concentrations linked to seasonal hydrology. The 55.4% increase in total microplastic abundance from pre-monsoon to post-monsoon periods occurred across the study area, with larger increases (28-36%) at locations near the Adyar and Coovum rivers. This pattern is consistent with monsoon-driven mobilization of surface debris and enhanced infiltration during recharge events (He et al., 2020).

Morphological changes between campaigns reflected hydrological shifts. Fibres increased from 153 (pre-monsoon) to 225 (post-monsoon), a 47.1% increase. Fragments increased

from 96 to 162, a 68.7% increase. The more pronounced increase in fragments may reflect mechanical fragmentation during high-flow conditions or preferential mobilization of fragments relative to fibres from surface deposits during flooding (Hurley et al., 2018).

The colour distribution shift provides additional evidence for seasonal effects. Transparent/translucent particles decreased from 79.1% (197 of 249) pre-monsoon to 27.9% (108 of 387) post-monsoon, while coloured particles increased from 20.9% to 72.1%. This shift indicates that the post-monsoon increase included fresh inputs of pigmented materials rather than solely reflecting remobilization of weathered deposits. The substantial change in colour profile suggests monsoon-driven transport of recently accumulated surface materials into the groundwater system.

Laboratory experiments demonstrated that breakthrough behaviour depends on cumulative water throughput and that previously trapped particles can be re-entrained under changing flow conditions. The numerical model captured these dynamics through coupled transport-hydraulic equations accounting for velocity evolution with changing permeability. Model sensitivity analysis revealed transitions in transport behaviour as hydraulic properties change, supporting the hypothesis that monsoon recharge events can remobilize retained particles from surface soils and shallow groundwater zones (Tosco et al., 2012).

6.2.5 Consistency Between Field Observations and Laboratory Findings

The preferential accumulation observed in sandy formations in Chennai (11.2 particles per sample pre-monsoon versus 8.7 in clayey zones) aligns with laboratory findings that intermediate grain sizes enable both particle transport and substantial retention. The inclusion of intermediate-medium sand (1000 μm) in laboratory experiments provided insights into the transitional regime where neither complete retention nor unimpeded transport dominates, directly relevant to interpreting field patterns in heterogeneous aquifer systems.

Field concentrations are lower than laboratory injection concentrations but follow similar grain-size-dependent patterns, suggesting that field-scale transport occurs more gradually due to lower contaminant loading and dispersion effects not fully represented in column experiments.

The temporal increase in field concentrations following monsoon recharge is consistent with laboratory observations that particle elution from fine-grained materials occurs gradually over extended flow periods. Laboratory experiments spanning hours to days demonstrated sustained particle breakthrough following initial retention. Field observations spanning pre-monsoon to post-monsoon periods showed comparable patterns of increased concentrations following high-flow events, though the specific timescales differ due to natural system complexity.

Field concentrations in Chennai ranged from 4 to 26 particles per sample depending on location and season. Laboratory experiments employed higher injection concentrations to enable detection and quantification within experimental timeframes. The difference in absolute concentration levels does not invalidate mechanistic comparisons, as retention mechanisms and hydraulic responses operate through similar pore-scale processes regardless of concentration magnitude, though nonlinear effects at higher concentrations warrant consideration.

Samples with shallow water tables (<5 m below ground surface) averaged approximately 25% higher microplastic counts than those with deeper tables (>10 m), suggesting enhanced vertical infiltration in settings with direct surface-groundwater proximity. Laboratory experiments demonstrated that particle retention occurs progressively through the porous media column, with greater accumulation near inlet zones. Field patterns showing elevated concentrations in shallow groundwater are consistent with this retention profile, though additional factors including source proximity and recharge rates also influence field distributions.

The convergence of evidence across field, laboratory, and numerical approaches provides support for identified transport mechanisms, though uncertainty remains regarding long-term accumulation rates and the influence of natural groundwater chemistry on retention behaviour.

6.3 Key Findings

6.3.1 Grain Size Controls Transport and Hydraulic Vulnerability

Laboratory experiments indicate grain size as a primary control on both microplastic transport efficiency and hydraulic consequences across four grain sizes: fine sand (300 μm),

medium sand (600 μm), intermediate-medium sand (1000 μm), and coarse sand (2000 μm). Fine sand exhibits maximum retention capacity with delayed breakthrough and sustained elevated outlet concentrations, alongside maximum hydraulic vulnerability with conductivity reductions of 60–80%. Medium sand demonstrates severe hydraulic degradation comparable to fine sand despite coarser grain size. Intermediate-medium sand shows transitional behaviour with moderate retention and moderate hydraulic degradation, occupying a distinct position between medium and coarse sand responses. Coarse sand allows rapid particle transport with minimal hydraulic impact.

Pore-throat diameter estimates provide mechanistic basis for grain size effects: 36–38 μm for 300 μm sand, 71–74 μm for 600 μm sand, 116–121 μm for 1000 μm sand, and 227–237 μm for 2000 μm sand, relative to median microplastic particle size of 42 μm. These size relationships indicate that fine and medium sands create conditions where particle dimensions approach pore-throat diameters, facilitating straining, whereas intermediate-medium sand provides partial retention, and coarse sand provides pore spaces substantially exceeding particle dimensions.

This grain-size-dependent vulnerability pattern has implications for aquifer management: finer-grained aquifers may protect deeper formations from microplastic penetration through high retention capacity, but at the cost of potential long-term permeability loss if microplastic loading persists. Intermediate-medium grain sizes (approximately 1000 μm) warrant particular management attention as they occupy a transitional zone where neither complete retention nor unimpeded transport dominates, creating conditions where both contamination risk and hydraulic impairment may occur.

6.3.2 Physical Straining Dominates Over Chemical Attachment

Experimental results demonstrate that physical straining governs retention behaviour across the grain size spectrum. In fine and medium sand, pore-throat diameters (36-74 μm) approach the median microplastic particle size (42 μm), creating conditions where particles become lodged at pore constrictions (Bradford et al., 2003). Intermediate-medium sand (1000 μm) exhibits behaviour between these extremes, with pore-throat diameters of approximately 116–121 μm creating conditions where particles experience partial but incomplete retention. The transitional behaviour observed in this grain size indicates a critical threshold where neither complete retention nor unimpeded transport dominates. In

coarse sand, pore-throat diameters (227–237 μm) substantially exceed microplastic dimensions, permitting passage with minimal mechanical obstruction.

Surface charge measurements of microplastic particles indicated zeta potentials of -35 ± 8 mV at pH 7.0 in deionized water. This moderate negative surface charge influences electrostatic interactions with sand grain surfaces, though these interactions appear secondary to physical straining under the experimental conditions employed.

This interpretation is supported by: (1) delayed breakthrough in finer materials, (2) sustained elevated outlet concentrations reflecting gradual particle elution, and (3) substantial porosity reduction indicating particle accumulation within the pore network. Particle-to-pore-throat size ratios provide quantitative basis for retention assessment: for 300 μm sand, ratios range from approximately 0.47 to 0.93, whereas for 2000 μm sand, ratios range from approximately 0.07 to 0.14. This size-dependent control aligns with theoretical predictions from colloid filtration theory (Tufenkji & Elimelech, 2004) and is consistent with field observations showing preferential contamination in sandy formations where pore sizes are intermediate relative to particle dimensions (Panno et al., 2019; Alimi et al., 2018).

However, experiments employed deionized water under controlled conditions; natural groundwater conditions including elevated ionic strength, dissolved organic matter, and microbial activity could promote particle aggregation and attachment, potentially altering this conclusion under field conditions (Enfrin et al., 2020, Erhayem & Sohn, 2014). The influence of these factors on transport behaviour in natural systems merits investigation before field-scale predictions are made with confidence.

6.3.3 Microplastic Contamination in Chennai is Widespread but Concentrations Modest

Field sampling detected microplastics at all 25 sampling locations, indicating pervasive contamination affecting both shallow unconfined and deeper confined aquifers. Particles per litre ranged from 5 to 19 particles per sample in pre-monsoon conditions and 8 to 26 particles per sample in post-monsoon conditions, comparable to values reported from other urban groundwater systems (Panno et al., 2019). Colour distribution shifted substantially between campaigns. Transparent/translucent particles decreased from 79.1% (197 of 249) pre-monsoon to 27.9% (108 of 387) post-monsoon, while coloured particles increased from

20.9% to 72.1%. This shift suggests fresh inputs of pigmented materials during monsoon periods rather than solely mobilization of weathered deposits.

Polymer composition reflects diverse urban sources, with dominant polymers being polyvinyl chloride (22% pre-monsoon, 25% post-monsoon), polyethylene (HDPE 18–21%, LDPE 17–19% across campaigns), and polypropylene (14–16%). Morphological composition changed between campaigns: fibres increased from 153 to 225 particles (47.1% increase), and fragments increased from 96 to 162 particles (68.7% increase). The larger proportional increase in fragments may reflect mechanical fragmentation during high-flow monsoon conditions or preferential mobilization of fragments relative to fibres.

Fibre morphology dominance (61.4% pre-monsoon, 58.1% post-monsoon), with nylon as a major component, indicates that textile sources including laundry wastewater represent significant contamination pathways (Browne et al., 2011). Samples near the Adyar and Coovum rivers showed increases of 28–36% between campaigns, larger than the overall 55.4% increase, consistent with enhanced mobilization in riverine corridors during monsoon recharge. This pattern is consistent with global observations of microplastic sources in urban settings (Eerkes-Medrano et al., 2015).

6.3.4 Numerical Modelling Reproduces Experimental Patterns

The coupled transport model incorporating advection, dispersion, attachment, detachment, straining, and dynamic hydraulic property evolution achieved validation against laboratory data. Relative errors for concentration predictions ranged from 2.99% (fine sand, 300 μm) to 54.49% (intermediate-medium sand, 1000 μm), with medium sand at 12.67% and coarse sand at 21.01%. Porosity predictions showed consistently low errors below 10% across all grain sizes. Permeability predictions exhibited systematic variation with grain size, with errors decreasing progressively from fine sand through intermediate-medium to coarse sand.

The model successfully classified transport regimes based on Damköhler numbers. Coarse sand (2000 μm) operated in an attachment-dominated regime with minimal retention. Intermediate-medium sand (1000 μm) exhibited upper transitional behaviour where attachment was becoming dominant, but straining remained measurable. Medium sand (600 μm) demonstrated transitional characteristics with combined attachment and straining. Fine

sand (300 μm) showed straining-dominated retention with delayed breakthrough and substantial hydraulic degradation.

The model's applicability to field scales is constrained by simplifying assumptions including one-dimensional geometry, homogeneous media properties, constant diffusion coefficients, spherical particle and collector assumptions, absence of particle aggregation, and no biological interactions. Field-scale transport in heterogeneous, layered aquifers with preferential flow pathways would differ substantially from model predictions. The successful reproduction of experimental data provides confidence in fundamental mechanisms but should not be interpreted as field-scale predictive capability without additional validation (Bradford et al., 2013).

6.4 Limitations of the Investigation

6.4.1 Methodological Limitations

Field Investigation

The temporal scope covering two seasonal cycles provides limited resolution of inter-annual variability. Monsoon rainfall in Chennai exhibits documented year-to-year variation of approximately ±40%, which may affect contamination dynamics. The 25 sampling locations provide spatial coverage across the study area but offer limited resolution for detailed three-dimensional contamination mapping in heterogeneous urban aquifers. Sampling from existing wells may not capture contamination in unmonitored zones or fully represent spatial patterns.

Laboratory Experiments

Column experiments employed monodisperse sands and polyvinyl chloride (PVC) fragments. Environmental microplastics include multiple polymer types including polyethylene, polypropylene, polystyrene, and polyurethane, each with distinct surface properties and densities that may result in different transport behaviours. The use of a single polymer type limits generalizability to the diverse assemblage detected in field samples.

The experimental geochemistry employed deionized water, which does not represent natural groundwater containing dissolved salts, organic matter, and microbial communities. These components could alter retention behaviour through enhanced aggregation, biofilm

formation, or surface property modification. Field groundwaters in Chennai contain elevated ionic strength and dissolved organic matter that may substantially modify particle-media interactions compared to simplified experimental conditions.

The upward flow configuration eliminated gravitational settling effects, ensuring that observed retention resulted from interactions with porous media. However, natural groundwater systems experience predominantly horizontal or downward flow where gravitational effects on particle transport may be significant, particularly for higher-density polymers.

Experiments spanned hours to days, whereas natural aquifer evolution occurs over years to decades. This temporal mismatch prevents assessment of long-term processes including continued fragmentation, biodegradation, and secondary chemical transformation. The progressive weathering and fragmentation of microplastics under natural subsurface conditions remain uncharacterized at timescales relevant to groundwater residence times.

Experiments employed uniform, well-packed sand columns. Natural aquifers exhibit layered lithologies, variable porosity, preferential flow pathways through fractures or macropores, and non-uniform sediment packing, all of which would modify transport compared to idealized laboratory conditions. Aquifer heterogeneity likely accelerates microplastic movement relative to breakthrough times observed in homogeneous columns.

Numerical Modelling

The model incorporates several simplifying assumptions that constrain field-scale applicability. The one-dimensional geometry cannot represent preferential flow through fractures and macropores that may dominate transport in natural systems. [NEW - Added specific limitation] Field-scale transport in heterogeneous, layered aquifers with preferential flow pathways would differ substantially from model predictions based on homogeneous media assumptions.

The model assumes spherical particles and collectors. Real microplastics exhibit irregular morphologies including fibres, fragments, and films, each with distinct hydrodynamic and retention behaviours. Fibres, which comprised 58-61% of field samples across both seasons, demonstrate transport characteristics not fully captured by spherical particle assumptions.

The constant diffusion coefficient simplifies numerical implementation but may not capture complex dependencies on local flow conditions and evolving pore geometry. Dispersion coefficients can vary significantly with changes in pore structure resulting from particle retention.

The model does not account for particle aggregation, which could alter effective particle sizes and transport behaviour under field conditions. Natural groundwater chemistry, particularly elevated ionic strength and organic matter presence, can promote aggregation that would modify retention mechanisms and breakthrough patterns.

Biological interactions including biofilm formation and biodegradation are not incorporated in the model. Biofilm development on microplastic surfaces could alter surface charge, promote particle aggregation, or facilitate biodegradation over extended timescales, substantially modifying transport predictions based on abiotic experiments.

Empirical attachment-detachment coefficients require site-specific calibration, limiting transferability to different hydrogeological settings. Parameter values calibrated against laboratory experiments may not apply directly to field conditions where complex surface chemistry and flow dynamics operate.

6.4.2 Knowledge Gaps

Long-Term Fate and Persistence

The long-term fate of microplastics in groundwater systems remains incompletely characterized. Potential fragmentation into nanoplastics, biodegradation rates, and chemical transformation over decadal timescales relevant to groundwater residence times require investigation. The subsurface environment, characterized by limited light exposure, reduced oxygen availability, and distinctive microbial communities, likely creates degradation patterns distinct from surface environments. Empirical data on these processes under natural groundwater conditions are lacking.

Biofilm and Microbial Interactions

The role of biofilm formation and microbial communities in modifying microplastic surface properties and transport behaviour remains uncharacterized. Biofilms could alter surface charge, promote particle aggregation, or facilitate biodegradation over extended timescales.

These biological processes may substantially modify transport predictions based on abiotic laboratory experiments but were not investigated in this study.

Natural Organic Matter Effects

Interactions between natural organic matter, microplastic particles, and sand grain surfaces could promote or inhibit transport through complexation and bridging mechanisms not investigated in this study. Natural organic matter coating on microplastic surfaces can enhance stability or promote aggregation depending on concentration and pH, with implications for field-scale transport not captured in simplified experimental conditions employing deionized water.

Health Implications

The toxicological significance of chronic low-level exposure to microplastics through drinking water remains uncertain. Dose-response relationships and regulatory thresholds based on health outcomes do not exist. The potential for smaller particles and nanoplastics to cross biological barriers and accumulate in tissues raises concerns about long-term human health effects. Research on these aspects remains preliminary, and comprehensive risk assessment frameworks specific to groundwater-derived microplastics require development.

Climate Change Interactions

Potential interactions between climate change and microplastic transport in groundwater systems remain largely unexplored. Altered precipitation patterns may modify recharge dynamics and associated microplastic transport. Increased extreme precipitation events may enhance particle mobilization and infiltration, while drought conditions may concentrate contaminants and modify groundwater chemistry in ways that influence particle stability and transport. Temperature increases may accelerate degradation rates and fragmentation into smaller, more mobile particles. These climate-driven effects on microplastic fate and transport warrant investigation.

6.4.3 Generalization and Transferability

The findings from Chennai may not directly transfer to groundwater systems with different climatic regimes, urban development patterns, or hydrogeological characteristics. The tropical monsoon climate, warm temperatures favouring weathering processes, and specific

waste management practices in Chennai create conditions not universally applicable to other regions.

Laboratory results using polyvinyl chloride fragments with median particle size of 42 μm may not represent transport of other polymer types or size fractions with different densities, surface properties, or morphologies. Polyethylene and polypropylene, which together comprised 29-35% of field samples depending on season, have lower densities (0.91-0.97 g/cm³ and 0.85-0.94 g/cm³ respectively) compared to PVC (1.38 g/cm³), potentially resulting in different gravitational settling and transport behaviours under natural flow conditions.

The numerical model requires parameter calibration for different aquifer systems. Attachment coefficients, detachment coefficients, and porosity decay constants derived from laboratory experiments may not apply directly to field conditions without site-specific validation. The model cannot be applied to new settings without calibration against local observations or experimental data representative of site conditions.

The simplified geochemical conditions (deionized water) and uniform media properties employed in experiments create idealized conditions that differ from heterogeneous natural aquifers with complex groundwater chemistry. Extrapolation to field scales requires careful consideration of these differences and validation against field observations where available.

6.5 Implications for Groundwater Management

6.5.1 Aquifer Vulnerability Assessment

Laboratory experiments demonstrate that grain size controls microplastic transport efficiency and hydraulic consequences. Fine sand (300 μm) with pore-throat diameters of 36-38 μm exhibits substantial retention capacity and hydraulic conductivity reductions of 60-80%. Medium sand (600 μm) with pore-throat diameters of 71-74 μm shows comparable severe conductivity reduction. Intermediate-medium sand (1000 μm) with pore-throat diameters of 116-121 μm demonstrates transitional behaviour with moderate retention and hydraulic changes, occupying a position between severe degradation in finer materials and minimal impact in coarse materials. Coarse sand (2000 μm) with pore-throat diameters of 227-237 μm allows rapid particle transport with minimal hydraulic impact.

Field observations from Chennai indicate that sandy formations (11.2 particles per sample pre-monsoon, 15.5 post-monsoon) contain higher microplastic abundances than clayey

zones (8.7 and 11.8 particles respectively), consistent with laboratory findings that intermediate grain sizes enable both particle transport and substantial retention. Aquifers within the 600-1000 µm range warrant particular management attention as they occupy the transitional zone where neither complete retention nor unimpeded transport dominates, creating conditions where both contamination risk and hydraulic impairment may occur.

Areas with shallow water tables (<5 m below ground surface) showed approximately 25% higher microplastic counts than deeper tables (>10 m), suggesting enhanced vertical infiltration in settings with direct surface-groundwater proximity. Locations within 500 m of the Adyar and Coovum rivers showed approximately 32% higher counts than distant locations, indicating that riverine corridors represent elevated vulnerability zones where surface water-groundwater exchange facilitates microplastic transfer.

6.5.2 Monitoring Priorities

Field investigations demonstrate that microplastic detection in groundwater is technically feasible using established sampling and analytical protocols. The 55.4% increase in total microplastic abundance from pre-monsoon (249 particles) to post-monsoon (387 particles) periods, with larger increases (28-36%) at riverine locations, indicates that monitoring should capture seasonal variability. The shift in colour distribution from 79.1% transparent/translucent particles pre-monsoon to 27.9% post-monsoon, with coloured particles increasing from 20.9% to 72.1%, suggests that monsoon periods mobilize fresh pigmented materials requiring targeted sampling during and after high-flow events.

Continued monitoring in Chennai should address: (1) seasonal campaigns during monsoon transitions to capture mobilization events documented in riverine corridors; (2) focused sampling in sandy formations where field data indicate preferential accumulation (15.5 particles per sample post-monsoon versus 11.8 in clayey zones); (3) depth-stratified sampling given the observed relationship between water table depth and microplastic abundance; (4) polymer composition analysis tracking seasonal variation in PVC (22-27%), polyethylene (HDPE 18-21%, LDPE 17-19%), and polypropylene (14-16%) to identify source changes.

Alternative monitoring approaches using proxy indicators warrant exploration to reduce analytical costs and complexity while maintaining temporal resolution. Integration of

microplastic monitoring with existing groundwater quality networks would enable detection of trends.

6.5.3 Source Control Considerations

Field observations indicate multiple urban sources requiring different control strategies. Fibre dominance (61.4% pre-monsoon, 58.1% post-monsoon) with nylon as a major component indicates textile sources including laundry wastewater. Polymer composition analysis identified polyvinyl chloride (22-25%), reflecting piping and construction materials; polyethylene (HDPE 18-21%, LDPE 17-19%) and polypropylene (14-16%), indicating packaging waste fragmentation; and polyurethane (9-10%), suggesting tire and shoe wear contributions from urban transportation.

Laboratory findings indicate that source control effectiveness depends on local aquifer characteristics. Areas with fine to medium sand (300-600 μm) beneath urban zones face hydraulic degradation risk from sustained microplastic loading, with conductivity reductions of 60-80% observed under experimental conditions. Areas with intermediate-medium sand (1000 μm) require management approaches addressing both transport potential and moderate hydraulic impairment. Areas with coarse sand (2000 μm) warrant focus on preventing downgradient transport rather than near-source retention.

The colour distribution shift and the larger increases in fragments (68.7%) compared to fibres (47.1%) from pre-monsoon to post-monsoon periods indicate that storm-driven surface runoff mobilizes diverse plastic debris. The substantial post-monsoon increases observed near rivers (28-36% at specific locations versus 55.4% overall increase) indicate that bank infiltration and urban runoff represent pathways requiring management attention during monsoon periods. Implementation of stormwater management practices in urban areas could reduce microplastic loading to surface waters and associated infiltration to groundwater.

Source control efforts should prioritize zones within 500 m of the Adyar and Coovum rivers where elevated microplastic abundances were documented (approximately 32% higher than distant locations). Sandy formations in these riverine corridors showed the highest post-monsoon counts (15.5 particles per sample on average), indicating that these areas require integrated surface water and groundwater protection measures.

6.6 Recommendations for Future Research

6.6.1 Extended Field Investigation

Long-term monitoring programs spanning multiple years would characterize inter-annual variability in microplastic occurrence and assess accumulation trends. Monsoon rainfall in Chennai exhibits year-to-year variation, suggesting that observations from two seasonal cycles may not represent longer-term patterns. Monitoring should include depth-stratified sampling to assess vertical migration and identify aquifer layers experiencing elevated contamination.

Integration with regional hydrogeological mapping would enable identification of preferential transport pathways and vulnerable zones . Complementary monitoring of surface water and soil microplastic concentrations would improve source attribution and pathway assessment (Panno et al., 2019). Integration of microplastic data with conventional groundwater quality parameters including major ions, dissolved organic carbon, and microbial indicators would clarify relationships between contamination sources and aquifer conditions (Koelmans et al., 2019).

Monitoring design should account for the spatial clustering observed near riverine corridors (28-36% higher increases at locations near the Adyar and Coovum rivers) and the seasonal timing of monsoon-driven mobilization. Sampling frequencies should capture both baseline conditions during dry periods and peak mobilization during and immediately following monsoon events (He et al., 2020).

Source attribution methodologies warrant development, potentially incorporating polymer fingerprinting techniques to distinguish contributions from different urban sources (Dris et al., 2018). The diverse polymer assemblage observed in Chennai samples (PVC 22-27%, PE 18-21%, PP 14-16%) suggests multiple contributing sources requiring differentiation for effective management.

6.6.2 Advanced Experimental Approaches

Laboratory experiments should extend to longer timescales (months to years) to assess long-term accumulation and potential recovery. Current experiments spanning hours to days cannot capture processes operating over timescales relevant to groundwater residence times

(Gewert et al., 2015). Experiments should incorporate heterogeneous media including natural sediment mixtures and clay lenses to better represent field conditions.

Hydrogeochemical conditions should include varied pH, ionic strength, and dissolved organic matter concentrations representative of natural groundwater (Xu et al., 2021). Experiments employed deionized water; natural groundwater chemistry including elevated ionic strength and organic matter may substantially modify particle aggregation and retention through mechanisms not captured in simplified experimental conditions (Erhayem & Sohn, 2014).

Additional grain sizes within the 600-2000 μm range would improve characterization of the transitional regime where retention mechanisms shift from straining-dominated to attachment-dominated behaviour (Chapter 4). The four grain sizes investigated provide initial coverage but additional resolution in the intermediate range would refine mechanistic understanding.

Mixed polymer assemblages reflecting field observations (PVC, PE, PP, polyurethane) should replace monodisperse PVC particles used in experiments (Chapter 4). Different polymer types exhibit distinct surface properties and densities that may result in different transport behaviours (Hartmann et al., 2019). Variable flow conditions simulating seasonal hydrology, including periods of enhanced flow representing monsoon conditions, would improve environmental relevance.

Pore-scale imaging techniques including X-ray computed tomography would provide detailed visualization of particle distributions and retention mechanisms at the pore scale (Karadimitriou et al., 2019). These techniques could clarify selective blockage phenomena suggested by the disproportionate hydraulic conductivity reduction (60-80%) relative to porosity changes observed in fine and medium sand experiments (Chapter 4).

Investigation of biofilm formation on microplastics and its effects on transport behaviour would address a knowledge gap relevant to long-term field conditions (Rummel et al., 2017). Biofilms could alter surface charge, promote particle aggregation, or facilitate biodegradation over extended timescales not captured in short-duration experiments.

6.6.3 Numerical Modelling Enhancement

Extension to two- and three-dimensional domains incorporating heterogeneous media properties and preferential flow paths would enable assessment of field-scale transport (Chapter 5). The one-dimensional model assumption limits field-scale applicability where preferential flow through fractures and macropores may dominate transport (Tufenkji & Elimelech, 2004). Spatial heterogeneity in aquifer properties observed in Chennai (sandy, clayey, and hard-rock zones) cannot be represented in homogeneous one-dimensional simulations.

Integration of chemical speciation models could address the role of natural organic matter and electrolyte effects on retention (Xu et al., 2021). The model assumes constant surface chemistry; natural groundwater conditions with varying ionic strength and organic matter could substantially modify particle-media interactions through mechanisms including enhanced aggregation and surface property modification (Wang et al., 2021).

Coupling with vadose zone transport models would enable assessment of contamination pathways from surface sources through soil to groundwater . Current model focuses on saturated zone transport; the vadose zone represents a critical pathway for vertical infiltration that requires separate modelling approaches incorporating unsaturated flow dynamics.

Extension of the model to incorporate particle aggregation processes would improve representation of field conditions (Chapter 5). The model assumes non-aggregating particles; natural groundwater chemistry may promote aggregation that alters effective particle sizes and transport behaviour. Biological interactions including biofilm formation represent additional processes not currently incorporated (Rummel et al., 2017).

Machine learning approaches incorporating diverse datasets including field observations, experimental results, and remote sensing information could complement mechanistic models .These approaches may identify patterns in complex, non-linear relationships though they require substantial training data and face interpretability challenges.

6.6.4 Health and Ecological Risk Assessment

Quantitative assessment of human health risks from microplastic ingestion through groundwater-based drinking water supply requires toxicological studies establishing dose-response relationships for chronic low-level exposure (Koelmans et al., 2019). No regulatory

thresholds based on health outcomes currently exist. Particle size fractionation analysis would assess bioavailability of smaller particles, particularly those below 10 μm that present analytical challenges but potentially enhanced biological uptake (Mintenig et al., 2018).

Evaluation of polymer-specific health effects should prioritize the dominant polymers identified in Chennai groundwater: PVC (22-27%), HDPE (18-21%), LDPE (17-19%), and PP (14-16%) (Chapter 3). Different polymers may exhibit distinct toxicological profiles based on their chemical composition and associated additives (Hahladakis et al., 2018).

Assessment of microplastics as vectors for co-contaminant transport warrants investigation (Hüffer et al., 2018). The capacity for microplastics to sorb and transport organic compounds and heavy metals may enhance contaminant bioavailability through mechanisms not captured in conventional risk assessments focusing on microplastics alone.

Ecological risk assessment should evaluate potential effects on aquifer microbial communities and the broader subsurface ecosystem (Griebler & Avramov, 2015). Groundwater ecosystems including diverse microbial communities and specialized invertebrate fauna may experience exposure to microplastic particles with consequences for community structure and ecological function that remain unexplored.

Investigation of interactions between microplastics and other contaminants including metals and persistent organic pollutants could reveal synergistic or antagonistic effects relevant to risk assessment (Koelmans et al., 2016). Natural organic matter interactions with microplastics may influence contaminant sorption and bioavailability through complexation and bridging mechanisms (Erhayem & Sohn, 2014).

6.6.5 Climate Change Considerations

Potential interactions between climate change and microplastic transport in groundwater systems warrant investigation. Altered precipitation patterns may modify recharge dynamics and associated microplastic transport (Allen et al., 2019). Increased extreme precipitation events may enhance particle mobilization and infiltration, potentially amplifying the seasonal effects observed in Chennai where post-monsoon samples showed 55.4% higher total microplastic abundance compared to pre-monsoon conditions (Chapter 3).

Temperature increases may accelerate degradation rates and fragmentation into smaller, more mobile particles (Romera-Castillo et al., 2018). Altered groundwater chemistry

resulting from climate-induced changes in water-rock interactions, redox conditions, or saline intrusion may influence particle surface properties and attachment behaviours (Galloway et al., 2017). Climate adaptation measures including increased groundwater extraction, artificial recharge, and land use changes may create secondary effects on microplastic transport and distribution.

Research integrating climate projections with microplastic transport models would provide insights into long-term contamination trajectories (Allen et al., 2019). Development of monitoring networks designed to detect climate-microplastic interactions would provide observational data to complement modelling approaches.

6.7 Conclusions

This integrated investigation examined microplastic transport in Chennai's groundwater systems through field observations, laboratory experimentation, and numerical modelling. The research addressed four objectives established in Chapter 1: characterizing microplastic occurrence and spatial distribution in groundwater; investigating transport mechanisms in porous media through controlled experiments; developing numerical models for predicting transport; and discussing implications for groundwater quality and aquifer behaviour.

Achievement of Research Objectives

Objective 1 (Characterization): Field sampling detected microplastics at all 25 locations across Chennai's aquifer systems. Particles per litre ranged from 5 to 19 particles per sample in pre-monsoon conditions (August 2024) and 8 to 26 particles per sample in post-monsoon conditions (February 2025). Total counts increased from 249 particles pre-monsoon to 387 particles post-monsoon. Sandy formations averaged 11.2 particles per sample pre-monsoon (15.5 post-monsoon) compared to 8.7 particles in clayey zones (11.8 post-monsoon). Samples near the Adyar and Coovum rivers showed increases of 28-36% between sampling periods, larger than the overall 55.4% increase.

Objective 2 (Transport Investigation): Laboratory experiments across four sand grain sizes (300 μm, 600 μm, 1000 μm, 2000 μm) quantified transport and retention mechanisms. Fine and medium sand exhibited delayed breakthrough with sustained elevated outlet concentrations and hydraulic conductivity reductions of 60-80%. Intermediate-medium sand showed transitional behaviour with moderate retention and hydraulic changes. Coarse sand

demonstrated early breakthrough with minimal hydraulic impact. Pore-throat diameter estimates (36-38 μm for 300 μm sand, 71-74 μm for 600 μm sand, 116-121 μm for 1000 μm sand, 227-237 μm for 2000 μm sand) relative to median microplastic particle size (42 μm) indicate size-dependent retention mechanisms (Bradford et al., 2003).

Objective 3 (Numerical Modelling): The coupled transport model achieved validation against laboratory data across four grain sizes, with consistently low errors for porosity predictions. The model incorporated advection-dispersion equations with retention terms for attachment, detachment, and straining, and accounted for porosity and permeability evolution. Relative errors for concentration predictions ranged from 2.99% (fine sand, 300 μm) to 54.49% (intermediate-medium sand, 1000 μm), with medium sand at 12.67% and coarse sand at 21.01%. Porosity predictions showed consistently low errors below 10% across all grain sizes. Model validation indicated that physical straining represents a primary retention mechanism, with particle-to-grain size ratios serving as a controlling parameter (Tufenkji & Elimelech, 2004).

Objective 4 (Implications): The investigation identified grain size distribution as a factor in aquifer vulnerability. Fine to medium sand (300-600 μm) experiences retention capacity alongside hydraulic degradation risk, while coarser materials enable particle transport with less hydraulic impact. Intermediate-medium sand (1000 μm) occupies a transitional zone where neither complete retention nor unimpeded transport dominates. Field observations of preferential accumulation in sandy formations and temporal increases following monsoon recharge align with laboratory findings and model predictions.

Primary Findings

Grain Size Controls: Laboratory experiments demonstrate that grain size controls microplastic transport efficiency and hydraulic consequences across four grain sizes. Fine sand (300 μm) exhibited delayed breakthrough with sustained outlet concentrations and hydraulic conductivity reductions of 60-80%. Medium sand (600 μm) demonstrated behaviour similar to fine sand with substantial conductivity reductions. Intermediate-medium sand (1000 μm) showed transitional behaviour with moderate retention and moderate hydraulic degradation. Coarse sand (2000 μm) allowed early breakthrough with minimal hydraulic impact.

Physical Straining Mechanism: Experimental results indicate that physical straining governs retention behaviour. In fine and medium sand, pore-throat diameters (45-180 μm) are of similar magnitude to median microplastic particle size (42 μm), creating conditions where particles lodge at pore constrictions (Bradford et al., 2003). In intermediate-medium sand (1000 μm), pore-throat diameters of approximately 150-300 μm create partial retention conditions. In coarse sand, pore-throat diameters (300-600 μm) substantially exceed microplastic dimensions, permitting passage with minimal mechanical obstruction. Microplastic particles exhibited zeta potentials of -35 ± 8 mV at pH 7.0, influencing electrostatic interactions though appearing secondary to physical straining under experimental conditions.

Field Contamination: Field sampling detected microplastics at all 25 locations. Particles per litre ranged from 5 to 19 particles per sample pre-monsoon and 8 to 26 particles per sample post-monsoon. Colour distribution shifted substantially between campaigns. Transparent/translucent particles decreased from 79.1% (197 of 249) pre-monsoon to 27.9% (108 of 387) post-monsoon. Coloured particles increased from 20.9% to 72.1%. This shift indicates fresh inputs of pigmented materials during monsoon periods. Polymer composition reflects diverse urban sources: polyvinyl chloride (22% pre-monsoon, 25% post-monsoon), polyethylene (HDPE 18-21%, LDPE 17-19%), and polypropylene (14-16%). Synthetic fibre prevalence (61.4% pre-monsoon, 58.1% post-monsoon) indicates textile sources (Browne et al., 2011).

Morphological Changes: Morphological composition changed between campaigns. Fibres increased from 153 to 225 particles (47.1% increase). Fragments increased from 96 to 162 particles (68.7% increase). The larger proportional increase in fragments may reflect mechanical fragmentation during high-flow monsoon conditions or preferential mobilization of fragments relative to fibres. Samples near the Adyar and Coovum rivers showed increases of 28-36%, larger than the overall 55.4% increase, consistent with enhanced mobilization in riverine corridors during monsoon recharge (He et al., 2020).

Numerical Model Performance: The coupled transport model achieved validation against laboratory data across four grain sizes, with consistently low errors for porosity predictions. Concentration prediction errors ranged from 6% (fine sand) to 23% (coarse sand). Porosity predictions showed errors below 10% across all grain sizes. Permeability predictions

exhibited systematic variation with grain size. The model classified transport regimes based on Damköhler numbers. Coarse sand operated in an attachment-dominated regime with minimal retention. Intermediate-medium sand exhibited upper transitional behaviour. Medium sand demonstrated transitional characteristics with combined attachment and straining. Fine sand showed straining-dominated retention.

Methodological Constraints

Field investigations covering two seasonal cycles provide limited resolution of inter-annual variability. The 25 sampling locations provide spatial coverage but limited resolution for detailed three-dimensional contamination mapping. Laboratory experiments employed polyvinyl chloride fragments; environmental microplastics include multiple polymer types with varying properties (Hartmann et al., 2019). Experimental geochemistry employed deionized water, which does not represent natural groundwater containing dissolved salts, organic matter, and microbial communities. These components could alter retention behaviour through enhanced aggregation, biofilm formation, or surface property modification (Rummel et al., 2017). Experiments spanned hours to days; natural aquifer evolution occurs over years to decades. Experiments employed uniform sand columns; natural aquifers exhibit layered lithologies and non-uniform characteristics.

The numerical model incorporates simplifying assumptions including one-dimensional geometry, homogeneous media properties, constant diffusion coefficients, spherical particle assumptions, and absence of particle aggregation or biological interactions (Chapter 5 Section 5.2.4). Field-scale transport in heterogeneous, layered aquifers with preferential flow pathways would differ from model predictions. Parameter calibration was conducted for each grain size; empirical coefficients require site-specific calibration for field applications.

Knowledge Gaps

Long-term fate and persistence of microplastics in groundwater systems remain incompletely characterized (Wagner & Lambert, 2018). Potential fragmentation into nanoplastics, biodegradation rates, and chemical transformation over decadal timescales relevant to groundwater residence times require investigation. The role of biofilm formation and microbial communities in modifying microplastic surface properties and transport behaviour remains uncharacterized (Rummel et al., 2017). Interactions between natural

organic matter, microplastic particles, and sand grain surfaces require investigation (Xu et al., 2021). The toxicological significance of chronic low-level exposure to microplastics through drinking water remains uncertain (Wright & Kelly, 2017).

Potential interactions between climate change and microplastic transport in groundwater systems remain largely unexplored (Allen et al., 2019).

Management Implications

The investigation identifies grain size distribution as a factor in aquifer vulnerability. Fine to medium sand (300-600 μm) experiences retention capacity but faces hydraulic degradation risk with conductivity reductions of 60-80% under experimental conditions. Intermediate-medium sand (1000 μm) occupies a transitional zone requiring management approaches addressing both transport potential and moderate hydraulic impairment. Coarse sand enables particle transport with minimal hydraulic impact.

Field investigations demonstrate that microplastic detection in groundwater is feasible using established protocols. The 55.4% increase in total abundance from pre-monsoon to post-monsoon periods, with larger increases (28-36%) at riverine locations, indicates that monitoring should capture seasonal variability. The colour distribution shift from 79.1% transparent pre-monsoon to 27.9% post-monsoon suggests that monsoon periods mobilize fresh pigmented materials requiring targeted sampling during and after high-flow events.

Source control efforts should address multiple urban sources. Fibre dominance (61.4% pre-monsoon, 58.1% post-monsoon) indicates textile sources. Polymer composition analysis identified polyvinyl chloride (22-25%), polyethylene (18-21%), and polypropylene (14-16%), reflecting diverse urban sources including piping materials, packaging waste, and tire wear. The colour distribution shift and larger increases in fragments (68.7%) compared to fibres (47.1%) indicate that storm-driven surface runoff mobilizes diverse plastic debris.

Future Research Directions

Long-term monitoring programs spanning multiple years would characterize inter-annual variability and assess accumulation trends. Integration with regional hydrogeological mapping would enable identification of preferential transport pathways. Laboratory experiments should extend to longer timescales, heterogeneous media, varied hydrogeochemical conditions, mixed polymer assemblages, and variable flow conditions.

Investigation of biofilm formation and its effects on transport behaviour would address a knowledge gap. Additional grain sizes within the 600-2000 μm range would improve characterization of transitional transport regimes.

Numerical modelling extensions to two- and three-dimensional domains incorporating heterogeneous media properties and preferential flow paths would enable field-scale assessment. Integration of chemical speciation models could address natural organic matter and electrolyte effects. Quantitative assessment of human health risks requires toxicological studies establishing dose-response relationships. Ecological risk assessment should evaluate potential effects on aquifer microbial communities. Research integrating climate projections with microplastic transport models would provide insights into long-term contamination trajectories (Allen et al., 2019).

Closing Statement

This investigation addressed microplastic transport and retention in groundwater systems through integrated field, laboratory, and modelling approaches. The four research objectives were addressed through field characterization across 25 locations, laboratory experiments across four grain sizes, numerical model development and validation, and assessment of implications for groundwater quality. The convergence of evidence across investigative approaches provides support for identified transport mechanisms. The findings have applications for groundwater monitoring and management in Chennai and similar tropical urban aquifer systems. Substantial knowledge gaps remain regarding long-term fate, biological interactions, and health implications, requiring continued research combining field investigations, laboratory experimentation, and advanced analytical approaches.

Chapter 7- Bibliography

Alimi, O. S., Budarz, J. F., Hernandez, L. M., & Tufenkji, N. (2018). Microplastics and nano plastics in aquatic environments: Aggregation, deposition, and enhanced contaminant transport. Environmental Science & Technology, 52(4), 1704-1724. https://doi.org/10.1021/acs.est.7b05559

Allen, S., Allen, D., Phoenix, V. R., Le Roux, G., Durántez Jiménez, P., Simonneau, A., Binet, S., & Galop, D. (2019). Atmospheric transport and deposition of microplastics in a remote mountain catchment. Nature Geoscience, 12, 339-344. https://doi.org/10.1038/s41561-019-0335-5

Anbumani, S., & Kakkar, P. (2018). Ecotoxicological effects of microplastics on biota: A review. Environmental Science and Pollution Research, 25(15), 14373-14396. https://doi.org/10.1007/s11356-018-1999-x

Andrady, A. L. (2011). Microplastics in the marine environment. Marine Pollution Bulletin, 62(8), 1596-1605. https://doi.org/10.1016/j.marpolbul.2011.05.030

Andrady, A. L. (2017). The plastic in microplastics: A review. Marine Pollution Bulletin, 119(1), 12-22. https://doi.org/10.1016/j.marpolbul.2017.01.082

ASTM D4253-16. (2016). Standard test methods for maximum index density and unit weight of soils using a vibratory table. ASTM International. https://doi.org/10.1520/D4253-16

Ballent, A., Corcoran, P. L., Madden, O., Helm, P. A., & Longstaffe, F. J. (2016). Sources and sinks of microplastics in Canadian Lake Ontario nearshore, tributary and beach sediments. Marine Pollution Bulletin, 110(1), 383-395. https://doi.org/10.1016/j.marpolbul.2016.06.037

Barnes, D. K. A., Galgani, F., Thompson, R. C., & Barlaz, M. (2009). Accumulation and fragmentation of plastic debris in global environments. Philosophical Transactions of the Royal Society B: Biological Sciences, 364(1526), 1985-1998. https://doi.org/10.1098/rstb.2008.0205

Besseling, E., Quik, J. T. K., Sun, M., & Koelmans, A. A. (2017). Fate of nano- and microplastic in freshwater systems: A modelling study. Environmental Pollution, 220(Part A), 540-548. https://doi.org/10.1016/j.envpol.2016.10.001

Bouwman, H., Minnaar, K., Bezuidenhout, C., & Verster, C. (2018). A SCOPING STUDY. https://www.wrc.org.za/wp-content/uploads/mdocs/2610-1-18.pdf

Bradford, S. A., & Bettahar, M. (2006). Concentration dependent transport of colloids in saturated porous media. Journal of Contaminant Hydrology, 82(1–2), 99–117. https://doi.org/10.1016/j.jconhyd.2005.09.006

Bradford, S. A., Morales, V. L., Zhang, W., Harvey, R. W., Packman, A. I., Mohanram, A., & Welty, C. (2013). Transport and Fate of Microbial Pathogens in Agricultural Settings. *Critical Reviews in Environmental Science and Technology*, *43*(8), 775–893. https://doi.org/10.1080/10643389.2012.710449

Bradford, S. A., Simunek, J., Bettahar, M., van Genuchten, M. T., & Yates, S. R. (2003). Modeling colloid attachment, straining, and exclusion in saturated porous media. Environmental Science & Technology, 37(10), 2242-2250. https://doi.org/10.1021/es025899u

Bradford, S. A., Torkzaban, S., & Shapiro, A. (2013). A theoretical analysis of colloid attachment and straining in chemically heterogeneous porous media. *Langmuir*, *29*(23), 6944-6952. https://doi.org/10.1021/la4011357

Bradford, S. A., Torkzaban, S., & Simunek, J. (2012). Modeling colloid transport and retention in saturated porous media under unfavourable attachment conditions. Water Resources Research, 47(10), W10503. https://doi.org/10.1029/2011WR010812

Bradford, S. A., Torkzaban, S., Leij, F., & Simunek, J. (2015). Equilibrium and kinetic models for colloid release under transient solution chemistry conditions. Journal of Contaminant Hydrology, 181, 141-152. https://doi.org/10.1016/j.jconhyd.2015.04.003

Bradford, S. A., Yates, S. R., Bettahar, M., & Simunek, J. (2002). Physical factors affecting the transport and fate of colloids in saturated porous media. Water Resources Research, 38(12), 1327. https://doi.org/10.1029/2002WR001340

Brander, S. M., Renick, V. C., Foley, M. M., Steele, C., Woo, M., Lusher, A., Carr, S., Helm, P., Box, C., Cherniak, S., Andrews, R. C., & Rochman, C. M. (2020). Sampling and quality assurance and quality control: A guide for scientists investigating the occurrence of microplastics across matrices. Applied Spectroscopy, 74(9), 1099–1125. https://doi.org/10.1177/0003702820945713

Browne, M. A., Crump, P., Niven, S. J., Teuten, E., Tonkin, A., Galloway, T., & Thompson, R. (2011). Accumulation of microplastic on shorelines worldwide: Sources and sinks. Environmental Science & Technology, 45(21), 9175–9179. https://doi.org/10.1021/es201811s

Browne, M. A., Underwood, A. J., Chapman, M. G., Williams, R., Thompson, R. C., & van Franeker, J. A. (2015). Linking effects of anthropogenic debris to ecological impacts. Proceedings of the Royal Society B: Biological Sciences, 282(1807), 20142929. https://doi.org/10.1098/rspb.2014.2929

Burns, E. E., & Boxall, A. B. A. (2018). Microplastics in the aquatic environment: Evidence for or against adverse impacts and major knowledge gaps. Environmental Toxicology and Chemistry, 37(11), 2776-2796. https://doi.org/10.1002/etc.4268

Cao, S., Dong, S., Wang, L., Suakollie, E. B., Wu, H., & Yu, Y. (2023). Transport of polypropylene, polyvinyl chloride, polyethylene terephthalate and polymethyl methacrylate microplastics in porous media under gradient ionic strength. *Environmental Pollutants and Bioavailability*, *35*(1). https://doi.org/10.1080/26395940.2023.2269315

Ceylan, E., Bartan, D.B., Öztürk-Ufuk, İ., Topuz, E., Ayral-Çınar, D. (2024). Interactıon of Micro-Nanoplastics and Heavy Metals in Soil Systems: Mechanism and Implication. In: Bhat, S.A., Kumar, V., Li, F., Kumar, S. (eds) Management of Micro and Nano-plastics in Soil and Biosolids. Springer, Cham. https://doi.org/10.1007/978-3-031-51967-3_7

Chamas, A., Moon, H., Zheng, J., Qiu, Y., Tabassum, T., Jang, J. H., Abu-Omar, M., Scott, S. L., & Suh, S. (2020). Degradation rates of plastics in the environment. ACS Sustainable Chemistry & Engineering, 8(9), 3494-3511. https://doi.org/10.1021/acssuschemeng.9b06635

Chen, M., Xu, J., Tang, R., Yuan, S., Min, Y., Xu, Q., & Shi, P. (2022). Roles of microplastic-derived dissolved organic matter on the photodegradation of organic micropollutants. Journal of hazardous materials, 440, 129784. https://doi.org/10.1016/j.jhazmat.2022.129784

Chia, R. W., Lee, J. Y., Kim, H., & Jang, J. (2021). Microplastic pollution in soil and groundwater: A review. Environmental Chemistry Letters, 19(6), 4211–4224. https://doi.org/10.1007/s10311-021-01297-6

Chubarenko, I., Bagaev, A., Zobkov, M., & Esiukova, E. (2016). On some physical and dynamical properties of microplastic particles in marine environment. Marine Pollution Bulletin, 108(1–2), 105–112. https://doi.org/10.1016/j.marpolbul.2016.04.048

De Falco, F., Di Pace, E., Cocca, M., & Avella, M. (2019). The contribution of washing processes of synthetic clothes to microplastic pollution. Scientific Reports, 9, 6633. https://doi.org/10.1038/s41598-019-43023-x

Dehaut, A., Hermabessiere, L., & Duflos, G. (2019). Current frontiers and recommendations for the study of microplastics in seafood. TrAC Trends in Analytical Chemistry, 116, 346–359. https://doi.org/10.1016/j.trac.2018.11.011

Dioses-Salinas, D. C., Pizarro-Ortega, C. I., & De-la-Torre, G. E. (2020). A methodological approach of the current literature on microplastic contamination in terrestrial environments: Current

knowledge and baseline considerations. Science of The Total Environment, 730, 139164. https://doi.org/10.1016/j.scitotenv.2020.139164

Dong, S., Gao, B., Sun, Y., Guo, H., Wu, J., Cao, S., & Wu, J. (2021). Transport characteristics of fragmental polyethylene glycol terephthalate (PET) microplastics in porous media under various chemical conditions. Chemosphere, 276, 130214. https://doi.org/10.1016/j.chemosphere.2021.130214

Dong, Z., Zhu, L., Zhang, W., Huang, R., Lv, X., Jing, X., ... & Qiu, Y. (2019). Role of surface functionalities of nanoplastics on their transport in seawater-saturated sea sand. *Environmental Pollution*, *255*, 113177. https://doi.org/10.1016/j.envpol.2019.113177

Dowarah, K., & Devipriya, S. P. (2019). Microplastic prevalence in the beaches of India and its correlation with fishing and tourism/recreational activities. Marine Pollution Bulletin, 149, 110582. https://doi.org/10.1016/j.marpolbul.2019.07.066

Dris, R., Gasperi, J., & Tassin, B. (2018). Sources and fate of microplastics in urban areas: A focus on Paris megacity. In M. Wagner & S. Lambert (Eds.), Freshwater microplastics (pp. 69-83). Springer. https://doi.org/10.1007/978-3-319-61615-5_4

Dris, R., Gasperi, J., Rocher, V., Saad, M., Renault, N., & Tassin, B. (2015). Microplastic contamination in an urban area: A case study in Greater Paris. Environmental Chemistry, 12(5), 592-599. https://doi.org/10.1071/EN14167

Dümichen, E., Barthel, A. K., Braun, U., Bannick, C. G., Brand, K., Jekel, M., & Senz, R. (2015). Analysis of polyethylene microplastics in environmental samples, using a thermal decomposition method. Water research, 85, 451-457. https://doi.org/10.1016/j.watres.2015.09.002

Eerkes-Medrano, D., Leslie, H. A., & Quinn, B. (2019). Microplastics in drinking water: A review and assessment. Current Opinion in Environmental Science & Health, 7, 69-75. https://doi.org/10.1016/j.coesh.2018.12.001

Eerkes-Medrano, D., Thompson, R. C., & Aldridge, D. C. (2015). Microplastics in freshwater systems: A review of the emerging threats, identification of knowledge gaps and prioritisation of research needs. Water Research, 75, 63–82. https://doi.org/10.1016/j.watres.2015.02.012

Enfrin, M., Dumée, L. F., & Lee, J. (2019). Nano/microplastics in water and wastewater treatment processes – Origin, impact and potential solutions. Water Research, 161, 621-638. https://doi.org/10.1016/j.watres.2019.06.049

Enfrin, M., Lee, J., Le-Clech, P., & Dumée, L. F. (2020). Kinetic and mechanistic aspects of ultrafiltration membrane fouling by nano- and microplastics. Journal of Membrane Science, 601, 117890. https://doi.org/10.1016/j.memsci.2020.117890

Erhayem, M., & Sohn, M. (2014). Effect of humic acid source on humic acid adsorption onto titanium dioxide nanoparticles. Science of The Total Environment, 470-471, 92-98. https://doi.org/10.1016/j.scitotenv.2013.09.063

Felsing, S., Kochleus, C., Buchinger, S., Brennholt, N., Stock, F., & Reifferscheid, G. (2018). A new approach in separating microplastics from environmental samples based on their electrostatic behaviour. Environmental Pollution, 234, 20-28. https://doi.org/10.1016/j.envpol.2017.11.013

Freeze, R. A., & Cherry, J. A. (1979). Groundwater. Prentice-Hall Inc.

Frei, S., Piehl, S., Gilfedder, B. S., Löder, M. G., Krutzke, J., Wilhelm, L., & Laforsch, C. (2019). Occurrence of microplastics in the hyporheic zone of rivers. Scientific Reports, 9(1), 15256. https://doi.org/10.1038/s41598-019-51741-5

Frias, J. P. G. L., & Nash, R. (2019). Microplastics: Finding a consensus on the definition. Marine Pollution Bulletin, 138, 145-147. https://doi.org/10.1016/j.marpolbul.2018.11.022

Galloway, T. S., Cole, M., & Lewis, C. (2017). Interactions of microplastic debris throughout the marine ecosystem. Nature Ecology & Evolution, 1, 0116. https://doi.org/10.1038/s41559-017-0116

Gewert, B., Plassmann, M. M., & MacLeod, M. (2015). Pathways for degradation of plastic polymers floating in the marine environment. Environmental Science: Processes & Impacts, 17(9), 1513-1521. https://doi.org/10.1039/C5EM00207A

Geyer, R., Jambeck, J. R., & Law, K. L. (2017). Production, use, and fate of all plastics ever made. Science Advances, 3(7), e1700782. https://doi.org/10.1126/sciadv.1700782

Gigault, J., ter Halle, A., Baudrimont, M., Pascal, P. Y., Gauffre, F., Phi, T. L., El Hadri, H., Grassl, B., & Reynaud, S. (2018). Current opinion: What is a nanoplastic? Environmental Pollution, 235, 1030-1034. https://doi.org/10.1016/j.envpol.2018.01.024

Griebler, C., & Avramov, M. (2015). Groundwater ecosystem services: A review. Freshwater Science, 34(1), 355-367. https://doi.org/10.1086/679903

Groh, K. J., Backhaus, T., Carney-Almroth, B., Geueke, B., Inostroza, P. A., Lennquist, A., Leslie, H. A., Maffini, M., Slunge, D., Trasande, L., Warhurst, A. M., & Muncke, J. (2019). Overview of

known plastic packaging-associated chemicals and their hazards. Science of The Total Environment, 651(Part 2), 3253-3268. https://doi.org/10.1016/j.scitotenv.2018.10.015

Hahladakis, J. N., Velis, C. A., Weber, R., Iacovidou, E., & Purnell, P. (2018). An overview of chemical additives present in plastics: Migration, release, fate and environmental impact during their use, disposal and recycling. Journal of Hazardous Materials, 344, 179-199. https://doi.org/10.1016/j.jhazmat.2017.10.014

Hartmann, N. B., Huffer, T., Thompson, R. C., Hassellov, M., Verschoor, A., Daugaard, A. E., ... & Wagner, M. (2019). Are we speaking the same language? Recommendations for a definition and categorization framework for plastic debris. https://doi.org/10.1021/acs.est.8b05297

He, B., Goonetilleke, A., Ayoko, G. A., & Rintoul, L. (2020). Abundance, distribution patterns, and identification of microplastics in Brisbane River sediments, Australia. Science of the Total Environment, 700, 134467. https://doi.org/10.1016/j.scitotenv.2019.134467

Hermsen, E., Mintenig, S. M., Besseling, E., & Koelmans, A. A. (2018). Quality criteria for the analysis of microplastic in biota samples: A critical review. Environmental Science & Technology, 52(18), 10230-10240. https://doi.org/10.1021/acs.est.8b01611

Hidalgo-Ruz, V., Gutow, L., Thompson, R. C., & Thiel, M. (2012). Microplastics in the marine environment: A review of the methods used for identification and quantification. Environmental Science & Technology, 46(6), 3060-3075. https://doi.org/10.1021/es2031505

Horton, A. A., & Dixon, S. J. (2018). Microplastics: An introduction to environmental transport processes. Wiley Interdisciplinary Reviews: Water, 5(2), e1268. https://doi.org/10.1002/wat2.1268

Horton, A. A., Walton, A., Spurgeon, D. J., Lahive, E., & Svendsen, C. (2017). Microplastics in freshwater and terrestrial environments: Evaluating the current understanding to identify the knowledge gaps and future research priorities. Science of The Total Environment, 586, 127-141. https://doi.org/10.1016/j.scitotenv.2017.01.190

Hurley, R. R., & Nizzetto, L. (2018). Fate and occurrence of micro(nano)plastics in soils: Knowledge gaps and possible risks. Current Opinion in Environmental Science & Health, 1, 6-11. https://doi.org/10.1016/j.coesh.2017.10.006

Hurley, R., Woodward, J., & Rothwell, J. J. (2018). Microplastic contamination of river beds significantly reduced by catchment-wide flooding. Nature Geoscience, 11(4), 251–257. https://doi.org/10.1038/s41561-018-0080-1

Jambeck, J. R., Geyer, R., Wilcox, C., Siegler, T. R., Perryman, M., Andrady, A., Narayan, R., & Law, K. L. (2015). Plastic waste inputs from land into the ocean. Science, 347(6223), 768-771. https://doi.org/10.1126/science.1260352

Jin, G., Zhang, Z., Tang, H., Xiaoquan, Y., Li, L., & Barry, D. A. (2019). Colloid transport and distribution in the hyporheic zone. *Hydrological Processes*, *33*(6), 932-944. https://doi.org/10.1002/hyp.13375

Johnson, P. R., & Elimelech, M. (1995). Dynamics of colloid deposition in porous media: Blocking based on random sequential adsorption. Langmuir, 11(3), 801–812. https://doi.org/10.1021/la00003a023

Jung, M. R., Horgen, F. D., Orski, S. V., Rodriguez, C. V., Beers, K. L., Balazs, G. H., Jones, T. T., Work, T. M., Brignac, K. C., Royer, S. J., & Hyrenbach, K. D. (2018). Validation of ATR FT-IR to identify polymers of plastic marine debris, including those ingested by marine organisms. Marine Pollution Bulletin, 127, 704–716. https://doi.org/10.1016/j.marpolbul.2017.12.061

Käppler, A., Fischer, D., Oberbeckmann, S., Schernewski, G., Labrenz, M., Eichhorn, K.-J., & Voit, B. (2016). Analysis of environmental microplastics by vibrational microspectroscopy: FTIR, Raman or both? Analytical and Bioanalytical Chemistry, 408(29), 8377-8391. https://doi.org/10.1007/s00216-016-9956-3

Käppler, A., Fischer, M., Scholz-Böttcher, B. M., Oberbeckmann, S., Labrenz, M., Fischer, D., Eichhorn, K. J., & Voit, B. (2018). Comparison of μ-ATR-FTIR spectroscopy and py-GCMS as identification tools for microplastic particles and fibers isolated from river sediments. Analytical and Bioanalytical Chemistry, 410(21), 5313–5327. https://doi.org/10.1007/s00216-018-1185-5

Karadimitriou, N. K., Mahani, H., Steeb, H., & Niasar, V. (2019). Nonmonotonic effects of salinity on wettability alteration and two-phase flow dynamics in PDMS micromodels. Water Resources Research, 55(11), 9826-9837. https://doi.org/10.1029/2018WR024252

Karadimitriou, N. K., Mahani, H., Steeb, H., & Niasar, V. (2019). Nonmonotonic effects of salinity on wettability alteration and two-phase flow dynamics in PDMS micromodels. Water Resources Research, 55(11), 9826–9837. https://doi.org/10.1029/2018WR024252

Karthik, R., Robin, R. S., Purvaja, R., Ganguly, D., Anandavelu, I., Raghuraman, R., Hariharan, G., Ramakrishna, A., & Ramesh, R. (2018). Microplastics along the beaches of southeast coast of India. Science of the Total Environment, 645, 1388–1399. https://doi.org/10.1016/j.scitotenv.2018.07.242

Kataoka, T., Nihei, Y., Kudou, K., & Hinata, H. (2019). Assessment of the sources and inflow processes of microplastics in the river environments of Japan. Environmental Pollution, 244, 958-965. https://doi.org/10.1016/j.envpol.2018.10.111

Keller, A. A., & Lazareva, A. (2014). Predicted releases of engineered nanomaterials: From global to regional to local. Environmental Science & Technology Letters, 1(1), 65-70. https://doi.org/10.1021/ez400106t

Keller, A. S., Jimenez-Martinez, J., & Mitrano, D. M. (2019). Transport of nano-and microplastic through unsaturated porous media from sewage sludge application. Environmental Science & Technology, 54(2), 911-920. https://doi.org/10.1021/acs.est.9b06483

Koelmans, A. A., Bakir, A., Burton, G. A., & Janssen, C. R. (2016). Microplastic as a vector for chemicals in the aquatic environment: Critical review and model-supported reinterpretation of empirical studies. Environmental Science & Technology, 50(7), 3315-3326. https://doi.org/10.1021/acs.est.5b06069

Koelmans, A. A., Besseling, E., Foekema, E. M., Kooi, M., Mintenig, S., Ossendorp, B. C., Redondo-Hasselerharm, P. E., Verschoor, A., Van Wezel, A. P., & Scheffer, M. (2018). Risks of plastic debris: Unravelling fact, opinion, perception, and belief. Environmental Science & Technology, 51(20), 11513-11519. https://doi.org/10.1021/acs.est.7b02219

Koelmans, A. A., Mohamed Nor, N. H., Hermsen, E., Kooi, M., Mintenig, S. M., & De France, J. (2019). Microplastics in freshwaters and drinking water: Critical review and assessment of data quality. Water Research, 155, 410-422. https://doi.org/10.1016/j.watres.2019.02.054

Koelmans, A. A., Redondo-Hasselerharm, P. E., Mohamed Nor, N. H., & Kooi, M. (2020). Solving the nonalignment of methods and approaches used in microplastic research to consistently characterize risk. Environmental Science & Technology, 54(19), 12307-12315. https://doi.org/10.1021/acs.est.0c02982

Kole, P. J., Löhr, A. J., Van Belleghem, F. G., & Ragas, A. M. (2017). Wear and tear of tyres: A stealthy source of microplastics in the environment. International Journal of Environmental Research and Public Health, 14(10), 1265. https://doi.org/10.3390/ijerph14101265

Kooi, M., Besseling, E., Kroeze, C., van Wezel, A. P., & Koelmans, A. A. (2018). Modeling the fate and transport of plastic debris in freshwaters: Review and guidance. In M. Wagner & S. Lambert (Eds.), Freshwater Microplastics (pp. 125-152). Springer, Cham. https://doi.org/10.1007/978-3-319-61615-5_7

Kooi, M., Nes, E. H. V., Scheffer, M., & Koelmans, A. A. (2017). Ups and downs in the ocean: Effects of biofouling on vertical transport of microplastics. Environmental Science & Technology, 51(14), 7963-7971. https://doi.org/10.1021/acs.est.6b04702

Kooi, M., Primpke, S., Mintenig, S. M., Lorenz, C., Gerdts, G., & Koelmans, A. A. (2021). Characterizing the multidimensionality of microplastics across environmental compartments. Environmental Science & Technology, 55(19), 13170–13179. https://doi.org/10.1016/j.watres.2021.117429

Lambert, S., & Wagner, M. (2016). Characterisation of nanoplastics during the degradation of polystyrene. Chemosphere, 145, 265–268. https://doi.org/10.1016/j.chemosphere.2015.11.078

Lassen, C., Hansen, S. F., Magnusson, K., Norén, F., Bloch Hartmann, N. I., Jensen, P. R., Nielsen, T. G., & Brinch, A. (2015). Microplastics: Occurrence, effects and sources of releases to the environment in Denmark. Environmental Project No. 1793. Danish Environmental Protection Agency.

Li, C., Busquets, R., & Campos, L. C. (2020). Assessment of microplastics in freshwater systems: A review. Science of the Total Environment, 707, 135578. https://doi.org/10.1016/j.scitotenv.2019.135578

Li, J., Liu, H., & Chen, J. P. (2018). Microplastics in freshwater systems: A review on occurrence, environmental effects, and methods for microplastics detection. Water Research, 137, 362–374. https://doi.org/10.1016/j.watres.2017.12.056

Li, P., Wang, X., Su, M., Zou, X., Duan, L., & Zhang, H. (2020). Characteristics of plastic pollution in the environment: A review. Bulletin of Environmental Contamination and Toxicology, 107(4), 577-584. https://doi.org/10.1007/s00128-020-02820-1

Liao, Y. L., Gan, C. D., Zhao, X., Du, X. Y., & Yang, J. Y. (2025). Insight into the interactions between microplastics and heavy metals in agricultural soil solution: adsorption performance influenced by microplastic types. Environmental Science: Processes & Impacts. https://doi.org/10.1039/D5EM00144G

Lim, S. J., Seo, J., Hwang, M., Kim, H. C., Kim, E. J., Lee, J., Hong, S. W., Lee, S., & Chung, J. (2023). A multi-scale framework for modeling transport of microplastics during sand filtration: Bridging from pore to continuum. Journal of Hazardous Materials, 443, 130219. https://doi.org/10.1016/j.jhazmat.2022.130219

Liu, K., Wang, X., Fang, T., Xu, P., Zhu, L., & Li, D. (2019). Source and potential risk assessment of suspended atmospheric microplastics in Shanghai. Science of the Total Environment, 675, 462–471. https://doi.org/10.1016/j.scitotenv.2019.04.110

Löder, M. G. J., & Gerdts, G. (2015). Methodology used for the detection and identification of microplastics—A critical appraisal. In M. Bergmann, L. Gutow, & M. Klages (Eds.), Marine anthropogenic litter (pp. 201-227). Springer. https://doi.org/10.1007/978-3-319-16510-3_8

Luo, H., Chang, L., Ju, T., & Li, Y. (2024). Factors influencing the vertical migration of microplastics up and down the soil profile. ACS Omega, 9(51), 50064–50077. https://doi.org/10.1021/acsomega.4c04083

Lusher, A. L., Welden, N. A., Sobral, P., & Cole, M. (2017). Sampling, isolating and identifying microplastics ingested by fish and invertebrates. Analytical Methods, 9(9), 1346–1360. https://doi.org/10.1039/C6AY02415G

Mai, L., You, S. N., He, H., Bao, L. J., Liu, L. Y., & Zeng, E. Y. (2019). Riverine microplastic pollution in the Pearl River Delta, China: are modeled estimates accurate?. Environmental science & technology, 53(20), 11810-11817. https://doi.org/10.1021/acs.est.9b04838

Masura, J., Baker, J., Foster, G., & Arthur, C. (2015). Laboratory methods for the analysis of microplastics in the marine environment: Recommendations for quantifying synthetic particles in waters and sediments. NOAA Technical Memorandum NOS-OR&R-48. https://dx.doi.org/10.25607/OBP-604

Messina, F., Marchisio, D. L., & Sethi, R. (2015). An extended and total flux normalized correlation equation for predicting single-collector efficiency. Journal of Colloid and Interface Science, 446, 185-193. https://doi.org/10.1016/j.jcis.2015.01.024

Miller, M. E., Kroon, F. J., & Motti, C. A. (2017). Recovering microplastics from marine samples: A review of current practices. Marine Pollution Bulletin, 123(1-2), 6-18. https://doi.org/10.1016/j.marpolbul.2017.08.058

Mintenig, S. M., Int-Veen, I., Löder, M. G. J., Primpke, S., & Gerdts, G. (2018). Identification of microplastic in effluents of waste water treatment plants using focal plane array-based micro-Fourier-transform infrared imaging. Water Research, 108, 365-372. https://doi.org/10.1016/j.watres.2016.11.015

Mintenig, S. M., Löder, M. G. J., Primpke, S., & Gerdts, G. (2019). Low numbers of microplastics detected in drinking water from ground water sources. Science of The Total Environment, 648, 631-635. https://doi.org/10.1016/j.scitotenv.2018.08.178

Mitrano, D. M., Beltzung, A., Frehland, S., Schmiedgruber, M., Cingolani, A., & Schmidt, F. (2019). Synthesis of metal-doped nanoplastics and their utility to investigate fate and behaviour in complex environmental systems. Nature Nanotechnology, 14(4), 362-368. https://doi.org/10.1038/s41565-018-0360-3

Mitrano, D. M., Wick, P., & Nowack, B. (2021). Placing nanoplastics in the context of global plastic pollution. Nature Nanotechnology, 16(5), 491-500. https://doi.org/10.1038/s41565-021-00888-2

Molnar, I. L., Johnson, W. P., Gerhard, J. I., Willson, C. S., & O'Carroll, D. M. (2015). Predicting colloid transport through saturated porous media: A critical review. Water Resources Research, 51(9), 6804-6845. https://doi.org/10.1002/2015WR017318

Molnar, I. L., Pensini, E., Asad, M. A., Mitchell, C. A., Nitsche, L. C., Pyrak-Nolte, L. J., Miño, G. L., & Krol, M. M. (2019). Colloid transport in porous media: A review of classical mechanisms and emerging topics. Transport in Porous Media, 130, 129-156. https://doi.org/10.1007/s11242-019-01270-6

Napper, I. E., Bakir, A., Rowland, S. J., & Thompson, R. C. (2015). Characterisation, quantity and sorptive properties of microplastics extracted from cosmetics. Marine Pollution Bulletin, 99(1-2), 178-185. https://doi.org/10.1016/j.marpolbul.2015.07.029

Nizzetto, L., Bussi, G., Futter, M. N., Butterfield, D., & Whitehead, P. G. (2016). A theoretical assessment of microplastic transport in river catchments and their retention by soils and river sediments. Environmental Science: Processes & Impacts, 18(8), 1050-1059. https://doi.org/10.1039/c6em00206d

Nizzetto, L., Futter, M., & Langaas, S. (2016). Are agricultural soils dumps for microplastics of urban origin? Environmental Science & Technology, 50(20), 10777-10779. https://doi.org/10.1021/acs.est.6b04140

O'Connor, D., Pan, S., Shen, Z., Song, Y., Jin, Y., Wu, W. M., & Hou, D. (2019). Microplastics undergo accelerated vertical migration in sand soil due to small size and wet-dry cycles. Environmental Pollution ,249, 527-534. https://doi.org/10.1016/j.envpol.2019.03.092

Panno, S. V., Kelly, W. R., Scott, J., Zheng, W., McNeish, R. E., Holm, N., Hoellein, T. J., & Baranski, E. L. (2019). Microplastic contamination in karst groundwater systems. Groundwater, 57(2), 189-196. https://doi.org/10.1111/gwat.12862

PlasticsEurope. (2023). Plastics – the facts 2023: An analysis of European plastics production, demand and waste data. PlasticsEurope Association. https://plasticseurope.org/knowledge-hub/plastics-the-facts-2023/

Praetorius, A., Scheringer, M., & Hungerbühler, K. (2012). Development of Environmental Fate Models for Engineered Nanoparticles A Case Study of TiO2 Nanoparticles in the Rhine River. Environmental science & technology, 46(12), 6705-6713. https://doi.org/10.1021/es204530n

Prata, J. C., da Costa, J. P., Duarte, A. C., & Rocha-Santos, T. (2019). Methods for sampling and detection of microplastics in water and sediment: A critical review. TrAC Trends in Analytical Chemistry, 110, 150–159. https://doi.org/10.1016/j.trac.2018.10.029

Prata, J. C., da Costa, J. P., Lopes, I., Duarte, A. C., & Rocha-Santos, T. (2019). Environmental exposure to microplastics: An overview on possible human health effects. Science of The Total Environment, 702, 134455. https://doi.org/10.1016/j.scitotenv.2019.134455

Primpke, S., Christiansen, S. H., Cowger, W., De Frond, H., Deshpande, A., Fischer, M., Holland, E. B., Meyns, M., O'Donnell, B. A., Ossmann, B. E., Pittroff, M., Sarau, G., Scholz-Böttcher, B. M., & Wiggin, K. J. (2020). Critical assessment of analytical methods for the harmonized and cost-efficient analysis of microplastics. Applied Spectroscopy, 74(9), 1012-1047. https://doi.org/10.1177/0003702820921465

Primpke, S., Dias, P. A., & Gerdts, G. (2019). Automated identification and quantification of microfibres and microplastics. Analytical Methods, 11(16), 2138-2147. https://doi.org/10.1039/C9AY00126C

Primpke, S., Fischer, M., Lorenz, C., Gerdts, G., & Scholz-Böttcher, B. M. (2020). Comparison of pyrolysis gas chromatography/mass spectrometry and hyperspectral FTIR imaging spectroscopy for the analysis of microplastics. Analytical and Bioanalytical Chemistry, 412(24), 8283-8298. https://doi.org/10.1007/s00216-020-02979-w

Primpke, S., Lorenz, C., Rascher-Friesenhausen, R., & Gerdts, G. (2017). An automated approach for microplastics analysis using focal plane array (FPA) FTIR microscopy and image analysis. Analytical Methods, 9(9), 1499–1511. https://doi.org/10.1039/C6AY02476A

Primpke, S., Wirth, M., Lorenz, C., & Gerdts, G. (2018). Reference database design for the automated analysis of microplastic samples based on Fourier transform infrared (FTIR) spectroscopy. Analytical and Bioanalytical Chemistry, 410(21), 5131-5141. https://doi.org/10.1007/s00216-018-1156-x

Ramachandran, A., Praveen, D., Jaganathan, R., & Palanivelu, K. (2019). Spatiotemporal analysis of fine particulate matter and associated mortality in Chennai, India. Environmental Science and Pollution Research, 26(28), 28757–28769. https://doi.org/10.1007/s11356-019-06074-w

Re, V. (2019). Shedding light on the invisible: Addressing the potential for groundwater contamination by plastic microfibers. Hydrogeology Journal, 27(7), 2719-2727. https://doi.org/10.1007/s10040-019-01998-x

Reichstein, M., Camps-Valls, G., Stevens, B. et al. Deep learning and process understanding for data-driven Earth system science. Nature 566, 195–204 (2019). https://doi.org/10.1038/s41586-019-0912-1

Rillig, M. C., Ingraffia, R., & de Souza Machado, A. A. (2017). Microplastic incorporation into soil in agroecosystems. Frontiers in Plant Science, 8, 1805. https://doi.org/10.3389/fpls.2017.01805

Rochman, C. M. (2018). Microplastics research—from sink to source. Science, 360(6384), 28–29. https://doi.org/10.1126/science.aar7734

Rochman, C. M., Brookson, C., Bikker, J., Djuric, N., Earn, A., Bucci, K., Athey, S., Huntington, A., McIlwraith, H., Munno, K., De Frond, H., Kolomijeca, A., Erdle, L., Grbic, J., Bayoumi, M., Borrelle, S. B., Wu, T., Santoro, S., Werbowski, L. M., … Hung, C. (2019). Rethinking microplastics as a diverse contaminant suite. Environmental Toxicology and Chemistry, 38(4), 703-711. https://doi.org/10.1002/etc.4371

Rochman, C. M., Hoh, E., Kurobe, T., & Teh, S. J. (2014). Ingested plastic transfers hazardous chemicals to fish and induces hepatic stress. Scientific Reports, 3, 3263. https://doi.org/10.1038/srep03263

Rochman, C. M., Kross, S. M., Armstrong, J. B., Bogan, M. T., Darling, E. S., Green, S. J., Smyth, A. R., & Veríssimo, D. (2015). Scientific evidence supports a ban on microbeads. Environmental Science & Technology, 49(18), 10759-10761. https://doi.org/10.1021/acs.est.5b03909

Romera-Castillo, C., Pinto, M., Langer, T. M., Álvarez-Salgado, X. A., & Herndl, G. J. (2018). Dissolved organic carbon leaching from plastics stimulates microbial activity in the ocean. Nature Communications, 9(1), 1430. https://doi.org/10.1038/s41467-018-03798-5

Rummel, C. D., Jahnke, A., Gorokhova, E., Kuhnel, D., & Schmitt-Jansen, M. (2017). Impacts of biofilm formation on the fate and potential effects of microplastic in the aquatic environment. Environmental Science & Technology Letters, 4(7), 258–267. https://doi.org/10.1021/acs.estlett.7b00164

Santana, M. F., Ascer, L. G., Custódio, M. R., Moreira, F. T., & Turra, A. (2020). Microplastic contamination in natural mussel beds from a Brazilian urbanized coastal region: Rapid evaluation through bioassessment. Marine Pollution Bulletin, 140, 98–105. https://doi.org/10.1016/j.marpolbul.2019.01.006

Setälä, O., Fleming-Lehtinen, V., & Lehtiniemi, M. (2014). Ingestion and transfer of microplastics in the planktonic food web. Environmental Pollution, 185, 77-83. https://doi.org/10.1016/j.envpol.2013.10.013

Shen, C., Huang, Y., Li, B., & Jin, Y. (2010). Effects of solution chemistry on straining of colloids in porous media under unfavorable conditions. Water Resources Research, 46(7), W07511. https://doi.org/10.1029/2007WR006580

Shen, X., He, Y., Zhu, X., & Ren, H. (2010). Concentration-dependent transport of colloids in saturated porous media. Journal of Contaminant Hydrology, 113(1–4), 96–108. https://doi.org/10.1029/2010WR009218

Šimůnek, J., Jarvis, N. J., Van Genuchten, M. T., & Gärdenäs, A. (2003). Review and comparison of models for describing non-equilibrium and preferential flow and transport in the vadose zone. *Journal of hydrology*, *272*(1-4), 14-35. https://doi.org/10.1016/S0022-1694(02)00252-4

Song, Y. K., Hong, S. H., Jang, M., Han, G. M., Jung, S. W., & Shim, W. J. (2017). Combined effects of UV exposure duration and mechanical abrasion on microplastic fragmentation by polymer type. Environmental Science & Technology, 51(8), 4368-4376. https://doi.org/10.1021/acs.est.6b06155

Stock, F., Kochleus, C., Bänsch-Baltruschat, B., Brennholt, N., & Reifferscheid, G. (2019). Sampling techniques and preparation methods for microplastic analyses in the aquatic environment – A review. TrAC Trends in Analytical Chemistry, 113, 84-92. https://doi.org/10.1016/j.trac.2019.01.014

Stock, V., Böhmert, L., Lisicki, E., Block, R., Cara-Carmona, J., Pack, L. K., Selb, R., Lichtenstein, D., Voss, L., Henderson, C. J., Zabinsky, E., Sieg, H., Braeuning, A., & Lampen, A. (2020). Uptake and effects of orally ingested polystyrene microplastic particles in vitro and in vivo. Archives of Toxicology, 94(4), 1541-1551. https://doi.org/10.1007/s00204-019-02478-7

Sudhakar, M., Doble, M., Murthy, P. S., & Venkatesan, R. (2008). Marine microbe-mediated biodegradation of low-and high-density polyethylenes. International Biodeterioration & Biodegradation, 61(3), 203-213.https://doi.org/10.1016/j.ibiod.2007.07.011

Sun, J., Dai, X., Wang, Q., van Loosdrecht, M. C. M., & Ni, B. J. (2019). Microplastics in wastewater treatment plants: Detection, occurrence and removal. Water Research, 152, 21-37. https://doi.org/10.1016/j.watres.2018.12.050

Thompson, R. C., Olsen, Y., Mitchell, R. P., Davis, A., Rowland, S. J., John, A. W. G., McGonigle, D., & Russell, A. E. (2004). Lost at sea: Where is all the plastic? Science, 304(5672), 838. https://doi.org/10.1126/science.1094559

Tosco, T., Bosch, J., Meckenstock, R. U., & Sethi, R. (2012). Transport of ferrihydrite nanoparticles in saturated porous media: role of ionic strength and flow rate. Environmental science & technology, 46(7), 4008-4015. https://doi.org/10.1021/es202643c

Tosco, T., Tiraferri, A., & Sethi, R. (2009). Ionic strength dependent transport of microparticles in saturated porous media: Modeling mobilization and immobilization phenomena under transient chemical conditions. Environmental Science & Technology, 43(12), 4425-4431. https://doi.org/10.1021/es900245d

Triebskorn, R., Braunbeck, T., Grummt, T., Hanslik, L., Huppertsberg, S., Jekel, M., Knepper, T. P., Krais, S., Müller, Y. K., Pittroff, M., Ruhl, A. S., Schmieg, H., Schür, C., Strobel, C., Wagner, M., Zumbülte, N., & Köhler, H.-R. (2019). Relevance of nano- and microplastics for freshwater ecosystems: A critical review. TrAC Trends in Analytical Chemistry, 110, 375-392. https://doi.org/10.1016/j.trac.2018.11.023

Tufenkji, N., & Elimelech, M. (2004). Correlation equation for predicting single-collector efficiency in physicochemical filtration in saturated porous media. Environmental Science & Technology, 38(2), 529-536. https://doi.org/10.1021/es034049r

Tufenkji, N., & Elimelech, M. (2005). Breakdown of colloid filtration theory: Role of the secondary energy minimum and surface charge heterogeneities. Langmuir, 21(3), 841-852. https://doi.org/10.1021/la048102g

Tufenkji, N., Miller, G. F., Ryan, J. N., Harvey, R. W., & Elimelech, M. (2004). Transport of Cryptosporidium oocysts in porous media: Role of straining and physicochemical filtration. Environmental science & technology, 38(22), 5932-5938. https://doi.org/10.1021/es049789u

Van Sebille, E., Wilcox, C., Lebreton, L., Maximenko, N., Hardesty, B. D., van Franeker, J. A., Eriksen, M., Siegel, D., Galgani, F., & Law, K. L. (2015). A global inventory of small floating plastic debris. Environmental Research Letters, 10(12), 124006. https://doi.org/10.1088/1748-9326/10/12/124006

Veerasingam, S., Mugilarasan, M., Venkatachalapathy, R., & Vethamony, P. (2016). Influence of 2015 flood on the distribution and occurrence of microplastic pellets along the Chennai coast, India. Marine Pollution Bulletin, 109(1), 196–204. https://doi.org/10.1016/j.marpolbul.2016.05.082

Wagner, M., & Lambert, S. (Eds.). (2018). Freshwater microplastics: Emerging environmental contaminants? Springer, Cham. https://doi.org/10.1007/978-3-319-61615-5

Wagner, M., Scherer, C., Alvarez-Muñoz, D., Brennholt, N., Bourrain, X., Buchinger, S., Fries, E., Grosbois, C., Klasmeier, J., Marti, T., Rodriguez-Mozaz, S., Urbatzka, R., Vethaak, A. D., Winther-Nielsen, M., & Reifferscheid, G. (2014). Microplastics in freshwater ecosystems: What we know and what we need to know. Environmental Sciences Europe, 26(1), 12. https://doi.org/10.1186/s12302-014-0012-7

Waldschläger, K., & Schüttrumpf, H. (2019). Effects of particle properties on the settling and rise velocities of microplastics in freshwater under laboratory conditions. Environmental Science & Technology, 53(4), 1958-1966. https://doi.org/10.1021/acs.est.8b06794

Waldschläger, K., & Schüttrumpf, H. (2020). Infiltration behaviour of microplastic particles with different densities, sizes, and shapes—From glass spheres to natural sediments. Environmental Science & Technology, 54(15), 9366-9373. https://doi.org/10.1021/acs.est.0c01722

Waldschläger, K., Lechthaler, S., Stauch, G., & Schüttrumpf, H. (2020). The way of microplastic through the environment – Application of the source-pathway-receptor model. Science of The Total Environment, 713, 136584. https://doi.org/10.1016/j.scitotenv.2020.136584

Wan, Y., Wu, C., Xue, Q., & Hui, X. (2019). Effects of plastic contamination on water evaporation and desiccation cracking in soil. Science of the Total Environment, 654, 576–582. https://doi.org/10.1016/j.scitotenv.2018.11.123

Wander, L., Vianello, A., Vollertsen, J., Westad, F., Braun, U., & Paul, A. (2020). Exploratory analysis of hyperspectral FTIR data obtained from environmental microplastics samples. Analytical Methods, 12(6), 781-791. https://doi.org/10.1039/C9AY02483B

Wang, F., Wang, F., & Zeng, E. Y. (2020). Sorption of toxic chemicals on microplastics. In Y. Zeng (Ed.), Microplastic contamination in aquatic environments (pp. 225-247). Elsevier. https://doi.org/10.1016/B978-0-12-813747-5.00007-2

Wang, F., Wong, C. S., Chen, D., Lu, X., Wang, F., & Zeng, E. Y. (2018). Interaction of toxic chemicals with microplastics: A critical review. Water Research, 139, 208–219. https://doi.org/10.1016/j.watres.2018.04.003

Wang, W., Gao, H., Jin, S., Li, R., & Na, G. (2020). Microplastics in surface waters of Dongting Lake and Hong Lake, China. Science of the Total Environment, 718, 137368. https://doi.org/10.1016/j.scitotenv.2020.137368

Wang, Z., Chen, M., Zhang, L., Wang, K., Yu, X., Zheng, Z., & Zheng, R. (2021). Sorption behaviors of phenanthrene on the microplastics identified in a mariculture farm in Xiangshan Bay, southeastern China. Science of the Total Environment, 761, 143175. https://doi.org/10.1016/j.scitotenv.2018.02.146

Weber, C. J., Opp, C., Prume, J. A., Koch, M., Andersen, T. J., & Chifflard, P. (2021). Deposition and in-situ translocation of microplastics in floodplain soils. Science of the Total Environment, 758, 143593. https://doi.org/10.1016/j.scitotenv.2020.143593

Wesch, C., Elert, A. M., Wörner, M., Braun, U., Klein, R., & Paulus, M. (2017). Assuring quality in microplastic monitoring: About the value of clean-air devices as essentials for verified data. Scientific Reports, 7(1), 5424. https://doi.org/10.1038/s41598-017-05838-4

Woodall, L. C., Gwinnett, C., Packer, M., Thompson, R. C., Robinson, L. F., & Paterson, G. L. J. (2015). Using a forensic science approach to minimize environmental contamination and to identify microfibres in marine sediments. Marine Pollution Bulletin, 95(1), 40–46. https://doi.org/10.1016/j.marpolbul.2015.04.044

World Health Organization (WHO). (2019). Microplastics in drinking-water. World Health Organization. https://apps.who.int/iris/handle/10665/326499

Wright, S. L., & Kelly, F. J. (2017). Plastic and human health: A micro issue? Environmental Science & Technology, 51(12), 6634-6647. https://doi.org/10.1021/acs.est.7b00423

Wright, S. L., Thompson, R. C., & Galloway, T. S. (2013). The physical impacts of microplastics on marine organisms: A review. Environmental Pollution, 178, 483-492. https://doi.org/10.1016/j.envpol.2013.02.031

Xu, B., Liu, F., Brookes, P. C., & Xu, J. (2018). Microplastics play a minor role in tetracycline sorption in the presence of dissolved organic matter. *Environmental Pollution*, *240*, 87-94. https://doi.org/10.1016/j.envpol.2018.04.113

Xu, B., Liu, F., Cryder, Z., Huang, D., Lu, Z., He, Y., Wang, H., Lu, Z., Brookes, P. C., Tang, C., Gan, J., & Xu, J. (2020). Microplastics in the soil environment: Occurrence, risks, interactions and fate – A review. Critical Reviews in Environmental Science and Technology, 50(21), 2175-2222. https://doi.org/10.1080/10643389.2019.1694822

Xu, J. L., Thomas, K. V., Luo, Z., & Gowen, A. A. (2019). FTIR and Raman imaging for microplastics analysis: State of the art, challenges and prospects. TrAC Trends in Analytical Chemistry, 119, 115629. https://doi.org/10.1016/j.trac.2019.115629

Xu, S., Gao, B., & Saiers, J. E. (2006). Straining of colloidal particles in saturated porous media. Water Resources Research, 42(12), W12S16. https://doi.org/10.1029/2006WR004948

Zettler, E. R., Mincer, T. J., & Amaral-Zettler, L. A. (2013). Life in the "plastisphere": Microbial communities on plastic marine debris. Environmental Science & Technology, 47(13), 7137-7146. https://doi.org/10.1021/es401288x

Zhang, K., Hamidian, A. H., Tubić, A., Zhang, Y., Fang, J. K., Wu, C., & Lam, P. K. (2021). Understanding plastic degradation and microplastic formation in the environment: A review. *Environmental Pollution*, 274, 116554. https://doi.org/10.1016/j.envpol.2021.116554

Zhang, Y., Kang, S., Allen, S., Allen, D., Gao, T., & Sillanpää, M. (2020). Atmospheric microplastics: A review on current status and perspectives. Earth-Science Reviews, 203, 103118. https://doi.org/10.1016/j.earscirev.2020.103118 .

Zhong, S., Zhang, K., Bagheri, M., Burken, J. G., Gu, A., Li, B., ... & Zhang, H. (2021). Machine learning: new ideas and tools in environmental science and engineering. Environmental science & technology, 55(19), 12741-12754. https://doi.org/10.1021/acs.est.1c01339

Zhu, D., Chen, Q. L., An, X. L., Yang, X. R., Christie, P., Ke, X., ... & Zhu, Y. G. (2018). Exposure of soil collembolans to microplastics perturbs their gut microbiota and alters their isotopic composition. Soil Biology and Biochemistry, 116, 302-310.https://doi.org/10.1016/j.soilbio.2017.10.027